Physiological traits determining yield tolerance of wheat to foliar diseases

van den Berg, F; Paveley, ND; Bingham, IJ; van den Bosch, F

Published in:
Phytopathology

DOI:
10.1094/PHYTO-07-16-0283-R

First published: 10/10/2017

Document Version
Peer reviewed version

Physiological Traits Determining Yield Tolerance of Wheat to Foliar Diseases

F. van den Berg, N. D. Paveley, I. J. Bingham, and F. van den Bosch

First author: Agriculture and Horticulture Department, Fera Science Ltd., Sand Hutton, York, YO41 1LZ; second author: Plant pathology department, ADAS, High Mowthorpe, Duggleby, Malton, North Yorkshire, YO17 8BP, UK; third author: Crop & Soils Systems, SRUC, Kings Buildings, West Mains Road, Edinburgh EH9 3JG, UK; fourth author: Computational and Systems Biology, Rothamsted Research, Harpenden, Hertfordshire, AL5 2JQ, UK

Corresponding author: F. van den Berg

Email address: Femke.vandenberg@fera.co.uk

ABSTRACT

van den Berg, F., Paveley, N. D., Bingham, I. J., van den Bosch, F.. Physiological traits determining yield tolerance of wheat to foliar diseases. Phytopathology x:x-x.

Tolerance is defined as the ability of one cultivar to yield more than another cultivar, under similar disease severity. If both cultivars suffer an equal loss in healthy (green) leaf area duration (HAD) over the grain filling period due to disease presence, then the yield loss per unit HAD loss is smaller for a more tolerant cultivar. Little is understood of what physiological and developmental traits of cultivars determine disease tolerance. In this study we use a mathematical model of wheat to investigate the effect of a wide range of wheat phenotypes on tolerance. During the phase from stem extension to anthesis, the model calculates the assimilate source and sink potential, allowing for dynamic changes to the source sink balance by partitioning assimilates between ear development and storage of water soluble carbon (WSC) reserves, according to assimilate availability. To quantify tolerance, rates of epidemic progress were varied on each phenotype, leading to different levels of HAD loss during the post-anthesis, grain filling period. Model outputs show that the main determinant of tolerance is the total amount of assimilate produced per grain during the rapid grain fill period, leading to a strong positive correlation between HAD per grain and tolerance. Reductions in traits that affect carbon assimilation rate, and increases in traits that determine the amount of structural biomass in the plant, increase disease tolerance through their associated reduction in number of grains per ear. Some of the most influential traits are the canopy green area index, carbon use efficiency and leaf specific weight. Increased WSC accumulation can either increase or decrease tolerance. Furthermore, a cultivar is shown to

be maximally tolerant when a crop is able to just fill its total sink size in the presence of disease. The model has identified influential functional traits and established that their associations with tolerance have a mechanistic basis.

Keywords: Septoria tritici blotch; *Zymoseptoria tritici*; source:sink balance; stem reserves; tolerance; *Triticum aestivum* L.; wheat; yield

INTRODUCTION

Minimising losses from disease requires the development of integrated and sustainable approaches to disease management that couple techniques to maximise plant defence (disease tolerance and resistance) with appropriate methods of chemical and cultural control. Cultivars that are tolerant to disease have higher yields than intolerant cultivars at the same disease severity (Parker et al. 2004). There is a clear relationship between measures of disease severity such as the area under the disease progress curve (AUDPC) and yield, whereby shallow slopes represent little yield loss per unit disease increase, and hence a high disease tolerance. However, the use of AUDPC to measure tolerance has the clear disadvantage that, especially near the end of the growing season, it is difficult to distinguish between diseased and senesced leaf tissues. AUDPC is also related to the healthy (green) area duration (HAD) of a crop and HAD is in turn related to yield. A measure of tolerance based on HAD which has proven useful in experimental studies for foliar wheat diseases, such as *Zymoseptoria tritici*, is yield loss per unit loss in HAD of the crop canopy over the grain-filling period (Foulkes et al. 2006; Parker et al. 2004). HAD is hereby quantified as the healthy area index of the crop canopy, integrated over time, as defined by Waggoner and Berger (1987). Yield loss per unit HAD loss is smaller for more tolerant cultivars. This metric of tolerance can be expressed as the slope of the straight line of yield (t ha^{-1}) on HAD when there is a range of disease severities leading to a range of HAD values (Fig. 1). Cultivars with smaller slopes are classed as more tolerant. Waggoner and Berger (1987) described why disease-induced HAD loss can be more predictive of yield loss than the more usual use of integrals of symptom area, such as area under the disease progress curve (AUDPC). The latter are generally based on relative measures of disease severity (i.e. percentages or fractions of leaf surface occupied by lesions) which, unlike HAD, do not take

into account the amount of green canopy area that remains. Parker et al. (2004) showed that for *Z. tritici* tolerance was indeed better quantified based on HAD loss than AUDPC.

Any single metric used to quantify tolerance (Bingham et al. 2009) will, however, inevitably be a simple summary of complex underlying processes and relationships. In this case, yield loss per unit HAD is the result of the complex, and often, non-linear, interactions by which crop-development and canopy characteristics affect the crop's response to disease-induced changes in light capture, assimilate production and allocation and grain filling. Our model considers these complex mechanistic interactions to study how phenotypic traits and the dynamics of underlying variables affect the relationship of yield loss per unit HAD loss, as measured in the field.

> *Note:* We distinguish here between tolerance and partial resistance, whereas the former is often used loosely in the literature as a synonym for the latter. The difference can be illustrated from figure 1. Tolerance is expressed as a smaller slope of the yield-HAD loss relationship, resulting in a reduced yield loss for any given disease-induced HAD loss. Resistance is expressed through a reduction in disease severity, resulting in a smaller disease-induced loss of HAD. For any given size and duration of crop canopy (and hence HAD) in the absence of disease, a more resistant cultivar will be further to the right along the x-axis compared to a more susceptible cultivar.

Progress with breeding cultivars for tolerance is hindered by lack of understanding about the traits and physiological processes that determine tolerance. Tolerance is believed to be associated with a high HAD per unit grain number, suggesting that plants for which source capacity is in excess of sink capacity, are more tolerant of disease (see e.g. Bingham et al. 2009). Source and sink capacities are, however, inter-related and are each determined by a

number of physiological traits (for example, Sinclair and Jamieson (2006)). Insight into the effect of physiological traits on source and sink dynamics, and how these feed through to tolerance, is thus needed to guide breeding.

The methods used to determine tolerance in the field are labour intensive, which may explain why few experimental studies (Foulkes et al. 2006; Parker et al. 2004) have been published comparing tolerance values across a range of cultivars or near isogenic lines. Reliable guidance to plant breeders depends on being able to identify correlations between crop traits and tolerance that are a result of true mechanistic links. In field experiments some correlations might arise by chance or because of correlations between traits (due to genetic linkage or concurrent selection in breeding programs). Such spurious correlations can be confirmed or refuted in mathematical models since they allow traits to be varied independently. Although HAD per grain was strongly correlated with tolerance in the experiments of Foulkes et al. (2006) it is not clear which underlying physiological traits drive this correlation. A mechanistic rationale is needed to add confidence that the relationship is causal. Furthermore, as HAD per grain is a compound variable (HAD combines green canopy size and duration) it is important to establish which crop characteristics and physiological processes are most influential. The study presented here therefore uses a mathematical model to identify and understand which traits determine the level of disease tolerance observed in wheat (*Triticum aestivum* L.).

Madden and Nutter (1995) discuss a wide range of models describing the relationship between yield and different injury mechanisms, including models that provide a detailed description of the spatial and temporal dynamics of the disease. However, most of these models use a rather simple description of the development and growth of the ear and its grain. Others do not keep track of the accumulation of reserves of water soluble carbohydrate (WSC) in the stem, despite the fact that these dynamics strongly influence the source-sink

balance, which is believed to be a major effector of tolerance (Sinclair and Jamieson 2006). The same is true for the crop growth models that have been developed to support plant breeding (Beasse et al. 2000; Bingham and Topp 2009; Carretero et al. 2010). In this paper we describe a new model that encompasses the physiological processes deemed important for disease tolerance, without making the model overly complex and hard to parameterise.

The work addresses the following questions with respect to septoria tritici blotch, the major foliar disease of wheat in cool temperate cropping systems:

- What physiological and developmental crop traits determine tolerance?
- What trait combination makes a cultivar maximally tolerant?
- Do the correlations between traits and tolerance reported in the experimental literature have a mechanistic rationale or are they likely to be spurious correlations?

MATERIALS AND METHODS

Model development. This section describes the biological processes in the model. For the model equations, parameter derivation and trait value ranges refer to the **Supporting Information 1** (**SI1**). A graphical representation of the model is given in Fig. 2, whereas Table 1 highlights which plant traits are considered to be subject to targeted breeding and will therefore be varied within the model simulations.

Assumptions: The model tracks plant development and growth, and disease progress, across a crop growing season. The Decimal Code system for wheat growth stages using the prefix GS is described in Zadoks et al. (1974). Model calculations start at the onset of stem extension (GS31) as yield components affected by septoria tritici blotch are those which are determined after the start of stem extension.

Many tillers are aborted between GS31 and GS61 (Sylvester-Bradley et al. 2008). More recently developed tillers, i.e. those with the highest probability of being aborted after GS31,

tend to be small and located at the bottom of the canopy. These tillers are unlikely to interfere significantly with light interception of the leaf tissues of the main shoot. Furthermore, ear numbers per m^2 is a yield component seldom affected by septoria tritici blotch in northern Europe (Robert et al. 2014). Tiller abortion is therefore not explicitly modelled. In a well established crop, grown at typical (commercial) plant population densities, the number of ears produced per plant tends to be small (main shoot ear plus two primary tiller ears) and the synchrony in flowering between main shoot and first and second tillers tends to be high. All tillers are therefore modelled as being at the same growth stage, whereby the shoot density is represented by the number of fertile ears m^{-2}.

The dynamics and quantification of assimilate accumulation are accounted for on the basis of an individual shoot. However, to enable the model to represent a crop as a population of shoots at a field scale, light interception by an individual shoot is based on the leaf area index of the crop (i.e. per unit ground area) – inter-shoot competition for light is therefore accounted for.

Crop development. The model tracks the green area index (GAI) of individual leaf layers (lamina and sheath), representing leaf growth and natural senescence. Leaf growth is described by a monomolecular growth function (Thornley and Johnson 1990). Each leaf has a specific leaf longevity related to its size after which leaf senescence commences **SI2**.

Zymoseptoria tritici is a hemi-biotrophic foliar pathogen infecting wheat leaves and causing septoria tritici blotch. The effect of *Z. tritici* lesions is to reduce the green leaf area, thus reducing the photosynthetic capacity of the crop canopy (Paveley et al. 2012). Necrotic lesions intercept solar radiation, but are not photosynthetically active (Robert et al. 2006).The epidemic progress on each leaf layer is modelled according to a logistic equation, which provides an accurate presentation of the progress of septoria tritici blotch under a range of

conditions (Paveley et al. 2000). It is assumed that diseased and senesced tissues (i.e. infectious and post-infectious) no longer contribute to photosynthesis (Robert et al. 2006).

Biomass accumulation through photosynthesis. The mean irradiance for a specific leaf layer is calculated using the Lambert-Beer relationship describing light interception (Thornley and Johnson 1990), whereby the light extinction coefficient represents both light transmission through the leaves and leaf angle. The average daily rate of gross photosynthesis is then calculated using the standard non-rectangular hyperbola (Johnson and Thornley 1984) and converted to total CO_2 fixed per shoot per day. Subtracting the carbon that is lost to maintenance and growth respiration gives the daily net CO_2 fixation. Net CO_2 fixed is then converted to total C fixed per shoot per day and finally to dry matter accumulated per shoot per day ('a' in Fig. 2).

Pre-anthesis biomass partitioning. The total dry matter biomass accumulated per shoot from GS31 to anthesis (GS61) is firstly partitioned to plant leaves, structural stem and roots according to organ sizes and specific weights ('b' in Fig. 2). It is assumed that total biomass accumulation is always sufficient to meet these demands, otherwise plants are not viable. Subsequently, the remainder of the biomass accumulated pre-anthesis is partitioned to either ear growth or stem reserves. Few experimental data exist on what drives this partitioning and how the assimilates are split between ear growth and building up stem reserves. This part of the model is hence necessarily of a descriptive nature rather than mechanistic. There is, however, evidence that ear/grain growth may be maintained over that of stem & leaf structural growth when conditions are limiting. For example, the harvest index of cereals (barley) is increased by nitrogen deficiency as ear and grain growth is maintained relatively more than stem and leaf growth (Bingham et al. 2012). Furthermore, early post-anthesis shading of barley reduces stem WSC concentrations but not soluble sugar concentration in developing grain (unpublished data by Kennedy). Hence, we assume that the fraction that is

partitioned to the ear is a function of the total biomass accumulated pre-anthesis such that when there is little biomass to invest a proportionally larger fraction is allocated to the ear, whereas when there is a lot of biomass to invest a proportionally larger fraction is allocated to the stem reserves ('c' in Fig. 2). All remaining biomass is partitioned to the stem as water soluble carbohydrate (WSC) for storage. If the total amount of WSC partitioned to the stem reserves exceeds the stem storage capacity the excess is lost due to assimilate degradation or a temporary feedback inhibition of photosynthesis. Additionally, it is assumed that increased stem heights lead to a relatively higher assimilate pull from the stem since Clarke et al. (2012) showed that partitioning to the ear decreases non-linearly with an increased stem height.

Number of grains per ear. If a floret does not accumulate sufficient biomass it will not reach the development stage (anther initials in full development) required for successful fertilisation, leading to the abortion of the floret (Bancal 2008; Gonzalez et al. 2011). These processes are summarised by modelling a direct relationship between pre-anthesis biomass allocated to the ear and number of grains per ear ('d' in Fig. 2).

Post-anthesis biomass partitioning. The leaves and ear are now fully developed and all further biomass accumulated is partitioned to structural stem biomass, the stem reserves and grain expansion/filling. The post-anthesis period is split into two distinct periods: the slow fill and rapid grain fill periods (Bingham et al. 2007b; Xie et al. 2015).

The *slow fill period* takes on average 2 to 3 weeks. There is a continued allocation of assimilates to the stem reserves during this period (Sylvester-Bradley et al. 2008; Schnyder 1993). This continued allocation to the stem reserves is associated with some further stem growth (Sylvester-Bradley 1998a). A fraction of the biomass accumulated during the slow fill period, and not invested in stem growth, is partitioned to the grain for endosperm formation whereas the rest is partitioned to the stem reserves. As during the pre-anthesis

period it is assumed that when there is little biomass to invest a larger fraction is allocated to the grain ('e' in Fig. 2) and when the stem storage capacity is exceeded 'excess' assimilates are lost due to assimilate degradation or feedback inhibition of photosynthesis.

Assimilate supply during the slow fill period determines the number of cell divisions that take place within the grain endosperm (Singh and Jenner 1984). The resultant number of cells in turn determines the capability of the grain to store water that can be replaced by dry matter during the rapid fill period (Hasan et al. 2011). These dynamics are summarised by a curvilinear relationship between the dry matter allocation to an individual grain during the slow fill period and the maximum potential grain DM content of the grain ('f' in Fig. 2).

The final realised grain dry weight per ear at harvest is determined during the *rapid fill period*. Any biomass accumulated during this period as a result of further light interception is directly invested in grain filling. At the same time the stem reserves are remobilised to the grains. Grain filling is, however, limited by the potential grain dry matter (DM) content determined during the slow fill period and the number of fertile grains set at anthesis. The resultant grain yield is expressed as tonnes per hectare at 85% dry matter.

Regression analysis to estimate tolerance. For each disease pressure simulated, HAD (in m^2 green leaf area per m^2 ground area times duration in days) is calculated over the duration of the grain-fill period across the top four leaves. Rates of epidemic progress are varied such that disease-induced HAD losses ranged between 5 and 50% under default conditions. The chosen HAD loss range is based on the observations that disease severities > 50% are rare and epidemics are unlikely to impact materially on yield for severities < 5%. Our measure for tolerance expressed as t ha^{-1} per HAD is then calculated as the slope of the yield-HAD relation (Figure 1), whereby small slopes denote more tolerant crops. We then analyse how changes in parameters representing underlying source and sink traits affect the slope of this relationship.

By the definition used here, a crop is more tolerant when disease presence results in a smaller yield loss per unit HAD lost to disease. Yield is the product of the crop's total sink size and the percentage of the total sink the crop is able to fill during the grain-fill period. This can be summarised by

$$\frac{1}{\text{Tolerance}} \propto \frac{\Delta\text{yield}}{\Delta\text{HAD}} = \frac{\Delta(\text{Total sink size} * \frac{\%\text{ sink filled}}{100})}{\Delta\text{HAD}} \qquad (1)$$

where Δ indicates the difference between a healthy and diseased crop. The equation shows that it is the balance between ΔTotal sink size, Δ% sink filled and ΔHAD that determines the level of tolerance. A central question is whether one of these three factors is the key variable in explaining tolerance or whether they are all similarly important. Insight at that level can guide us to characterise the crop physiological processes that are most influential to tolerance.

The percentage of the sink that can be filled depends on the total amount of assimilate available for grain filling and the total sink size (number of grains per ear multiplied by the potential maximum grain volume), i.e.

$$\%\text{ sink filled} \propto \frac{\text{HAD during grain fill+WSC reserves}}{\#\text{ grains per ear} * \text{potential maximum grain volume}} * 100. \qquad (2)$$

The measure of % sink filled is a good indicator for the source:sink balance, whereby 100% sink filled indicates a fully sink limited crop (i.e. yield is limited by sink capacity). The effect of a particular trait on tolerance is therefore determined by its *relative* effects on source and sink.

Model calibration and validation. The model was calibrated according to data obtained from the HGCA wheat growth guide (Sylvester-Bradley et al. 2008) and its underlying reports (Spink et al. 2000a; Spink et al. 2004; Spink et al. 2000b; Sylvester-Bradley 1998a; Sylvester-Bradley 1998b; Sylvester-Bradley 1998c). These data give the most comprehensive set of parameter estimates, based on many field experiments, for a single cultivar (Mercia) within the published literature (**SI1**). Mercia is thus our benchmark

cultivar. A literature search was performed to determine the current genotypic variability of plant traits (Table 1 and **SI1**), representing the variability in these traits across different cultivars.

Some trait change correlations. Increases in maximum canopy GAI are simulated by increasing all leaf sizes by the same percentage. When the leaf area distribution is changed, the total canopy GAI is kept constant by reducing the total area of leaves 2 to 5 by the same amount that the flag leaf is increased.

Two sets of traits were treated as being closely related, as they are unlikely to be varied independently in practice. Changes to growth periods are assumed to be directly related to changes in canopy dynamics, whereby an increased pre-anthesis period is assumed to be associated with an equal percentage increase in phyllochron length. An increased slow-fill or rapid-fill period goes paired with an increase in leaf longevity of the top five leaves by an equal number of days.

Model validation. We validated the model using three distinct approaches. Firstly, we tested the model's power to predict yield and yield components by comparing model predictions with published data from five independent field experiments. This validation is reported in the **SI3** as it does not directly relate to tolerance but presents evidence for the validity of our model. Secondly, as a quantitative validation with respect to tolerance the range of published tolerance values was compared with the range of tolerance values predicted by the model. Thirdly, a qualitative validation is performed by comparing published and model derived trends between plant traits and tolerance. None of the papers and data sets used within this validation exercise were used for model calibration.

Testing diverse parameter sets. We used the cultivar Mercia as the default parameter set (Table 1), and studied the effect of changes in parameters relative to this default set. The question then is whether our conclusions would also hold for other parameter value

sets. To test this we simulated parameter sets by randomly selecting values from the ranges determined (Table 1). For each of these parameter sets we first determined the yield of the crop. Since the aim was to identify trait combinations that will lead to improved disease tolerance, but at the same time maintain acceptable yields, we only determine tolerance as described above for those parameter sets that lead to crop yields greater than or equal to Mercia (9 t/ha in the field crops reported by Sylvester-Bradley (1998c)).

RESULTS

What physiological crop traits determine tolerance? The yield of a more tolerant plant is less strongly affected by disease presence than an intolerant plant. We therefore studied how trait changes affect certain source and sink components in the presence of the disease as compared to in the absence of disease (see individual lines in for example Figure 3). Trait changes leading to increased tolerance might then be identified by a smaller effect of disease on the source and/or sink components (the lines for disease absence and presence lie closer together, with the difference denoted by Δ). Equation (1) shows that the level of tolerance experienced by a plant is determined by the balance between $\Delta\text{Total sink size}$, $\Delta\%\text{ sink filled}$ and ΔHAD. In this section we look at whether one of these three factors is the key variable in explaining tolerance.

Let's first consider the cases where a trait change has no effect on HAD and where additionally $\Delta\%\text{ sink filled} \neq 0$ (e.g. Fig. 3C for carbon use efficiency > 0.64). For these cases the results show that tolerance generally increases when $\Delta\%\text{ sink filled}$ decreases and vice versa (Fig. 3A, 4A). There are few exceptions to this finding: these being for a small part of the trait range for the maximum number of grains per ear and maximum potential grain volume; Fig. 4A. For trait changes that have an opposing effect on $\Delta\text{Total sink size}$

and Δ% sink filled it is found that in most cases Δ% sink filled determines the overall effect on tolerance (Fig. 3B, 5B; **SI4** (panel B in all figures)). When trait changes also affect ΔHAD, such as for GAI in Fig. 5 (and traits with closed symbols in Fig. 4A), the negative relation between Δ% sink filled and tolerance is maintained for most traits (Fig. 4A), although the effect is less pronounced than in cases where the trait change does not affect Δ HAD (open symbols in Fig. 4A). Only two traits, the durations of the pre-anthesis period and the rapid grain fill period, show slightly different behaviour.

Now, consider the case where the yield is fully sink limited., i.e. the plant is able to completely fill its available sink irrespective of whether disease is present or not). In the figures these cases are denoted by trait value ranges for which the % sink filled is the same in the presence and absence of disease ($\Delta\%\ \text{sink filled} = 0\ \&\ \frac{\%\ \text{sink filled}}{100} = 1$ in eqn. (1); Fig. 3C CUE < 0.64). In these extreme cases we still detect an effect on tolerance despite Δ% sink filled not being affected and hence in these cases ΔTotal sink size and ΔHAD control whether tolerance increases or decreases with a change in parameter (trait) value (Fig. 3, **SI4** panels B-D).

For all trait ranges investigated the change in total sink size is driven predominantly by the number of grains per ear (Fig. 4D; **SI4**). In combination with the finding that there is a direct correlation between Δ% sink filled and tolerance, equation 2 shows that tolerance is therefore closely related to the total assimilate available per grain. The total assimilate available per grain is determined by both HAD and the WSC reserves. Although the results reveal a significant correlation between tolerance and HAD per grain (Fig. 4F), no clear trend between WSC reserves and tolerance can be identified (Fig. 4E).

For the traits CUE (Fig. 3), stem height at anthesis, stem diameter and leaf specific weight the tolerance curve has a clear maximum (see also figures in **SI4**), which coincides with the

trait value where Δ % sink filled goes from being larger than zero to zero. A pre-requisite for maximal tolerance is thus that the source is just large enough to fill the sink in both the absence and presence of disease. Note, however, that the plots have been created by simulating a single disease severity and that the exact location of the optimum depends on the disease severity encountered.

Results comparison against experimental data. This section presents results for correlations between specific pairs of traits which have previously been reported as being associated in experimental data. The discussion cites the relevant literature and describes the extent to which the modelling results agree with, or differ from, the experimental evidence.

The model predicts that: (i) an increase in the maximum number of grains per ear is negatively correlated to tolerance (Fig. 6A), (ii) flag leaf area relative to total leaf area (referred to as leaf distribution) and tolerance are positively correlated (Fig. 6B), (iii) reduced stem height leads to a strong reduction in tolerance (Fig. 6C), (iv) the maximum photosynthetic capacity ($P_{\max}^{0}$) is weakly negatively correlated with tolerance (Fig. 6D), (v) the maximum canopy GAI is positively correlated with tolerance (Fig. 6E) (vi) the light extinction coefficient is positively correlated with tolerance (Fig. 6F), and (vii) increased grain-fill periods, which lead to increased HADs, lead to increased tolerance (Fig. 6G), whilst the length of the pre-anthesis period has a more or less neutral effect on tolerance (Fig. 3H).

Results from diverse parameter sets. Figure 7 shows the correlation between HAD per grain and tolerance for a wide range of parameter sets representing different cultivars. Despite there being considerable scatter around the regression line, the linear regression reveals a highly significant regression slope ($p<0.00001$) with an overall R^2 of 0.48.

DISCUSSION

The model analysis provides insights into the physiological traits that determine tolerance and helps to understand previous correlations of traits with tolerance reported in the literature. Relationships between 'high level' factors (sink size, % sink filled and HAD) and tolerance are discussed first, then we consider whether the analysis supports or refutes relationships between specific traits and tolerance reported previously in the literature.

What physiological crop traits determine tolerance? There has been no previous consideration in the literature of whether there might be consistent patterns of association between high level factors and tolerance. Such patterns have been found here, but there is little literature against which to compare the new findings summarised below. When a trait change has no effect on HAD (and $\Delta\%\ \text{sink filled} \neq 0$) the $\Delta\%$ sink filled tends to be the main determinant of tolerance. The effect of *Z. tritici* on light interception and assimilation occurs predominantly post-anthesis (due to its long latent period relative to the rate of leaf emergence) at which point the number of grains per ear, i.e. the main determinant of the total sink size, has already been set. Hence, it is understandable that $\Delta\%$ sink filled rather than ΔTotal sink size is the main determinant of tolerance.

When trait changes also affect ΔHAD, $\Delta\%$ sink filled still tends to be the main determinant of tolerance. Equation 1, shows that if tolerance doesn't change much with changes in $\Delta\%$ sink filled, then either Δ total sink size has changed too or ΔHAD has changed (or both). As shown in **SI4.16**, increasing the pre-anthesis duration reduces % of sink filled in diseased but not non-diseased crops; reduces HAD in diseased but increases it in non-diseased and increases total sink in both. Thus, both $\Delta\%$ sink filled and ΔHAD are increased. The question is then why should an increase in the duration of the pre-anthesis period reduce HAD with disease but increase it without disease? A longer pre-anthesis period was assumed to be associated with an increased phyllochron length, which results in an increased HAD in the absence of disease. With the onset of the epidemic remaining constant this then means that

the disease has longer to develop, leading to an increased post-anthesis severity. This in turn leads to a reduced HAD in the presence of disease and therefore an increase in ΔHAD. Similar, but less strong, effects can be identified for the rapid grain-fill period, due to the underlying assumption that an increased rapid-fill period is associated with increased leaf longevities for L1 to L5 (see figure **SI4.18**).

When yield is fully sink limited, we find that ΔTotal sink size and ΔHAD control whether tolerance increases or decreases. This is counter-intuitive because if the sink is filled irrespective of whether disease is present or not one might expect the plant to be completely tolerant of disease. However, the definition of tolerance includes absolute (rather than %) yield per unit HAD and for those trait changes resulting in continually increasing sink limitation, ΔTotal sink size increases, leading to a decrease in tolerance.

Given that the main determinant of tolerance is the Δ% sink filled, equation 2 can now help understand the effect of individual trait changes on tolerance. Changes in total sink size were shown to be predominantly affected by the number of grains per ear rather than the potential maximum grain size, which means that tolerance is closely related to the total assimilate available per grain. Assimilate for grain filling comes from remobilised WSC reserves and assimilate produced by leaf photosynthesis during the rapid-fill period. The contribution of WSC reserves in the simulations ranged from 26 to 66 % of the total available assimilate. Hence, grain-filling relies heavily on assimilation by green leaf and sheath tissues during the rapid-fill period. This results in a close correlation between HAD per grain and tolerance. Despite its large contribution to yield, there is no consistent positive correlation between % yield from WSC reserves and tolerance that holds across a range of different traits/values (see later in discussion).

In the majority of cases (15 of the 21 traits studied), trait changes do not affect HAD and, given the discussion above, in these cases an increased number of grains per ear decreases

tolerance because it decreases HAD per grain. The number of grains per ear is determined by the amount of assimilate accumulated pre-anthesis and it is therefore straightforward to predict whether a change in trait value will affect the number of grains per ear and in what manner. For example, traits affecting assimilation rate (light extinction coefficient, $P_{\max}^{0}$ and carbon use efficiency (CUE)) are positively associated with pre-anthesis assimilate accumulation, leading to a larger number of grains per ear and reduced tolerance. Traits that determine the amount of structural biomass in the plant (stem height, stem diameter, fractional stem thickness, leaf specific weight, stem specific weight and root mass) are all negatively associated with the amount of assimilate available for ear development, leading to a reduction in number of grains per ear and increased tolerance. Surprisingly, traits regulating stem storage dynamics (stem storage efficiency and stem reserves remobilisation rate) did not affect the amount of assimilate available for ear development and thus had no effect on tolerance (See **SI4** for the associated figures). We conclude that in most cases the number of grains per ear is an indicator of tolerance, making it possible to predict the effect of trait changes on tolerance.

This leaves the cases for which a trait change does affect HAD, i.e. the developmental period and canopy size traits (maximum canopy size, leaf area distribution, shoot density, pre-anthesis period, slow-fill period and rapid-fill period). In all but one of these cases increased HAD coincides with increased HAD per grain and thus increased tolerance (See **SI4** for associated figures), because variation in these traits resulted in a stronger effect on HAD than on the number of grains per ear. The only exception is the duration of the pre-anthesis period, which has, as would be expected, a stronger effect on the number of grains per ear than on HAD post-anthesis.

Results comparison against experimental data. The analysis was designed to check whether associations between traits and tolerance reported from field experiments could be

explained mechanistically. Associations which cannot be readily explained are more likely to be spurious correlations. When varying the plant traits within the range of current genotypic variability, the model estimated a maximally achievable tolerance value (0.0171) close to the maximum reported in the literature (0.0141). Note that the values represent the slope of the HAD versus yield relationship and that smaller values therefore represent increased tolerance. The minimum tolerance values estimated by the model lie around 0.04, which compares well with the minimum of 0.036 reported within experimental studies (Foulkes et al. (2006) and Parker et al. (2004)). When varying CUE we however found tolerance values up to 0.063 (indicating extremely poor tolerance), but trait changes leading to extremely low tolerance also went paired with extremely low disease-free yield. Such wheat lines would not be selected as elite cultivars or be included in field experiments where the aim is to increase tolerance whilst maintaining high yield.

The effects of changes in traits on tolerance is largely in agreement with the trends derived experimentally or suggested within the literature. Most strikingly, Foulkes et al. (2006) found a significant negative correlation between grains m^{-2} and tolerance. This finding is in close agreement with our conclusion that in the absence of an effect on HAD the key determinant of tolerance is the number of grains ear^{-1}.

The model results suggest that traits that increase the plant's assimilation rate will result in a reduction in tolerance. Parker et al. (2004) compared the disease tolerance levels of plants with and without the 1BL/1RS translocation and found a negative correlation between the presence of the translocation and tolerance. This translocation has been associated with a possible increase in radiation use efficiency (RUE) (Foulkes et al., 2007) and thus an increased assimilation rate. This matches our prediction that tolerance is negatively associated with the plant's assimilation rate.

Bingham et al. (2009) infer that larger extinction coefficients should lead to increased tolerance through greater interception of solar radiation per unit green area by leaves in the upper canopy. This is in disagreement with our finding, although across the UK genotypic variability in light extinction coefficient, the effect on tolerance was estimated to be negligible.

The only experimental study to assess the effect on tolerance of traits that determine the amount of structural biomass is the field study by Foulkes et al. (2006). They found that the presence of Rht-D1b alleles (associated with semi-dwarfing) did not have a significant effect on tolerance. Their initial reasoning was that this is due to the Rht allele not affecting WSC reserves, but later argued that WSC might not affect tolerance anyway. This case presents the main discrepancy between model and data, as our analysis suggest that trait changes that increase the amount of structural biomass are positively correlated with tolerance. However, dwarfing genes have a number of pleiotropic effects such as increased ear fertility (Flintham et al. 1997), increased light extinction coefficients (Miralles and Slafer 2007) and shorter leaves (Calderini et al. 1996) with potentially opposing effects on tolerance. It may be that these pleiotropic effects cause the previously reported absence of changes in tolerance with dwarfing.

Previous work has suggested that increased WSC accumulation will increase disease tolerance, irrespective of the overall storage capacity (Bingham et al. 2009; Blum 1998; Ehdaie et al. 2006). The only study directly testing this hypothesis found that WSC reserves were negatively correlated with tolerance (Foulkes et al. 2006). The analysis reported here found that changes to plant traits that increase WSC reserves stored per shoot can either increase or decrease tolerance. There are two possible ways in which WSC reserves are related to tolerance. The first is in the case of trait changes where there is a direct trade-off between WSC reserves and number of grains per ear. The only trait for which this is the case

is the fraction ear versus stem reserves investment. Yet, even in this case it is HAD per grain that determines tolerance. The second is in the case of trait changes that lead to stem storage limitation during the slow-fill period. The only trait for which this is the case is the shoot density (**SI4** Fig. S13). Increased shoot densities lead to both an increased HAD and a decreased number of grains per ear and hence an increased HAD per grain, suggesting that tolerance will increase with increased shoot densities. However, an increased shoot density will also lead to an increased number of grains per m^2, suggesting that overall HAD per grain might not increase much with an increased shoot density, which is supported by the weak positive effect of shoot density on tolerance (with shoot density changes modelled by changes in ears m^{-2}). In this case it is WSC that determines Δ % sink filled and hence tolerance (**SI4** Fig. S6).

Finally, our results reveal that trait changes that increase HAD (with the exception of an increased pre-anthesis period) coincide with an increased HAD per grain and increased tolerance. The literature supports this finding. For example, Foulkes et al. (2006) found a positive correlation between flag leaf area and tolerance. Additionally, Bingham et al. (2009) infer that crops with large canopies might be more tolerant to disease through an increased ability to maintain radiation interception per unit green area loss to disease. Similarly, for doubled-haploid progeny from a cross between UK cultivars Cadenza and Lynx, tolerance was found to be associated with high post-anthesis HADs (Paveley 2008).

The model study has helped understand the processes involved in tolerance and has either supported, explained further or dispelled previously reported associations between certain traits and tolerance. Some findings remain unclear, with the main discrepancy between experimental data and model predictions regarding the effect of Rht-D1b alleles, as a proxy for changes in stem height, on tolerance.

Results from diverse parameter sets. The results presented in Figures 2-6 are all based on variations of single parameter values away from the benchmark Mercia parameter set. Our main conclusion based on these results is that HAD per grain is a good predictor of tolerance. The main question now is whether this conclusion is only valid for cultivars with parameter values very similar to Mercia or whether our conclusion would also hold for a wider range of cultivars. Running the results for a large range of diverse parameter sets (representing a range of different cultivars and potential within cultivar variability) has shown that despite there being quite some scatter around the tolerance and HAD per grain regression line, the relationship is highly significant, which generalises our main finding beyond Mercia.

Model assumptions and their potential implications. Tolerance is the result of the complex and nonlinear interactions of light capture, assimilate production and allocation, leaf and stem growth, ear development and grain filling. Currently there is no model available that dynamically simulates the dynamics of the determination of ear size, the determination of grain number and potential grain size as a function of assimilate availability, and then accurately models the final grain filling. We have therefore developed a model that incorporates all these processes. This implies that the model is complex, but even in a complex model some simplifying assumptions are made. Here we discuss the possible consequences of our assumptions.

Because of the limited data describing what drives the partitioning of assimilates between ear growth and accumulating stem reserves, this part of the model was necessarily descriptive rather than mechanistic. It was assumed that the fraction of available assimilate that is partitioned to the ear is a function of the total biomass accumulated pre-anthesis such that when there is little biomass to invest, a proportionally larger fraction is allocated to the ear, whereas when there is a lot of biomass to invest a proportionally larger fraction is allocated to

the stem reserves. When this dynamic partitioning fraction was replaced by a constant fraction, the results remained qualitatively unchanged (results not shown).

We have assumed the environment to be constant. This is because one of the aims was to provide guidance to breeders on physiological traits affecting tolerance. Disentangling the interacting effects of individual traits on source and sink capacities and tolerance is complex even under a constant environment (E); thus in this study we consider the genetic (G) effects only and for now not the GxE interactions. However, the model has the capacity for investigating effects of environmental conditions (e.g. temperature and radiation) and the timing of disease epidemics on tolerance.

Foliar pathogens can modify the growth of plants through multiple injury mechanisms (Boote et al., 1983; Gaunt 1995). The effects of injury on yield depend on the timing of the disease epidemic in relation to the phenology of the crop and the extent to which plants can compensate for the injury through adjustments in physiology and morphology (Boote et al. 1983; Gaunt 1995; Bingham et al. 2009; Ney et al. 2012). Late epidemics provide fewer opportunities for morphological adjustments to take place (Gaunt 1995; Bingham et al. 2009). In wheat, the maximum leaf number and size is set by flag emergence and, with the exception of occasional late tillering, the number of ears and grains is determined by anthesis.

In this study we have parameterised the model using data on *Z. tritici*. We have assumed that the contribution to tolerance of compensatory physiological and morphological adjustments (Bingham et al. 2009; Ney et al. 2013) in this pathosystem is small. In temperate climates, epidemics of septoria tritici blotch tend to develop late with disease reducing yield through effects on average grain weight and to a lesser extent grain number per ear rather than the number of ears (Forrer and Zadoks 1983; Robert et al. 2004). Epidemics are generally too late to induce differences in leaf size and number (Robert et al. 2004). Robert et al. (2006) reported that within *Z. tritici* infected leaves, reductions in net photosynthesis were

caused by the replacement of green tissue by necrotic lesions. In comparison with some other pathogens, reductions in net photosynthesis in asymptomatic tissue surrounding the visible lesions were small. Moreover, there is little evidence of compensatory adjustments in the photosynthetic rate or growth of non-infected leaves on wheat infected with *Z. tritici* (Bingham et al. 2009; Ney et al. 2013; but see Zuckerman et al. 1997). These observations are consistent with reports that septoria tritici blotch has little effect on the radiation use efficiency of field grown wheat (Serrago et al. 2009). Other foliar diseases share similar patterns of disease progress curves, because the timing of disease on each leaf layer is determined largely by leaf emergence (Paveley et al. 2000). The methods used should therefore be applicable to other foliar diseases of wheat. However, the model would need specific parametrisation to account for differences between pathogens on photosynthetic activity beyond visible disease lesions (Scholes and Rolfe 2009; Rolfe and Scholes 2010) and on potential compensatory adjustments in growth and photosynthetic activity (Ney et al. 2013).

Traits that confer tolerance in wheat might not do so in others crops. For example, barley is more sink limited than wheat (Bingham et al. 2007a, Bingham et al. 2007b), and early treatment of foliar disease often results in increases in sink components (shoots m^{-2} and grains ear^{-1}). Therefore, it would be inappropriate to extrapolate our results directly to other crop species. After suitable parameterisation the model can be used to simulate and investigate source-sink relations and their influence on disease tolerance in other cereal crops. As such, it promises to be a valuable tool for guiding the improvement of tolerance in a range of species.

SUPPLEMENTARY INFORMATION

The Supplementary Information contains a full model description including model equations, a parameter derivation, an overview of the current genotypic variability in plant traits, results for additional model testing and results for the effect of individual trait changes on tolerance trends.

ACKNOWLEDGEMENTS

Funding through the UK Department for Environment, Food and Rural Affairs (Defra) is gratefully acknowledged. Rothamsted Research receives support from the Biotechnology and Biological Sciences Research Council (BBSRC) of the United Kingdom. SRUC receives financial support from the Scottish Government's Rural and Environmental Science and Analytic Services (RESAS) division.

LITERATURE CITED

Bancal, P. 2008. Positive contribution of stem growth to grain number per spike in wheat. Field Crops Res. 105:27-39.

Beasse, C., Ney, B., and Tivoli, B. 2000. A simple model of pea (*Pisum sativum*) growth affected by *Mycosphaerella pinodes*. Plant Pathol. 49:187-200.

Bingham, I. J., Blake, J., Foulkes, M. J., and Spink, J. 2007a. Is barley yield in the UK sink limited? I. Post-anthesis radiation interception, radiation-use efficiency and source-sink balance. Field Crops Res. 101:198-211.

Bingham, I. J., Blake, J., Foulkes, M. J., and Spink, J. 2007b. Is barley yield in the UK sink limited? II. Factors affecting potential grain size. Field Crops Res. 101:212-220.

Bingham, I. J., Karley, A. J., White, P. J., Thomas, W. T. B., and Russell, J. R. 2012. Analysis of improvements in nitrogen use efficiency associated with 75 years of spring barley breeding. Eur. J. Agron. 42:49-58.

Bingham, I. J., and Topp, C. F. E. 2009. Potential contribution of selected canopy traits to the tolerance of foliar disease by spring barley. Plant Pathol. 58:1010-1020.

Bingham, I. J., Walters, D. R., Foulkes, M. J., and Paveley, N. D. 2009. Crop traits and tolerance of wheat and barley to foliar disease. Ann. Appl. Biol. 154:159-173.

Blum, A. 1998. Improving wheat grain filling under stress by stem reserve mobilisation. Euphytica 100:77-83.

Boote, K.J., Jones, J.W., Mishoe, J.W., and Berger, R.D. 1983. Coupling pests to crop growth simulations to predict yield reductions. Phytopathology 73:1581-1587.

Bryson, R. J., Paveley, N. D., Clark, N. D., Sylvester-Bradley, R. and Scott, R. K. 1997. Use of in-field measurements of green leaf area and incident radiation to estimate the effects of yellow rust epidemics on the yield of winter wheat. Eur. J. Agron., 7: 53–62.Calderini, D. F., Miralles, D. J., and Sadras, V. O. 1996. Appearance and growth of individual leaves as affected by semidwarfism in isogenic lines of wheat. Ann. Bot. 77:583-589.

Calderini, D. F., Miralles, D. J., and Sadras, V. O. 1996. Appearance and growth of individual leaves as affected by semidwarfism in isogenic lines of wheat. Ann. Bot. 77:583-589.

Carretero, R., Serrago, R. A., Bancal, M.-O., Perello, A. E., and Miralles, D. J. 2010. Absorbed radiation and radiation use efficiency as affected by foliar diseases in relation to their vertical position into the canopy in wheat. Field Crops Res. 116:184-195.

Clarke, S., Sylvester-Bradley, R., Foulkes, J., Ginsburg, D., Gaju, O., Wemer, P. J., Flatman, E., and Smith-Reeve, L. 2012. Adapting wheat to global warming. Report No. 496. Pages 1-131. HGCA.

Ehdaie, B., Alloush, G. A., Madore, M. A., and Waines, J. G. 2006. Genotypic variation for stem reserves and mobilization in wheat: I. Postanthesis changes in internode dry matter. Crop Sci. 46:735-746.

Espinosa, E. G., and Fornoni, J. 2006. Host tolerance does not impose selection on natural enemies. New Phytol. 170:609-614.

Flintham, J. E., Börner, A., Worland, A. J., and Gale, M. D. 1997. Optimizing wheat grain yield: effects of *Rht* (gibberellin-insensitive) dwarfing genes. J. Agri. Sci. 128:11-25.

Forrer, H.R., and Zadoks, J.C., 1983. Yield reduction in relation to leaf necrosis caused by Septoria tritici. Neth J. Pl. Path. 89:87-98.

Foulkes, M. J., Paveley, N. D., Worland, A., Welham, S. J., Thomas, J., and Snape, J. W. 2006. Major genetic changes in wheat with potential to affect disease tolerance. Phytopathology 96:680-688.

Foulkes, J., Snape, J. W., Shearman, V. J., and Sylvester-Bradley, R. 2005. Physiological processes associated with winter wheat yield potential progress. in: 7th International

Wheat Conference, H. T. Buck, J. E. Nisi and N. Salomon, eds. Springer, Mar del Plata, Argentina.

Gaunt, R. E., 1995. The relationship between plant disease severity and yield. Ann. Rev. Phytopathology 33:119-144.

Gonzalez, F., Miralles, D. J., and Slafer, G. A. 2011. Wheat floret survival as related to pre-anthesis spike growth. J. Exp. Bot. 62:4889-4901.

Hasan, A. K., Herrera, J., Lizana, C., and Calderini, D. F. 2011. Carpel weight, grain length and stabilized grain water content are physiological drivers of grain weight determination of wheat. Field Crops Res. 123:241-247.

Johnson, I. R., and Thornley, J. H. M. 1984. A model of instantaneous and daily canopy photosynthesis. J. Theor. Biol. 107:531–545.

Madden, L. V. and Nutter Jr, F. W. 1995. Modeling crop losses at the field scale. Can. J. Plant Pathol., 17: 124-137.

Miralles, D. J., and Slafer, G. A. 2007. Sink limitations to yield in wheat: how could it be reduced? J. Agri. Sci. 145:139-149.

Ney, B., Bancal, M.-O., Bancal, P., Bingham, I. J., Foulkes, J., Gouache, D., and Smith, J. 2013. Crop architecture and crop tolerance to fungal diseases and insect herbivory. Mechanisms to limit crop losses. Eur. J. Plant Pathol. 135: 561-580.

Parker, S. R., Welham, S., Paveley, N. D., Foulkes, J., and Scott, R. K. 2004. Tolerance of septoria leaf blotch in winter wheat. Plant Pathol. 53:1-10.

Paveley, N., Blake, J., Gladders, P., and Cockerell, V. 2012. HGCA wheat disease management guide 2012. Pages 1-32. HGCA.

Paveley, N. D., Lockley, D., Vaughan, T. B., Thomas, J., and Schmidt, K. 2000. Predicting effective fungicide doses through observation of leaf emergence. Plant Pathol. 49:748-766.

Paveley, N. D., Smith, J. S., and Foulkes, J. 2008. Traits for reduced fungicide dependence. Pages 35-47 in: BSPP Presidential Meeting, G. Jellis and C. Edwards, eds., Queen Mary, University of London.

Robert, C., Bancal, M-O., Nicolas, P., Lannou C., Ney, B., 2004. Analysis and modelling of effects of leaf rust and *Septoria tritici* blotch on wheat growth. J. Exp. Bot. 55:1079-1094

Robert, C., Bancal, M-O, Lannou, C. and Ney, B. 2006. Quantification of the effects of *Septoria tritici* blotch on wheat leaf gas exchange with respect to lesion age, leaf number, and leaf nitrogen status. J Exp. Bot. 57: 225-234.

Rolfe, S. A., and Scholes, J. D. 2010. Chlorophyll fluorescence imaging of plant-pathogen interactions. Protoplasma 247:163-175.

Schnyder, H. 1993. The role of carbohydrate storage and redistribution in the source-sink relations of wheat and barley during grain filling - a review. New Phytol. 123:233-245.

Serrago, R.A., Carretero R., Bancal, M-O., and Miralles, D.J., 2009. Foliar diseases affect the eco-physiological attributes linked with yield and biomass in wheat (*Triticum aestivum* L.) Eur J. Agron 31:195-203.

Scholes, J. D., and Rolfe, S. A. 2009. Chlorophyll fluorescence imaging as tool for understanding the impact of fungal diseases on plant performance: a phenomics perspective. Func. Plant Biol. 36:880-892.

Sinclair, T. R., and Jamieson, P. D. 2006. Grain number, wheat yield, and bottling beer: an analysis. Field Crops Res. 98:60-67.

Singh, B. K., and Jenner, C. F. 1984. Factors controlling endosperm cell number and grain dry weight in wheat: effects of shading on intact plants and of variation in nutritional supply to detached, cultured ears. Austr. J. Plant Physiol. 11:151-163.

Spink, J., Foulkes, J. M., Gay, A., Bryson, R., Berry, P., Sylvester-Bradley, R., Semere, T., Clare, R. W., Scott, R. K., Kettlewell, P. S., and Russell, G. 2000a. Reducing winter wheat production costs through crop intellegence information on variety and sowing date, rotational position, and canopy management in relation to drought and disease control. Pages 1-135. Project Report 235, HGCA.

Spink, J. H., Berry, P., Theobald, C., Sparkes, D., Wade, A., and Roberts, A. 2004. The effect of location and management on target drilling rate for winter wheat. Pages 1-154. Project Report 361, HGCA.

Spink, J. H., Whaley, J., Semere, T., Wade, A., Sparkes, D., and Foulkes, J. 2000b. Prediction of optimum plant population in winter wheat. Pages 1-59. Project Report No. 234, HGCA.

Sylvester-Bradley, R. 1998a. Assessments of wheat growth to support its production and improvement. Volume I: The wheat growth digest. Pages 1-128. Project Report 151, HGCA.

Sylvester-Bradley, R. 1998b. Assessments of wheat growth to support its production and improvement. Volume II: How to run a reference crop. Pages 1-78. Project Report 151, HGCA.

Sylvester-Bradley, R. 1998c. Assessments of wheat growth to support its production and improvement. Volume III: The dataset. Pages 1-50. Project Report 151, HGCA.

Sylvester-Bradley, R., Berry, P., Blake, J., Kindred, D., Spink, J., Bingham, I. J., McVittie, J., and Foulkes, J. 2008. The wheat growth guide. Pages 1-32. HGCA.

Thornley, J. H. M., and Johnson, I. R. 1990. Plant and crop modelling: a mathematical approach to plant and crop physiology. Clarendon Press, Oxford.

Waggoner, P. E. and Berger, R. D. 1987. Defoliation, disease, and growth. Phytopathology, 77: 393-398.

Xie, Q., Mayes, S., and Sparkes, D. L. 2015. Carpel size, grain filling, and morphology determine individual grain weight in wheat. J. Exp. Bot. 66:6715-6730.

Zadoks, J. C., Chang, T. T., and Konzak, C. F. 1974. A decimal code for the growth stages of cereals. Weed Res. 14:415-421.

Zuckerman, E., Eshel, A., and Eyal, Z. 1997. Physiological aspects related to tolerance of spring wheat cultivars to septoria tritici blotch. Phytopathology 87:60-65.

TABLE 1. Description of the traits that could be subject to targeted breeding. All default model parameters are representative for the wheat cultivar Mercia. The current trait ranges describe the current genotypic variability for each trait based on genotype means as found in the literature.

Trait description	**Units**	**Mercia trait value**	**Current trait range**
Pre-anthesis period	days	59	51-65
Slow-fill period	days	16	5-21
Rapid-fill period	days	34	24-37
Shoot density	m^{-2}	578	294-578
Maximum canopy GAI	-	6.03	3.26-7.51
Carbon use efficiency	-	0.79	0.62-0.79
Light extinction coefficient	-	0.53	0.37-0.58
Maximum photosynthetic capacity	mol CO_2 m^{-2} leaf d^{-1}	1.83	1.28-2.07
Fraction ear versus stem reserves investment	-	0.48	0.37-0.49
Maximum number of grains per ear	-	59.30	57.37-97.44
Fraction grain versus stem reserves investment	-	0.55	0.50-0.59

Maximum potential grain DM content	G	0.048	0.040-0.056
Leaf specific weight	g m^{-2}	32	31.8-54.0
Root mass	g $shoot^{-1}$	0.17	0.11-0.17
Stem specific weight	g m^{-1}	1.36	1.08-1.62
Stem height at anthesis	M	0.64	0.64-1.10
Stem diameter	M	0.0033	0.0032-0.0041
Factional stem thickness	-	0.35	0.33-0.38
Stem storage efficiency	g m^{-3}	287075	220341-353087
Stem reserves remobilisation rate	day^{-1}	0.088	0.081-0.125
Leaf distribution (flag leaf area / area of top five leaves)	-	0.23	0.23-0.43

Fig. 1 Linear regression through simulated data of yield on HAD (green tissue area per unit ground area integrated over time). The slope of the regression line is a measure for tolerance, whereby smaller slopes denote a more tolerant crop. The dots and solid line are for Mercia and the triangles and dotted line represent a more tolerant cultivar. Note that a decrease in HAD is the result of increased disease severity.

Fig. 2 Graphical representation of the model. Light interception and disease affect the dry matter accumulation of individual wheat shoots. The total biomass accumulated during the pre-anthesis period is firstly allocated to the leaves, roots and structural stem tissues. The remainder is then allocated to either the ear or stem reserves, whereby the ear investment determines the number of grains per ear. During the slow grain-fill period there is some further biomass allocation towards structural stem tissues, after which the remainder is partitioned to either stem reserves or endosperm cell division. The endosperm investment determines the maximum potential dry matter (DM) content of an individual grain. During the rapid-fill period, all additional biomass accumulated is directly allocated to the grain and the stem reserves are remobilised to the grain. Dashed lines denote feedback loops due to storage limitation. Note that the width of the columns is not indicative of the length of the growth periods. Letters refer to the main text of the materials and methods and illustrate the dynamics described therein.

Fig. 3 Effect of changes in carbon use efficiency (CUE) on disease tolerance. The trends in tolerance (squares in (**a**)) across the trait value range are explained according to the effects of the presence of a severe epidemic on four main components: (A) yield; (B) total realised sink size; (C) percentage of total sink filled at the end of the rapid-fill period and (D) healthy area duration (HAD). Panels (E) - (H) illustrate how the same trait change affects: (E) number of grains per ear; (F) amount of WSC per stem at the end of the slow grain-fill period; (G) percentage of stem storage capacity used at the end of the slow-fill period and (H) HAD per grain. Triangles represent disease-free/fully treated crops, whereas circles represent crops affected by a severe epidemic. Blank areas in the plot represent traits that lead to not viable plants, i.e. the assimilates collected pre-anthesis are not sufficient to cover the demand of the leaves, roots and stem structural tissues. Note that tolerance increases with a decreased yield loss per unit HAD loss. The x-axis is representative of the current genotypic variability for the trait in question as identified during a literature search.

Fig. 4 Correlation plots for a selection of traits tested across their full trait range. (A) tolerance versus Δ % sink filled; (B) tolerance versus Δ total sink filled; (C) tolerance versus Δ HAD; (D) grains per ear versus total sink size; (E) tolerance versus water soluble carbon (WSC) reserves and (F) tolerance versus HAD per grain, where HAD stands for the healthy area duration. Closed and open symbols represent traits affected by HAD and not affected by HAD, respectively. That trait changes for which $\Delta\,\%\,\text{sink filled} = 0$ have been excluded from (A), (B) and (F).

Fig. 5 Effect of changes in canopy size on disease tolerance. The layout and description for the figure are as for Fig. 3.

Fig. 6 Model validation. Panels (A) to (I) show the effect of a 10% increase or decrease of an individual trait value away from its default value (circle) which represents the wheat cultivar Mercia. The arrows indicate the predicted direction of effect according to the literature for the same or similar plant traits, whereas a horizontal line suggests no effect. Note that in most cases the effect has not been determined through experimentation. The steepness of the arrow is not indicative of the strength of the effect. 'Leaf distribution' refers to the fractional size of the flag leaf compared to the total leaf area of the top five leaves.

Fig. 7 Correlation between healthy area duration (HAD) per grain and tolerance for a large set of data sets randomly selected from the ranges in Table I. Note that for each of these randomly selected parameter sets the crop yields more than 9 t/ha. The solid line represents the linear regression through the data points ($p<0.00001$).

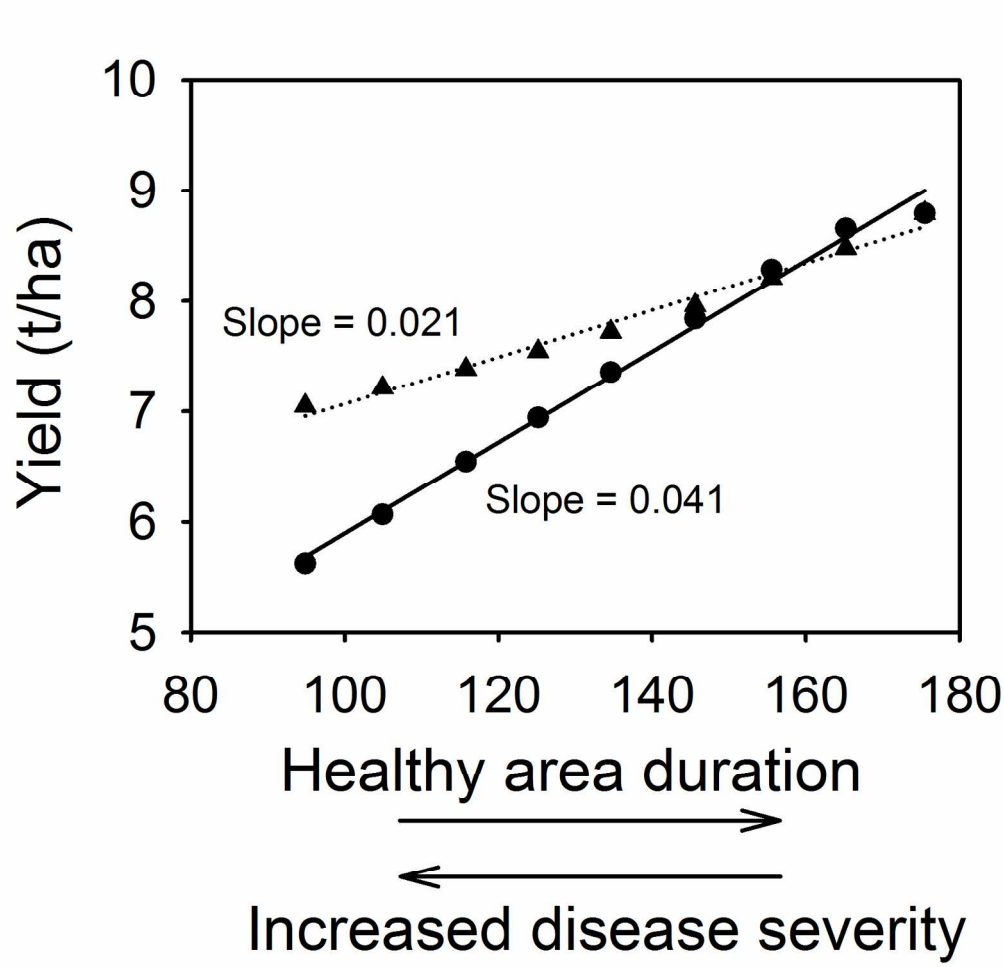

Fig. 1 Linear regression through simulated data of yield on HAD (green tissue area per unit ground area integrated over time). The slope of the regression line is a measure for tolerance, whereby smaller slopes denote a more tolerant crop. The dots and solid line are for Mercia and the triangles and dotted line represent a more tolerant cultivar. Note that a decrease in HAD is the result of increased disease severity.

162x157mm (300 x 300 DPI)

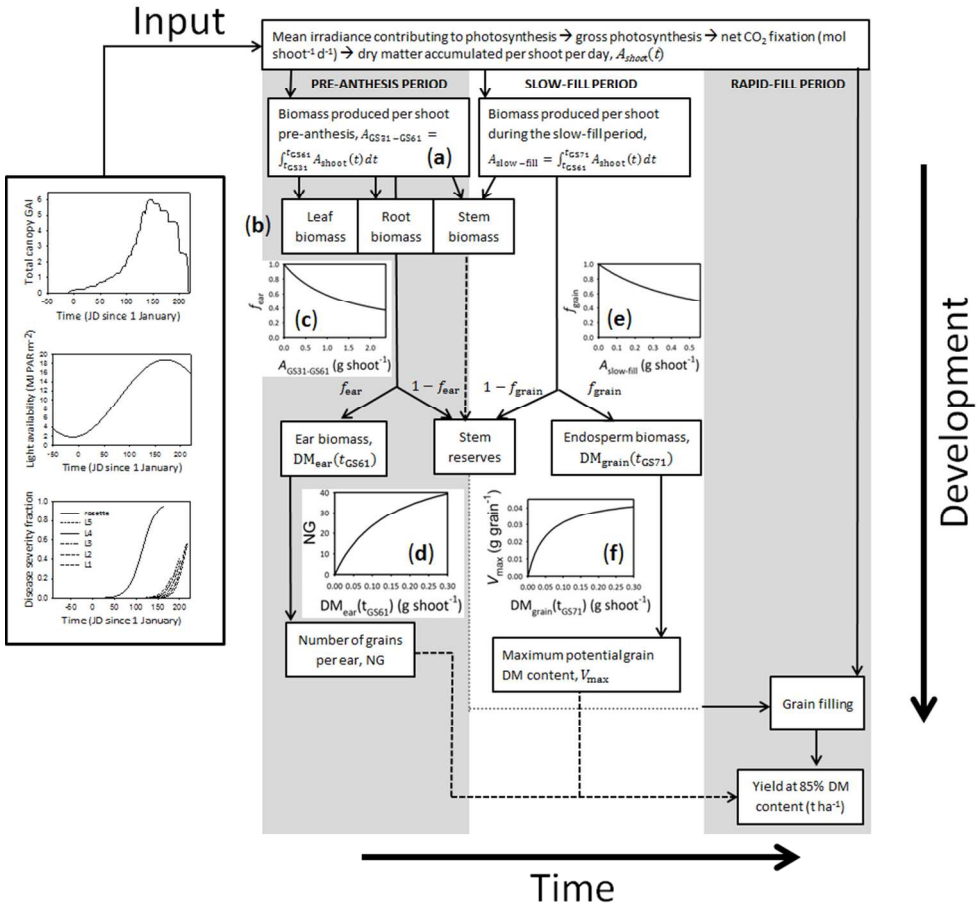

Fig. 2 Graphical representation of the model. Light interception and disease affect the dry matter accumulation of individual wheat shoots. The total biomass accumulated during the pre-anthesis period is firstly allocated to the leaves, roots and structural stem tissues. The remainder is then allocated to either the ear or stem reserves, whereby the ear investment determines the number of grains per ear. During the slow grain-fill period there is some further biomass allocation towards structural stem tissues, after which the remainder is partitioned to either stem reserves or endosperm cell division. The endosperm investment determines the maximum potential dry matter (DM) content of an individual grain. During the rapid-fill period, all additional biomass accumulated is directly allocated to the grain and the stem reserves are remobilised to the grain. Dashed lines denote feedback loops due to storage limitation. Note that the width of the columns is not indicative of the length of the growth periods. Letters refer to the main text of the materials and methods and illustrate the dynamics described therein.

266x255mm (96 x 96 DPI)

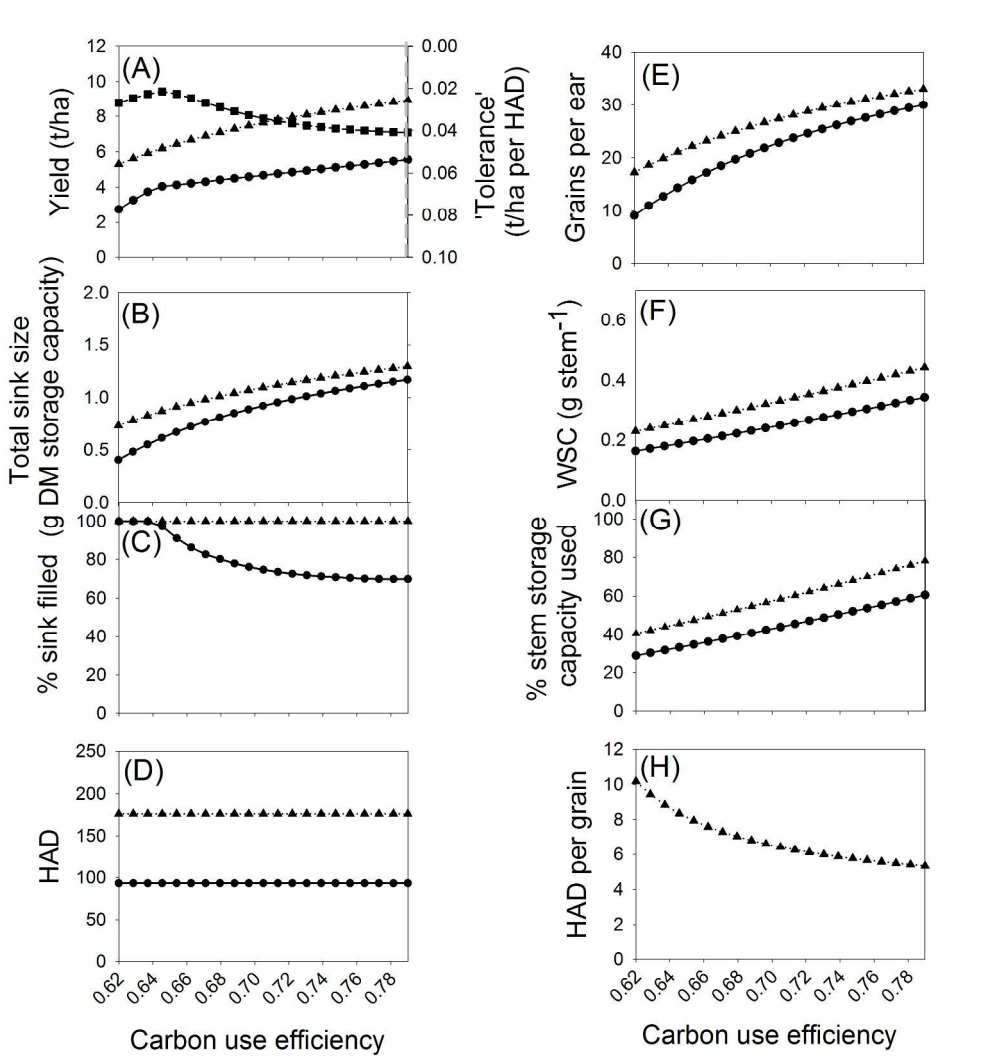

Fig. 3 Effect of changes in carbon use efficiency (CUE) on disease tolerance. The trends in tolerance (squares in (a)) across the trait value range are explained according to the effects of the presence of a severe epidemic on four main components: (A) yield; (B) total realised sink size; (C) percentage of total sink filled at the end of the rapid-fill period and (D) healthy area duration (HAD). Panels (E) - (H) illustrate how the same trait change affects: (E) number of grains per ear; (F) amount of WSC per stem at the end of the slow grain-fill period; (G) percentage of stem storage capacity used at the end of the slow-fill period and (H) HAD per grain. Triangles represent disease-free/fully treated crops, whereas circles represent crops affected by a severe epidemic. Blank areas in the plot represent traits that lead to not viable plants, i.e. the assimilates collected pre-anthesis are not sufficient to cover the demand of the leaves, roots and stem structural tissues. Note that tolerance increases with a decreased yield loss per unit HAD loss. The x-axis is representative of the current genotypic variability for the trait in question as identified during a literature search.

266x281mm (300 x 300 DPI)

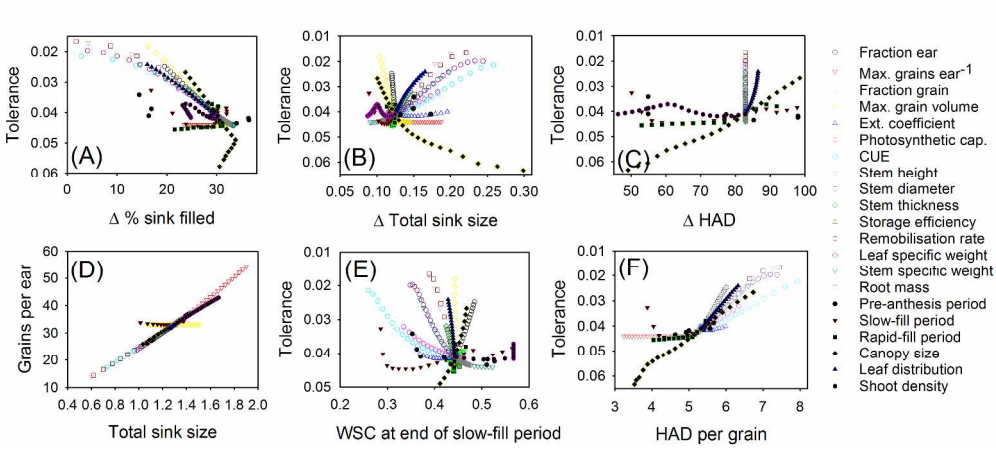

Fig. 4 Correlation plots for a selection of traits tested across their full trait range. (A) tolerance versus Δ % sink filled; (B) tolerance versus Δ total sink filled; (C) tolerance versus Δ HAD; (D) grains per ear versus total sink size; (E) tolerance versus water soluble carbon (WSC) reserves and (F) tolerance versus HAD per grain, where HAD stands for the healthy area duration. Closed and open symbols represent traits affected by HAD and not affected by HAD, respectively. That trait changes for which Δ % sink filled=0 have been excluded from (A), (B) and (F).

349x156mm (300 x 300 DPI)

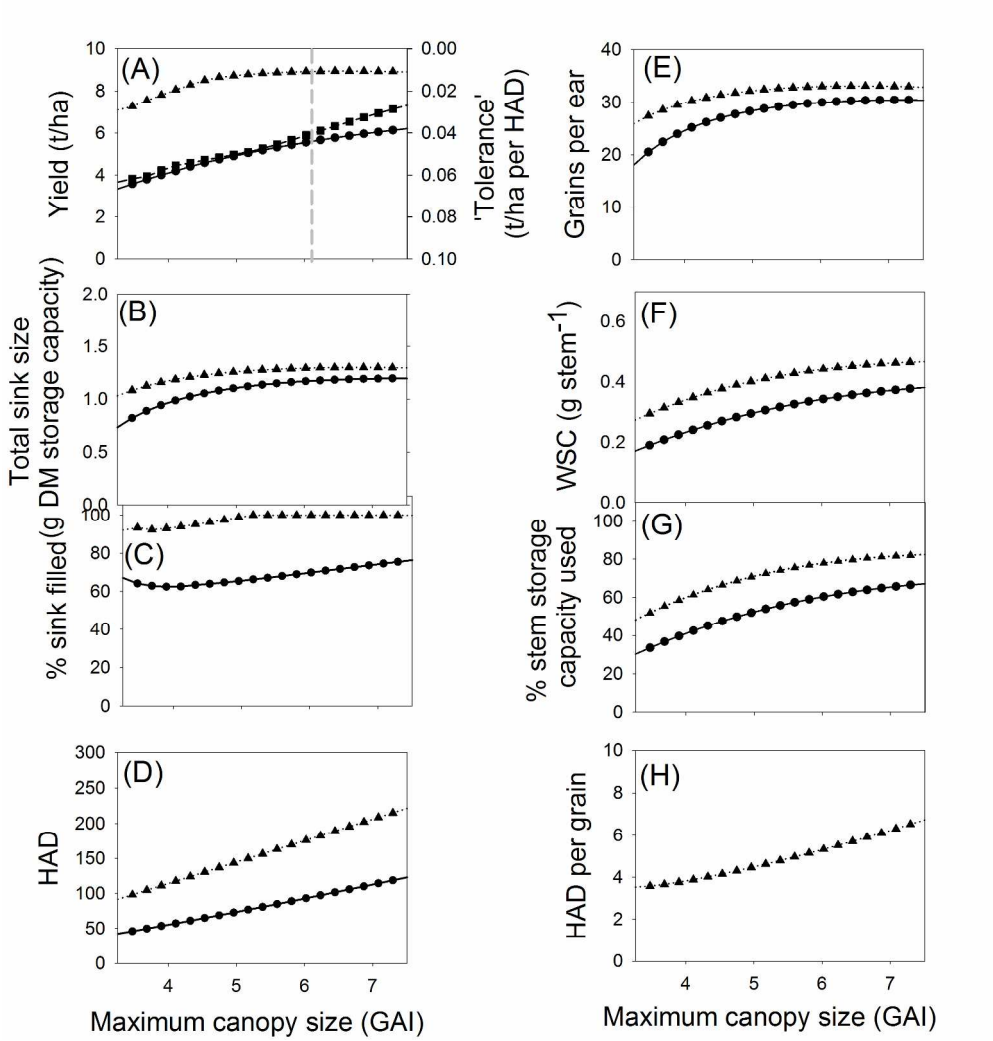

Fig. 5 Effect of changes in canopy size on disease tolerance. The layout and description for the figure are as for Fig. 3.

265x276mm (300 x 300 DPI)

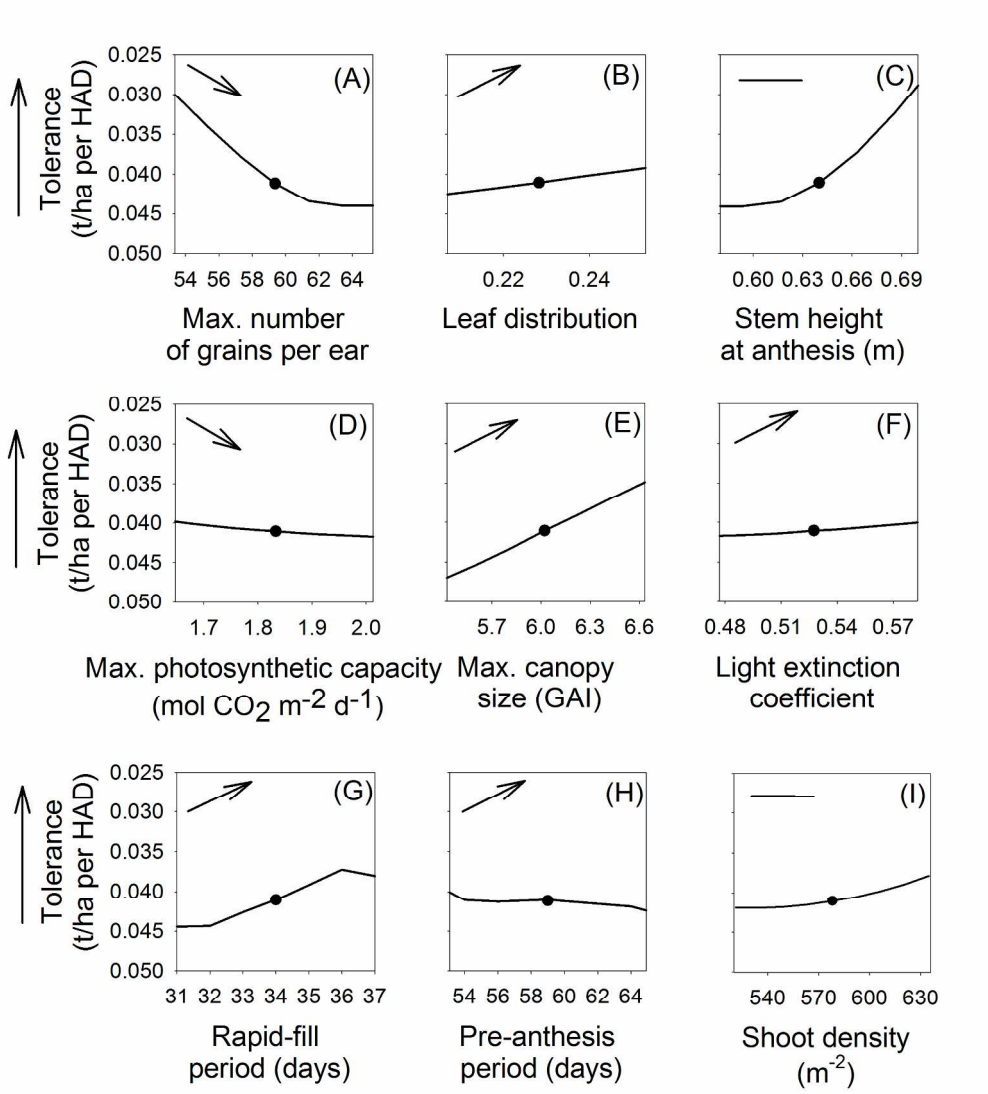

Fig. 6 Model validation. Panels (A) to (I) show the effect of a 10% increase or decrease of an individual trait value away from its default value (circle) which represents the wheat cultivar Mercia. The arrows indicate the predicted direction of effect according to the literature for the same or similar plant traits, whereas a horizontal line suggests no effect. Note that in most cases the effect has not been determined through experimentation. The steepness of the arrow is not indicative of the strength of the effect. 'Leaf distribution' refers to the fractional size of the flag leaf compared to the total leaf area of the top five leaves.

227x249mm (300 x 300 DPI)

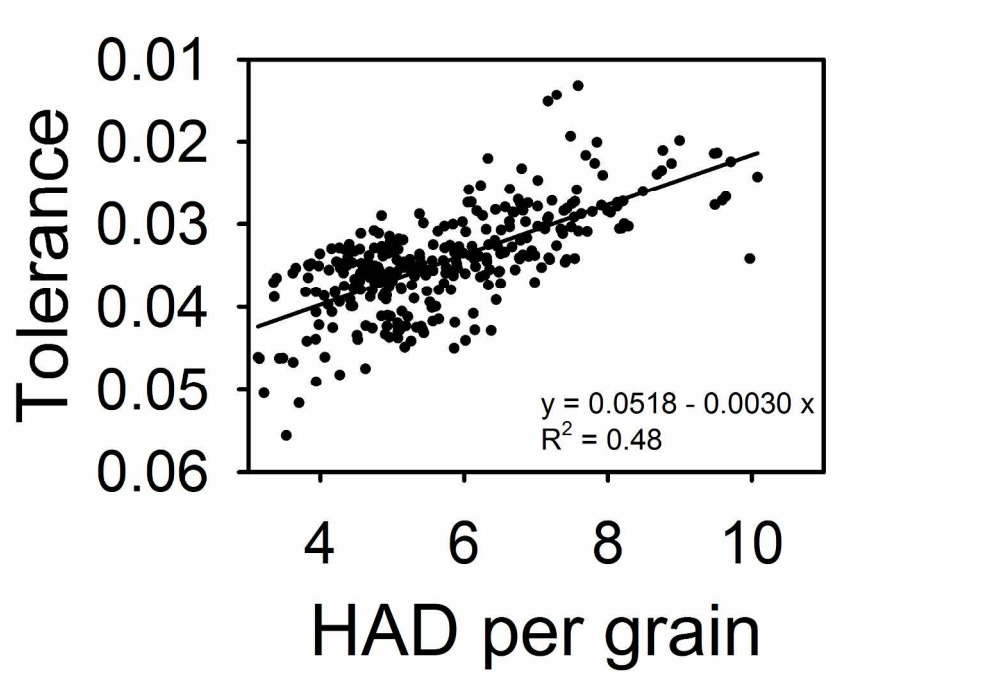

Fig. 7 Correlation between healthy area duration (HAD) per grain and tolerance for a large set of data sets randomly selected from the ranges in Table I. Note that for each of these randomly selected parameter sets the crop yields more than 9 t/ha. The solid line represents the linear regression through the data points ($p<0.00001$).

217x146mm (300 x 300 DPI)

Phytopathology Supporting Information SI1

Article title: **Physiological and developmental traits determining yield tolerance of wheat to foliar diseases**
Authors: van den Berg, F., Paveley, N. D., Bingham, I. J. and van den Bosch, F.

Model development

Crop development. *Tillering and shoot density.* It is assumed that aborting tillers are not a main drain on or source of remobilisation of assimilates and that flowering on main stems and tillers occurs close together. Therefore all tillers are modelled as main stems. The shoot density, *N*, is represented by the number of fertile ears per m^2.

Leaf area growth and senescence. Culm leaves are numbered down the shoot, such that the flag leaf is denoted by LI, the next leaf down by L2, and so on. The green area, GA, of a single leaf, *n*, is described by a monomolecular growth function (Thornley and Johnson 1990) followed by monomolecular decline due to leaf senescence, leading to

$$\mathrm{GA}_n(t) = \begin{cases} A_{\max_n} + \left(A_{\mathrm{ini}} - A_{\max_n}\right)e^{-g_n\left(t-t_{\mathrm{initiation}_n}\right)}, & t_{\mathrm{initiation}_n} \le t < t_{\mathrm{senescence}_n} \\ A_{\max_n} + \left(A_{\mathrm{death}} - A_{\max_n}\right)e^{s_n\left(t-t_{\mathrm{death}_n}\right)}, & t_{\mathrm{senescence}_n} \le t \le t_{\mathrm{death}_n} \\ 0, & t > t_{\mathrm{death}_n} \end{cases} \quad (1)$$

where $t_{\mathrm{initiation}_n}$, $t_{\mathrm{senescence}_n}$ and t_{death_n} are the times of leaf initiation, leaf senescence onset and leaf death, respectively; A_{ini} is the initial leaf size when the leaf first becomes visible; $A_{\max_n}$ is the maximum area leaf *n* attains (in cm^2); A_{death} is the healthy leaf area size below which the leaf is assumed dead; g_n is the leaf growth rate and s_n is the mean leaf senescence rate.

Note that here leaf initiation refers to the point at which the leaf becomes visible and starts to grow and not the initiation of the leaf primordial within the shoot apex. Throughout the text the phrase 'leaf' refers to the leaf lamina and its associated leaf sheath.

Green area index. The seasonal development of the green area index of a given leaf layer (GAI_n in m^2 leaf area per m^2 ground area) can be derived from the green leaf area of the leaf layer, GA_n, multiplied by the shoot density, *N* (in m^{-2} ground), such that

$$\mathrm{GAI}_n(t) = \frac{\mathrm{GA}_n(t)}{10000} N. \quad (2)$$

*Senesced area index (*DAI*).* Senesced tissues might behave different as compared to healthy tissues with regards to photosynthesis and/or light interception. It is therefore essential to track the dead area index for individual leaf layers (DAI_n in m^2 leaf per m^2 ground) separately, leading to

$$\mathrm{DAI}_n(t) = \begin{cases} 0, & t < t_{\mathrm{senescence}_n} \\ \frac{A_{\max_n}}{10000} N - \mathrm{GAI}_n(t), & t \ge t_{\mathrm{senescence}_n} \end{cases} \quad (3)$$

Disease dynamics. The epidemic progress on an individual leaf layer is modelled according to a logistic equation describing the seasonal increase in the fractional disease severity, S_n, such that

$$S_n(t) = \frac{S_{\max_n}}{1+\left(\frac{1-S_0/A_{\max_n}}{S_0/A_{\max_n}}\right)e^{-r_n\left(t-t_{\mathrm{onset}_n}\right)}} \quad (4)$$

and whereby S_0 is the area taken up by the lesions caused by the initial spore influx on a leaf, $S_{\max_n}$ is the maximum disease severity, r_n is the initial rate of epidemic progress and t_{onset_n} is the onset time of the epidemic. For the rosette leaves an average disease severity is calculated to represent the disease progress over the life-span of the rosette leaves.

Mean daily irradiance. The mean daily solar radiation in the UK, $I_{\text{PAR}}(t)$ in MJ PAR m^{-2} ground d^{-1}, can be represented by a cosine function (Sylvester-Bradley, Berry et al. 2005), i.e.

$$I_{\text{PAR}}(t) = i_{\text{vert}} + i_{\text{amp}} - i_{\text{amp}} \cos\left(\frac{t}{i_{\text{freq}}} + i_{\text{hor}}\right) \quad (5)$$

with i_{vert} the vertical location, i_{amp} the amplitude, i_{freq} the frequency and i_{hor} the horizontal location of the curve.

Light interception is calculated for the individual leaf layers, with the exception of leaf 6 and below, which form the rosette of the plant. The leaves forming the rosette are treated as a single leaf layer for light interception and photosynthesis. Light interception is traditionally represented by the Lambert-Beer relationship (Thornley and Johnson 1990) and hence given light extinction coefficient, k, the fraction of solar radiation intercepted by a leaf layer, F_n, is calculated from

$$F_n(t) = \left(1 - e^{-\left(k\text{GAI}_n(t) + k(1-k_{\text{reduction}})\text{DAI}_n(t)\right)}\right) e^{-\sum_{i=1}^{n-1}\left(k\text{GAI}_i(t) + k(1-k_{\text{reduction}})\text{DAI}_i(t)\right)} \text{ for } n \leq 5 \quad (6)$$

$$F_{\text{rosette}}(t) = \left(1 - e^{-\left(k\text{GAI}_{\text{rosette}}(t) + k(1-k_{\text{reduction}})\text{DAI}_{\text{rosette}}(t)\right)}\right) e^{-\sum_{i=1}^{5}\left(k\text{GAI}_i(t) + k(1-k_{\text{reduction}})\text{DAI}_i(t)\right)} \text{ for } n = 6 \quad (7)$$

with

$$\text{GAI}_{\text{rosette}}(t) = \sum_{n=6}^{11} \text{GAI}_n(t) \text{ and } \text{DAI}_{\text{rosette}}(t) = \sum_{n=6}^{11} \text{DAI}_n(t) \quad (8)$$

Although senesced tissues still contribute to light interception they might do so at a reduced level due to shrivelling of the tissues, which is denoted by a fractional reduction, $k_{reduction}$, in the light extinction coefficient. The mean irradiance, $I_n(t)$, in MJ PAR m^{-2} leaf d^{-1} is then given by

$$I_n(t) = \frac{I_{PAR}(t)F_n(t)}{GAI_n(t) + (1-k_{reduction})DAI_n(t)} \text{ for } n \leq 5 \text{ and}$$
$$I_{rosette}(t) = \frac{I_{PAR}(t)F_{rosette}(t)}{GAI_{rosette}(t) + (1-k_{reduction})DAI_{rosette}(t)} \text{ for } n = 6 \quad (9)$$

Biomass accumulation through photosynthesis. We assume that senesced and diseased tissues no longer contribute to photosynthesis and that there is no specific feedback of the disease on natural leaf senescence (i.e. the processes are independent). The mean irradiance intercepted by leaf n that is contributing to photosynthesis, I_{Photo_n}, is then given by

$$I_{\text{Photo}_n}(t) = I_n(t) \frac{\text{GA}_n}{\text{GA}_n + (1-k_{\text{reduction}})\text{DA}_n} (1 - S_n(t)) \quad (10)$$

The relationship between the average daily rate of gross photosynthesis, P_{gross_n}, in mol CO_2 m^{-2} leaf d^{-1} and the mean irradiance contributing to photosynthesis, I_{Photo_n}, on the leaf surface of leaf n can be described by a non-rectangular hyperbola (Johnson and Thornley 1984) such that

$$P_{\text{gross}_n}(t) = \frac{1}{2\theta}\left(\alpha I_{\text{Photo}_n}(t) + P_{\max_n} - \left[\left(\alpha I_{\text{Photo}_n}(t) + P_{\max_n}\right)^2 - 4\theta\alpha I_{\text{Photo}_n}(t) P_{\max_n}\right]^{1/2}\right) \quad (11)$$

Here, α is the photochemical efficiency represented by the initial slope of the photosynthesis-light response curve in mol CO_2 MJ^{-1}, $P_{\max}$ is the light-saturated rate of photosynthesis in mol CO_2 m^{-2} leaf d^{-1} and θ is a parameter describing the degree of curvature of the response. For the rosette $I_{\mathrm{Photo}_{\mathrm{rosette}}}(t)$ and $P_{\mathrm{gross}_{\mathrm{rosette}}}(t)$ are calculated according to $\mathrm{GAI}_{\mathrm{rosette}}(t)$ and $\mathrm{DAI}_{\mathrm{rosette}}(t)$.

Leaves containing a reduced nitrogen concentration have a lower $P_{\max_n}$ value. The distribution of nitrogen within the canopy tends to follow the canopy PAR profile and $P_{\max_n}$ can therefore be estimated from

$$P_{\max_n} = \begin{cases} P^0_{\max}, & n = 1 \\ P^0_{\max}\left[1 - \frac{\lambda}{2}\left(1 - e^{\sum_{i=2}^{n}\left(k\mathrm{GAI}_i(t) + k(1-k_{\mathrm{reduction}})\mathrm{DAI}_i(t)\right)}\right)\right], & n \geq 2 \end{cases} \quad (12)$$

where $P^0_{\max}$ is the light saturated rate of photosynthesis of the uppermost leaf layer, the exponent represents the total leaf area index below the upper canopy surface and λ is its rate of decline down the canopy (Thornley and Johnson 1990).

From here we calculate the total CO_2 fixed per shoot per day, C_{gross}.

$$C_{\mathrm{gross}}(t) = P_{\mathrm{gross}_{\mathrm{rosette}}}(t)GA_{\mathrm{rosette}}(t) + \sum_{i=1}^{5} P_{\mathrm{gross}_i}(t)GA_i(t) \quad (13)$$

It is assumed that a fraction of the carbon that is fixed daily is lost to maintenance and growth respiration such that the daily net CO_2 fixation, C_{net}, can be given by,

$$C_{\mathrm{net}}(t) = \mathrm{CUE}\ C_{\mathrm{gross}}(t), \quad (14)$$

where CUE is the carbon use efficiency as defined by Gifford (1995) and Albrizio and Steduto (2003). Net CO_2 fixed can be converted to total C fixed per shoot per day with the simple conversion factor $\mathrm{conv}_{\mathrm{mol\ CO2 \rightarrow g\ C}}$. The net CO_2 fixation in mol shoot^{-1} d^{-1} is then converted to dry matter accumulated per shoot per day, $A_{\mathrm{shoot}}(t)$, i.e.

$$A_{\mathrm{shoot}}(t) = C_{\mathrm{net}}(t)\mathrm{conv}_{\mathrm{mol\ CO2 \rightarrow g\ C}}\mathrm{conv}_{\mathrm{g\ C \rightarrow g\ DM}} \quad (15)$$

Pre-anthesis biomass partitioning. The dry matter biomass accumulated per shoot from GS31 to anthesis at GS61, $A_{\mathrm{GS31-GS61}}$, is calculated from the integral of $A_{\mathrm{shoot}}(t)$, such that

$$A_{\mathrm{GS31-GS61}} = \int_{t_{\mathrm{GS31}}}^{t_{\mathrm{GS61}}} A_{\mathrm{shoot}}(t)dt. \quad (16)$$

This biomass is partitioned to several different plant organs: plant leaves, structural stem, roots, stem reserves and the ear.

The stem reaches its maximum height around anthesis and the total amount of dry matter accumulated in the structural stem tissues between GS31 and GS61, A_{stem}, is then given by

$$A_{\mathrm{stem}} = (h_{\mathrm{stem}}(t_{\mathrm{GS61}}) - h_{\mathrm{stem}}(t_{\mathrm{GS31}}))c_{\mathrm{stem\ length \rightarrow volume}}c_{\mathrm{stem\ volume \rightarrow DM}} \quad (17)$$

with

$$c_{\mathrm{stem\ length \rightarrow volume}} = \pi(0.5D_{\mathrm{stem}})^2 T_{\mathrm{stem}}.$$

Here, $h_{\mathrm{stem}}(t_{\mathrm{GS31}})$ and $h_{\mathrm{stem}}(t_{\mathrm{GS61}})$ are the stem height at GS31 and GS61, respectively, $c_{\mathrm{stem\ length \rightarrow volume}}$ denotes the conversion from stem length to stem dry matter volume, $c_{\mathrm{stem\ volume \rightarrow DM}}$ denotes the conversion from stem dry matter volume to stem dry matter weight, D_{stem} is the stem diameter and T_{stem} is the fractional stem thickness.

Furthermore, artificial shading, which is also a surrogate for mutual shading of leaves (due to changes in leaf position across the main stem) and stems (due to changes in shoot density), is known to lead to a reduction in dry matter accumulation in the structural stem and leaf tissues (Beed, Paveley et al. 2007). Stem diameter and stem wall thickness are likely to be genetically determined traits and are thus unlikely to be affected by a reduced light availability and hence it is assumed that the reduction in structural stem dry matter

accumulation manifests itself through an decreased specific stem weight and hence a reduction in $c_{\text{stem volume}\rightarrow\text{DM}}$. The relationship is summarised in the model by,

$$c_{\text{stem volume}\rightarrow\text{DM}} = a + b * A_{\text{GS31}-\text{GS61}} \quad (18)$$

whereby *a* and *b* represent the intercept and the slope of the relationship, respectively.

All leaves emerge before anthesis and some leaves will have fully or partially senesced at anthesis. The total amount of dry matter accumulated in the leaves, A_{leaves}, between GS31 and GS61 is therefore

$$A_{\text{leaves}} = \Big(\big(\text{GA}(t_{\text{GS61}}) + \text{DA}(t_{\text{GS61}})\big) - \big(\text{GA}(t_{\text{GS31}}) + \text{DA}(t_{\text{GS31}})\big)\Big)\, c_{\text{leaf area}\rightarrow\text{DM}} \quad (19)$$

where DA represents the senesced tissue area on the shoot. The reduction in leaf specific weight, $c_{\text{leaf area}\rightarrow\text{DM}}$, due to reduced light availability is summarised by

$$c_{\text{leaf area}\rightarrow\text{DM}} = c + d * A_{\text{GS31}-\text{GS61}}.$$

The roots reach their maximum length around anthesis and the total amount of dry matter accumulated in the root tissues between GS31 and GS61, A_{roots}, is then given by

$$A_{\text{roots}} = m_{\text{roots}}(t_{\text{GS61}}) - m_{\text{roots}}(t_{\text{GS31}}) \quad (20)$$

where, $m_{\text{roots}}(t_{\text{GS31}})$ and $m_{\text{roots}}(t_{\text{GS61}})$ are the root masses of an individual plant at GS31 and GS61, respectively.

The remainder of the biomass, $A_{\text{remainder}}$, has been partitioned to either the ear or the stem reserves, i.e.

$$A_{\text{remainder}}(t_{\text{GS61}}) = A_{\text{GS31}-\text{GS61}} - A_{\text{stem}} - A_{\text{leaves}} - A_{\text{roots}}. \quad (21)$$

It is assumed that biomass production is always sufficient to meet the demand of the leaves, roots and structural stem and therefore only cases that lead to $A_{\text{remainder}}(t_{\text{GS61}}) \geq 0$ are considered.

Partitioning between the ear and the stem reserves. The fraction of $A_{\text{remainder}}$ that is partitioned to the ear, $f_{\text{ear}_{\text{pre}-\text{anthesis}}}$, is assumed to be a function of the total biomass produced, i.e. $A_{\text{GS31}-\text{GS61}}$ in such a way that when there is little biomass to invest a proportionally larger fraction is allocation to the ear, whereas when there is a lot of biomass to invest a proportionally larger fraction is allocated to the stem reserves. This leads to a total ear DM investment, A_{ear}, of

$$A_{\text{ear}} = f_{\text{ear}_{\text{pre}-\text{anthesis}}} A_{\text{remainder}} \quad (22)$$

with

$$f_{\text{ear}_{\text{pre}-\text{anthesis}}} = \frac{f_{\text{max}_{\text{pre}-\text{anthesis}}}}{1+\gamma A_{\text{GS31}-\text{GS61}}} \quad (23)$$

whereby $f_{\text{max}_{\text{pre}-\text{anthesis}}}$ the maximum $A_{\text{remainder}}$ fraction allocated to the ear and γ a shape parameter. Furthermore, Clarke, Sylvester-Bradley et al. (2012) showed that partitioning to the ear decreases non-linearly with an increased stem height, probably due to a relatively higher assimilate pull from the stem, which we model according to,

$$\gamma = s_1 h_{\text{stem}}(t_{\text{GS61}})\pi(0.5D_{\text{stem}})^2 T_{\text{stem}} \quad (24)$$

All the other biomass, $(1 - f_{\text{ear}_{\text{pre}-\text{anthesis}}})A_{\text{remainder}}$, has been partitioned to the stem for storage in the form of water soluble carbon (WSC; fructan based stem reserves stored within the vacuoles present within the structural stem tissues), leading to a WSC accumulation of

$$A_{\text{stem reserves}} = (1 - f_{\text{ear}_{\text{pre-anthesis}}})A_{\text{remainder}}. \quad (25)$$

The total amount of DM accumulated in the ear and in the form of stem reserves at anthesis $\text{DM}_{\text{ear}}(t_{\text{GS61}})$, and $\text{DM}_{\text{stem reserves}}(t_{\text{GS61}})$, respectively, are then given by

$$\text{DM}_{\text{ear}}(t_{\text{GS61}}) = A_{\text{ear}} + \text{DM}_{\text{ear GS31}} \quad (26)$$

$$\text{DM}_{\text{stem reserves}}(t_{\text{GS61}}) = A_{\text{stem reserves}} + \text{DM}_{\text{stem reserves GS31}} \quad (27)$$

with $\text{DM}_{\text{ear GS31}}$ and $\text{DM}_{\text{stem reserves GS31}}$ the ear and WSC dry matter weights at GS31.

However, we assume that the total amount of WSC that is actually stored in the stem is directly related to stem volume, whereby taller stems can store more assimilates. If the total amount of WSC partitioned to the stem reserves exceeds the stem storage capacity, S_{capacity}, the excess is lost due to assimilate degradation or a temporary reduction in photosynthesis. In summary this gives

$$S_{\text{capacity}} = h_{\text{stem}}(t_{\text{GS61}})\pi(0.5D_{\text{stem}})^2 T_{\text{stem}} s_2 \quad (28)$$

$$\text{DM}_{\text{stem reserves}}(t_{\text{GS61}}) = \begin{cases} \text{DM}_{\text{stem reserves}}(t_{\text{GS61}}), & \text{DM}_{\text{stem reserves}}(t_{\text{GS61}}) \le S_{\text{capacity}} \\ S_{\text{capacity}}, & \text{DM}_{\text{stem reserves}}(t_{\text{GS61}}) > S_{\text{capacity}} \end{cases} \quad (29)$$

Number of grains. The relationship between the pre-anthesis biomass allocated to the ear and the number of fertile florets is in the model represented by

$$\text{NG} = \frac{\tau \text{DM}_{\text{ear}}(t_{\text{GS61}})}{\upsilon + \text{DM}_{\text{ear}}(t_{\text{GS61}})} \quad (30)$$

with NG the average number of grains per ear and τ and υ genotype specific shape parameters.

Post-anthesis biomass partitioning. The leaves and ear are now fully developed and all further biomass accumulated is partitioned to the structural stem, the stem reserves or grain development/filling. The post-anthesis period is split into two distinct periods: i) the slow fill period during which endosperm cell division takes place and the grains grow largely by water uptake rather than dry matter uptake and ii) the rapid grain fill period during which stem reserves are relocated towards the grains and any biomass accumulated through photosynthesis is directly invested into grain filling.

The slow fill period. During this period there is a continued allocation of assimilates to the stem reserves and a small amount of further stem growth (Sylvester-Bradley 1998). It is assumed that a fraction $f_{\text{grain}_{\text{slow-fill}}}$ of the biomass accumulated during the slow fill period, and not invested in stem growth, is partitioned to the grain for endosperm formation whereas the rest is partitioned to the stem reserves. As during the pre-anthesis period it is assumed that when there is little biomass to invest a proportionally larger fraction is allocation to the grain. The dry matter content in the grain and the stem reserves at the start of the rapid fill period, $\text{DM}_{\text{grain}}(t_{\text{rapid-fill}})$ and $\text{DM}_{\text{stem reserves}}(t_{\text{rapid-fill}})$, respectively, can then be calculated to be

$$\text{DM}_{\text{grain}}(t_{\text{rapid-fill}}) = f_{\text{grain}_{\text{slow-fill}}}(A_{\text{slow-fill}} - A_{\text{stem}_{\text{slow-fill}}}) \quad (31)$$

$$\text{DM}_{\text{stem reserves}}(t_{\text{rapid-fill}}) = (1 - f_{\text{grain}_{\text{slow-fill}}})(A_{\text{slow-fill}} - A_{\text{stem}_{\text{slow-fill}}}) + \text{DM}_{\text{stem reserves}}(t_{\text{GS61}}) \quad (32)$$

with

$$A_{\text{slow-fill}} = \int_{t_{\text{GS61}}}^{t_{\text{rapid-fill}}} A_{\text{shoot}}(t)dt, \quad (33)$$

$$A_{\text{stem}_{\text{slow-fill}}} = (h_{\text{stem}}(t_{\text{rapid-fill}}) - h_{\text{stem}}(t_{\text{GS61}}))c_{\text{length}\to\text{volume}} c_{\text{volume}\to\text{DM}} \quad (34)$$

and

$$f_{\text{grain}_{\text{slow-fill}}} = \frac{f_{\text{max}_{\text{slow-fill}}}}{1 + \delta A_{\text{slow-fill}}}. \quad (35)$$

Note, that it is again assumed that i) the fraction that is partitioned to the grain depends on the stem storage volume whereby larger stems go paired with a relatively higher assimilate demand, such that $\delta = s_3 h_{\text{stem}}(t_{\text{rapid-fill}})\pi(0.5D_{\text{stem}})^2 T_{\text{stem}}$ and ii) the total amount of WSC that is actually stored in the stem is directly related to stem volume and that if the total amount of WSC partitioned to the stem reserves exceeds the stem storage capacity, S_{capacity}, the excess is lost due to assimilate degradation or a temporary reduction in photosynthesis. This gives

$$S_{\text{capacity}} = h_{\text{stem}}(t_{\text{rapid-fill}})\pi(0.5D_{\text{stem}})^2 T_{\text{stem}} s_2 \quad (36)$$

$$\text{DM}_{\text{stem reserves}}(t_{\text{rapid-fill}}) = \begin{cases} \text{DM}_{\text{stem reserves}}(t_{\text{rapid-fill}}), & \text{DM}_{\text{stem reserves}}(t_{\text{rapid-fill}}) \le S_{\text{capacity}} \\ S_{\text{capacity}}, & \text{DM}_{\text{stem reserves}}(t_{\text{rapid-fill}}) > S_{\text{capacity}} \end{cases} \quad (37)$$

The dry matter allocated to the grains affects the endosperm cell division and consequently has an impact on the maximum potential grain volume and hence the maximum potential grain dry weight. We summarise these dynamics by assuming a curvilinear relationship between the dry matter allocation to an individual grain during the slow fill period, $\frac{\text{DM}_{\text{grain}}(t_{\text{rapid-fill}})}{\text{NG}}$, and the maximum potential grain DM content of the grainV_{max}, , such that,

$$V_{\text{max}} = \frac{\varepsilon \frac{\text{DM}_{\text{grain}}(t_{\text{rapid-fill}})}{\text{NG}}}{\mu + \frac{\text{DM}_{\text{grain}}(t_{\text{rapid-fill}})}{\text{NG}}}. \quad (38)$$

and where ε and μ are shape parameters.

The rapid fill period. The final grain dry weight per ear at harvest is determined during the rapid fill period. Any biomass accumulated during this period as a result of further light interception is directly invested into grain filling. At the same time the stem reserves are being remobilised to the ear at a constant rate, r_{mob} and with an efficiency of m_{eff}, i.e. carbon translocation from the stem reserves to the grain comes at a cost and reserves might have partially been depleted due to respiration. Grain filling is however limited by the potential grain DM content determined during the slow fill period and the number of fertile grains set at anthesis. These dynamics are summarised by,

$$\frac{dG(t)}{dt} = \begin{cases} A_{\text{shoot}}(t) + m_{\text{eff}} r_{\text{mob}} \text{DM}_{\text{stem reserves}}(t), & G(t) < V_{\text{max}}\text{NG} \\ 0, & G(t) \ge V_{\text{max}}\,\text{NG} \end{cases} \quad (39)$$

with

$$\text{DM}_{\text{stem reserves}}(t) = \text{DM}_{\text{stem reserves}}(t_{\text{rapid fill}}) e^{-r_{\text{mob}}(t - t_{\text{rapid fill}})} \quad (40)$$

and the initial condition

$$G(t_{\text{rapid fill}}) = \text{DM}_{\text{grain}}(t_{\text{rapid fill}}).$$

The grain weight at harvest is then given by $G(t_{\text{harvest}})$. To estimate grain yield, two further conversion factors need to be applied. Firstly, the conversion from g m^{-2} to ton ha^{-1}, i.e. $c_{\text{gm}^{-2}\rightarrow\text{ton ha}^{-1}}$. Secondly, grain yields tend to be expressed as tonnes per hectare at 85% dry matter, leading to the conversion factor, $c_{85\%\,\text{DM}}$. The grain yield, *Y*, in ton per hectare is then calculated from

$$Y = \frac{G(t_{\text{harvest}}) N c_{\text{gm}^{-2}\rightarrow\text{ton ha}^{-1}}}{c_{85\%\,\text{DM}}}. \quad (41)$$

Parameter derivation

All default model parameters are where possible derived according to the HGCA wheat growth guide (HGCA 2008) and the data from its underlying reports (Sylvester-Bradley 1998, Sylvester-Bradley 1998, Sylvester-Bradley 1998, Spink, Foulkes et al. 2000, Spink, Whaley et al. 2000, Spink, Berry et al. 2004). These data sets give the most consistent set of parameter estimates for a single cultivar within the published literature. The benchmark cultivar used is Mercia. Having defined a consistent set of parameter values for an individual wheat cultivar, individual or sets of parameters can then be adjusted to represent other wheat cultivars and to study their effects on disease tolerance. With time, *t*, defined as the number of Julian Days since the first of January, sowing, GS31, GS39, GS61 and the onset of the rapid fill period take place at $t = -41$, $t = 109$, $t = 141$, $t = 168$ and $t = 184$, respectively. The model simulations are stopped at the end of the total grain-fill period, which occurs at $t = 218$.

Number of leaves and shoot density. A plant produces between 9 and 14 leaves per main shoot (HGCA 2008) and in the model each shoot therefore develops 11 leaves. The mean number of fertile ears per m^2 for the 18 site-years used in the experiments is 578 (Sylvester-Bradley 1998), leading to $N = 578$.

Maximum leaf areas and green area index. The average maximum GAI of all photosynthetic plant tissues is 6.8 (HGCA 2008). At flowering the ear contributes 7% to the total green area (HGCA 2008) leading to a maximum GAI for the leaves and sheaths of 6.3, which given a shoot density of 578 translates to a leaf (plus sheath) area of 109 cm^2 per shoot. Only the top 5 leaves are subject to stem extension and it is therefore assumed that only the sheaths associated with these leaves significantly contribute to light interception. At GS61 the sheaths account for 19% of the total GAI (HGCA 2008), i.e. 3.8% per leaf sheath. At this point the top 4 leaves make up 73% of the total available green area and hence it can be calculated that on average 17% of the green area of each leaf plus sheath can be attributed to the sheath. Consistent leaf area data are limited and highly variable and therefore we use maximum leaf area sizes for the top five leaves averaged over 22 winter wheat varieties as reported by Milne, Paveley et al. (2003) to determine the proportional differences in leaf areas. No data is available for the lower leaves, but a general assumption is that the leaf areas decrease with leaf number (e.g. Milne, Paveley et al. 2003). These data represent leaf lamina areas only and hence for the top five leaves an additional 17% due to leaf sheaths has to be added. Under the assumption that at GS39 only the top eight leaves are still alive, the total leaf and sheath area of 109 cm^2 is divided over these eight leaves according to their proportional area contributions. The resultant leaf areas are given in Table SI1.1.

Leaf development timings. Leaf emergence dates are given in the HGCA wheat growth guide (HGCA 2008) and were converted to Julian days. Leaves generally emerge a phyllocron (*P*) apart (HGCA 2008) and L1 has generally fully emerged 3*P* before anthesis (Jamieson, Semenov et al. 1998). For Mercia the average phyllocron length is 112 °C days (Sylvester-Bradley 1998). Leaf initiation occurs roughly 65 degree days before leaf emergence (Milne, Paveley et al. 2003). Given the average temperature at the time of leaf emergence the time of leaf initiation and the growth rates in Julian days can be determined, leading to growth rates of 0.38, 0.38, 0.38, 0.29, 0.29, 0.29, 0.21, 0.21, 0.18, 0.18 and 0.18 for leaves L1 to L11, respectively. Leaf life-spans are a function of both leaf size and the phyllocron length, with life-spans ranging between 4*P* and 9*P* and whereby larger leaves are associated with longer life-spans (Lawless, Semenov et al. 2005). Senescence occurs at a constant rate of 0.05 ℃ days and given the average phyllocron length at the onset of senescence the senescence rate can be calculated to be 0.85, 0.85, 0.85, 0.85, 0.7, 0.55, 0.55,

0.55, 0.55, 0.4 and 0.3 *JD*, for L1 to L11, respectively. In general the senescence period takes about 1.8*P* (Lawless, Semenov et al. 2005). See Table SI1.1 for a summary.

Disease dynamics. In the model we consider the presence of an epidemic caused by *Zymoseptoria tritici* comb. nov. (Septoria tritici leaf blotch; previously known as *Mycosphaerella graminicola*), the most damaging foliar disease of UK wheat, resulting in significant yield losses every year (Paveley, Blake et al. 2012). Although substantial *Z. tritici* infection is common on the leaf lamina of wheat, substantial infection on stems are rare and, hence, we ignore infections on the leaf sheaths. As previously defined, only the top five leaves have considerably sized leaf sheaths as a result of stem extension, whereby on average 17% of the green area of each leaf plus sheath can be attributed to the sheath. The maximum severity, S_{max}, of the top five leaves is therefore, 0.83, whereas it is 1 for the lower leaves. The area taken up by lesions caused by the initial spore influx on a leaf, S_0, is set to 0.022, i.e. a thousandth of the maximum flag leaf area. The epidemic on leaf *n* is assumed to commence when the leaf is halfway between initiation and emergence, i.e. $t_{\mathrm{onset}_n} = t_{\mathrm{initiation}_n} + 0.5(t_{\mathrm{emergence}_n} - t_{\mathrm{initiation}_n})$. For the rosette leaves $t_{\mathrm{onset}_{\mathrm{rosette}}} = t_{\mathrm{initiation}_{11}} + 0.5(t_{\mathrm{emergence}_{11}} - t_{\mathrm{initiation}_{11}})$. The initial growth rate of the epidemic on a leaf, r_n, can be approximated by $r_n = \frac{R_0}{\text{generation time}} \approx \frac{R_0}{(\mathrm{LP+IP})/\mathrm{Temp}(t_{\mathrm{initiation}_n}+0.5(t_{\mathrm{emergence}_n}-t_{\mathrm{initiation}_n}))}$, with LP and IP the latent period and infectious period, respectively. Estimates of r for the top three leaf layers combined were derived according to a large data set of disease severity observations (te Beest, Shaw et al. 2009). This data set contained leaf layer specific disease severity observations for 24 site/year/cultivar combinations including 7 sites, 10 susceptible cultivars with septoria leaf blotch resistance ratings ≤ 5 and 4 experimental years. Epidemics with a maximum disease severity $\leq 5\%$ were excluded from the analysis and observations of leaf 3 emergence (usually around GS32) were used to ensure that the canopy emergence was similar for all individual epidemics. This data analysis found r values ranging from 0.071 to 0.787 JD^{-1} with a mean of 0.192. Under outdoor conditions the latent period of *Z. tritici* was found to be around 275 °C days (Lovell, Hunter et al. 2004). The infectious period of the lesions can be derived from the experiments performed by Eyal (1971) and was found to be 30 days, i.e. around 450 °C days. Sylvester-Bradley (1998) report seasonal temperature, Temp, data averages for 6 UK sites. These data can be described well by the following sin function: $\mathrm{Temp} = 9.76 + 6.72\sin(0.93t + 260.12)$. With these data the LP and IP can be converted from degree days to *JD* by dividing the mean LP in degree days by the temperature experienced at the start of the epidemic. Given the average estimate of the generation time of 725 degree days and the average temperature around $t_{\mathrm{initiation}_n} + 0.5(t_{\mathrm{emergence}_n} - t_{\mathrm{initiation}_n})$ for the top three leaf layers of 12 °C, R_0 can be calculated to lie around 5.7. The leaf specific initial growth rates can then be calculated from $r_n = \frac{5.7}{725/\mathrm{Temp}(t_{\mathrm{initiation}_n}+0.5(t_{\mathrm{emergence}_n}-t_{\mathrm{initiation}_n}))}$. For the rosette leaves we define $A_{\mathrm{max}_{\mathrm{rosette}}}$ as $\sum_{i=6}^{11} A_{\mathrm{max}_i}$ and assume an average temperature of 8 °C, leading to an maximum severity on leaves 1 to 3 of around 60% which compares well with observations for typical *Z. tritici* epidemics in the absence of control (Paveley, Lockley et al. 2000).

Solar radiation and interception. Sylvester-Bradley et al. (2005) fitted a cosine function through mean daily incident solar radiation data for five sites in east, south and middle England, Wales and Scotland between 1989 and 1994, leading to $i_{\mathrm{vert}} = 1.8$, $i_{\mathrm{amp}} = 8.5$, $i_{\mathrm{freq}} = 58$ and $i_{\mathrm{hor}} = 6.5$.

Table SI1.1 Summary of the maximum leaf areas and leaf development timings with *P* the phyllocron and *JD* the number of calendar days since the 1st January. The average temperature during the life-span of the leaf is estimated according to: (temperature at leaf emergence + temperature two months after leaf emergence)/2.

Leaf	Max. leaf area (cm^2) $A_{\max_n}$	Temp. at emergence (°C)	Time of initiation $t_{\text{initiation}_n}$	Time of emergence $t_{\text{emergence}_n}$	Life-span			Senescence onset $t_{\text{senescence}_n}$	*P* length at senescence onset (JD)	Leaf death t_{death_n}
					in *P*	Av. Temp. [1]	in JD			
L1	21	11	135	141	8	14	64	205	7	218
L2	23	11	126	132	9	14	72	204	7	217
L3	19	11	118	124	8	14	64	188	7	201
L4	16	8	108	116	7	11	70	186	7	199
L5	13	8	98	106	6	11	60	166	8	180
L6	8	8	88	96	5	11	50	146	10	164
L7	5	6	74	85	4	9	48	133	10	151
L8	5	6	59	70	4	9	48	118	10	136
L9	5	5	41	54	4	7	64	118	10	136
L10	4	5	20	33	4	7	64	97	14	122
L11	4	5	-12	1	4	6	76	77	19	111

The mean light extinction coefficient of wheat, κ, is 0.53 (Shearman, Sylvester-Bradley et al. 2005). For simplicity it is assumed that senesced tissues still fully contribute to light interception, i.e. $k_{\text{reduction}} = 0$. Additional simulations for different $k_{\text{reduction}}$ values however show that the total DM fixated per shoot per day is hardly affected by the fractional contribution to light interception and shading by senesced tissues. This is probably because most senesced tissues are found relatively low down in the canopy and hence contribute little to light interception in the first place.

Photosynthesis and dry matter accumulation. Both senesced and diseased tissues are assumed to no longer contribute to photosynthesis. Bingham and Topp (2009) report a photochemical efficiency, α, of 0.23 mol CO_2 MJ^{-1}, a θ (degree of curvature of the gross photosynthesis versus intercepted radiation relationship) of 0.97 and rate of decline of the maximum rate of photosynthesis down the canopy, λ, of 0.7. Driever, Lawson et al. (2014) report a light saturated rate of photosynthesis of the uppermost leaf layer for Mercia of 28.2 μmol CO_2 m^{-2} s^{-1}.Given an average daily temperature of 15 °C during the months of April to August the light saturated rate of photosynthesis of the uppermost leaf layer, P^0_{max}, can be calculated to be 1.83 mol CO_2 m^{-2} leaf d^{-1}.

The carbon use efficiency, CUE, of wheat as reported in the literature varies considerably. For example, Monje and Bugbee (1998) report CUE values between 0.53 and 0.61 for different crop development stages, Tanaka and Osaki (1983) report a CUE value for wheat under field conditions, Gent (1994) reports a value of 0.73 at anthesis with an average of 0.6 and van den Boogaard et al. (1996) report values between 0.69 and 0.72. As shown by Albrizio and Steduto (2003) the CUE strongly depends on temperature, whereby higher CUE values are associated with lower temperatures. Most the fore mentioned experiments are performed at relatively high temperatures (up to 23 °C), whereas our model works with and average temperature of only 15 °C, which means that the above mentioned CUE values are too low. From Albrizio and Steduto (2003) we can derive the wheat CUE value for an average temperature of 15 °C to be 0.79. The amount of assimilates collected in mol CO_2 is converted to gram carbon by multiplying by a factor 12, such that $\text{conv}_{\text{mol CO2}\rightarrow\text{g C}} = 12$. The carbon mass fraction in wheat biomass is 0.47 (Vertregt and Penning de Vries 1987).

Pre-anthesis biomass partitioning. The average stem height at GS31 and GS61 and the start of the rapid-fill period, $h_{\text{stem}}(t_{\text{GS31}})$, $h_{\text{stem}}(t_{\text{GS61}})$ and $h_{\text{stem}}(t_{\text{rapid-fill}})$, are 0.11, 0.64 and 0.66 m, respectively. Given a stem diameter of 3.3 mm and a fractional stem thickness of 0.35 (Saint Pierre, Trethowan et al. 2010) we can calculate $c_{\text{stem length}\rightarrow\text{volume}} = \pi(0.5 \cdot 0.0033)^2 0.35 = 2.99 \cdot 10^{-6}$. Given a specific weight of the structural stem of 1.36 g DM m^{-1} stem (Sylvester-Bradley 1998), we can then calculate $c_{\text{stem volume}\rightarrow\text{DM}} = \frac{1.36}{2.99 \cdot 10^{-6}} = 454850$. The paper by Beed et al. (2007) suggests that a 57% reduction in light availability between GS31 and GS61 and hence a 57% reduction in $A_{\text{GS31-GS61}}$ (from 1.52 to 0.65 g C $stem^{-1}$), leads to a 13% reduction in dry matter accumulation within the structural stem and hence a 13% reduction in $c_{\text{stem volume}\rightarrow\text{DM}}$ (from 454850 to 395720). From this information we derive $a = 351113$ and $b = 68472$. The green and senesced leaf tissue areas at GS31 and GS61 can be derived from (1) and the specific leaf area weight, $c_{\text{leaf area}\rightarrow\text{DM}}$ is about 32 g m^{-2} (Gifford 1995). Beed et al. (2007) suggests that a 57% reduction in light availability between GS31 and GS61 leads to a 9% reduction in dry matter accumulation within the leaves and hence a 9% reduction in $c_{\text{leaf area}\rightarrow\text{DM}}$. From this information we derive $c = 26.7$ and $d = 3.5$. The root lengths of an

average shoot at GS31 and GS61 are 15 and 51 m per shoot, respectively (HGCA 2008). The shoot mass at anthesis is 1.05 t/ha, so given that root weight and length are proportional (HGCA 2008), the root masses at anthesis and GS61 can be calculated to be $m_{\text{roots}}(t_{\text{GS31}}) = 0.05$ and $m_{\text{roots}}(t_{\text{GS61}}) = 0.17$ g shoot^{-1}, respectively.

It is assumed that before GS31 all dynamics are roughly the same for all wheat cultivars and hence $\text{DM}_{\text{ear GS31}}$ and $\text{DM}_{\text{stem reserves GS31}}$ are set to the constant values of $\text{DM}_{\text{ear GS31}} = 0$ and $\text{DM}_{\text{stem reserves GS31}} = 0.05$ (Sylvester-Bradley 1998). Between GS31 and GS61 and under default conditions a total DM weight of about 1.52 g is fixated. Over this period the WSC increases from 0.05 to around 0.38 and the ear DM increases from 0 to around 0.3 (Sylvester-Bradley 1998), leading to $f_{\text{ear}_{\text{pre-anthesis}}} = 0.48$. Under the assumption of a maximum fractional investment into ear development, $f_{\text{max}_{\text{pre-anthesis}}}$, of 1, the shape parameter for the fractional contribution to the ear, γ, can then be calculated to be around 0.72. We subsequently choose the shape parameter for the function describing the relationship between the stem storage volume and γ such that for the default stem volume $\gamma = 0.72$ as previously calculated and such that when the stem volume is zero $\gamma = 0$, in which case all biomass available for the ear and stem reserves is allocated to the ear. This leads to $s_1 = 375808$.

Shearman, Sylvester-Bradley et al. (2005) find that the stem WSC DM weights at anthesis plus 75 °C days for 8 wheat cultivars lie within the range of 244 to 391 g m^{-2}. Given the stem storage capacity, S_{capacity}, equals $h_{\text{stem}}(t_{\text{GS61}})\pi(0.5D_{\text{stem}})^2 T_{\text{stem}} s_2$, the WSC DM weights per m^2 are then given by NS_{capacity}. Using the midpoint value of the Shearman, Sylvester-Bradley et al. (2005) data, i.e. 318 g m^{-2}, the stem storage capacity slope parameter, s_2, can then be calculated to be 287075.

Number of grains. The mean number of grains per ear at harvest for Mercia is 34 (Sylvester-Bradley 1998). Clarke et al. (2012) finds that the semi-dwarfing allele leads to an increase of 9% in the number of grains per m^2, which is associated with a 24% increase in ear DM at anthesis. In our model the shoot density is kept constant during the growing season and hence a 9% increase in the number of grains per m^2 means a 9% increase in the number of grains per ear. This suggests that $\tau = 59.30$ and $\upsilon = 0.15$.

Slow-fill period. Between GS61 and the onset of the rapid grain-fill period and under default conditions a total DM weight of 0.46 g is fixated. For two French wheat cultivars Bancal (unpublished data) recorded the increase in grain dry weights and WSC dry weights during the first 300 °C days after anthesis (roughly 3 weeks post-anthesis), which can be compared to the slow-fill period. From these values the fractional grain versus WSC investment post-anthesis can be calculated to vary between 0.50 and 0.59. The fractional grain versus WSC investment post-anthesis for Mercia is set to 0.55. Given the assumption of a maximum fractional investment into ear development, $f_{\text{max}_{\text{slow-fill}}}$, of 1, the shape parameter for the fractional contribution to the ear, δ, can be calculated to be around 1.79. We subsequently choose the shape parameter for the function describing the relationship between the stem volume and δ such that for the default stem volume $\delta = 1.79$ as previously calculated and such that when the stem volume is zero $\delta = 0$, in which case all biomass available for the ear and stem reserves is allocated to the ear. This leads to $s_3 = 903597$.

Trujillo (PhD, unpublished) reports the potential grain weight of 26 wheat cultivars to vary between 39.5 to 56.2 mg in de-grained ears which is believed to be a good indicator for potential grain weight. The upper asymptote, ε, of the relationship between the dry matter

allocation to an individual grain during the slow fill period, $\frac{\mathrm{DM_{grain}}(t_{\mathrm{rapid-fill}})}{\mathrm{NG}}$, and the maximum grain DM content of the grain, $V_{\max}$, is therefore set to 0.048. At harvest a Mercia grain weighs on average 39 mg at 100% DM (Sylvester-Bradley 1998), which given 34 grains per ear leads to a dry matter weight per shoot of 1.30 at 100% DM and a yield of 8.9 t/ha at 85% DM. There is a general view that under the 'light-limited' conditions experienced in the UK, the yield of current elite varieties is marginally sink limited. This means that in the absence of disease there is generally enough assimilate to fill all the grains to their maximum capacity. It is therefore assumed that under the default model parameters $V_{\max} = 0.039$, leading to $\mu = 0.0016$.

Rapid-fill period. On average five percent of the stem reserves does not get remobilised before harvest (Sylvester-Bradley 1998), leading to a remobilisation efficiency of $m_{eff} = 0.95$. The remobilisation rate, r_{mob}, was chosen such that at the end of the total grain-fill period, i.e. 50 days after anthesis (HGCA 2008), only five percent of the stem reserves remain and the maximum grain weight is reached, leading to $r_{mob} = 0.088$. The conversion factor $c_{gm^{-2}\rightarrow ton\ ha^{-1}}$ to convert from g m^{-2} to ton ha^{-1} is 0.01 and the conversion factor $c_{85\%\ DM}$ to convert pure dry weight to grain yields expressed as tonnes per hectare @ 85% DM is given by 0.85.

Current genotypic variability in plant traits

The trait ranges described here are based on genotype means as found in the literature.

Shoot density. For 64 wheat cultivars the number of ears per m2 at harvest was found to vary between 294 and 540, whereas the mean number of fertile ears per m^2 for the 18 site-years was 578 according tp Sylvester-Bradley (1998). In the model the shoot density is represented by the number of fertile ears per m^2 and the shoot densities is therefore assumed to vary between 294 and 578.

Growth periods. Shearman, Sylvester-Bradley et al. (2005) report GS31 and GS61 timings for eight UK-bred winter wheat cultivars, leading to a pre-anthesis period of 51-65 days. Bancal (2008) reports GS31 and GS61 timings for 6 French winter wheat cultivars, leading to a pre-anthesis period of 58-63 days. Clarke, Sylvester-Bradley et al. (2012) measured the pre-anthesis period for 64 wheat cultivars and found it to vary between 565 and 669 °C days. Given an average temperature of 10.3 degrees across this period (Clarke, Sylvester-Bradley et al. 2012), this gives a pre-anthesis period between 55 and 65 days. The range was hence set to 51 to 65 Julian days.

The HGCA report by Sylvester-Bradley (1998) states that the slow-fill period for cv. Mercia generally takes between two to three weeks. The cell division period for wheat cv. Sonora was found to take roughly 18 days (Singh and Jenner 1984) whereas Shearman (2001) found the cell division period of four winter wheat cultivars to vary between five and nine days. The range was hence set to 5 to 21 Julian days.

The total grain filling period was found to range between 605.5 and 698.7 degree days for 4 winter wheat cultivars (Shearman 2001) grown at Sutton Bonnington. With a long term average temperature of 15.2 degrees Celsius for this site across the grain-fill period (Clarke, Sylvester-Bradley et al. 2012) the total grain-fill period is found to vary between 40 and 46 days. For 64 wheat cultivars the total grain-fill period was found to vary between 711 and 827 degree days with an average temperature of 15.5 degrees Celcius (Clarke, Sylvester-Bradley et al. 2012), leading to a total grain-fill period of 46 to 53 days. Given a default slow-fill period of 16 days,

the rapid-fill period can be calculated to range between 24 and 37 days and remobilisation rate can be calculated to range between 0.081 and 0.125.

Carbon fixation traits. Bancal (unpublished data) recorded maximum canopy leaf area index values for 18 wheat cultivars between 3.26 and 7.51.

According to Shearman, Sylvester-Bradley et al. (2005) the range of flag leaf areas for UK winter wheat cultivars is 22.1 to 39.7 cm^2, based on eight cultivars. The benchmark flag leaf area of Mercia was calculated to be 21 cm^2 and hence the total flag leaf area range is set to vary between 21 and 40 cm^2.

Shearman, Sylvester-Bradley et al. (2005) report the light extinction coefficient of eight winter wheat cultivars to range between 0.48 and 0.58. Thorne, Pearman et al. (1988) report the light extinction coefficient of cultivars Hustler and Avalon to vary between 0.37 and 0.55 with a mean of 0.46. This leads to an overall range of 0.37 to 0.58.

For 64 different wheat genotypes the light saturated photosynthesis rate of the uppermost leaf layer (P_{max}^0) was found to vary between 19.8 and 32.0 µmol CO_2 m^{-2} s^{-1}, i.e. 1.71-2.76 mol CO2 m^{-2} d^{-1} (Driever, Lawson et al. 2014). In the experiments measurements took place at 20°C whereas in the model an average daily temperature of only 15°C is assumed. Since P_{max}^0 is temperature sensitive, the value was adjusted for the above described temperature difference according to Thornley and Johnson (1990) under the additional assumption that photosynthetic activity ceases at 0°C, leading to a range of 1.28-2.07.

Albrizio and Steduto (2003) report carbon use efficiency (CUE) values measured at different temperatures. For example, the CUE at 23°C is 0.71, whereas at 15°C (the temperature used in the model simulations) it is 0.78. Monje and Bugbee (1998) report the CUE to vary between 0.56 and 0.61 when measured at 23°C and van den Boogaard, Goubitz et al. (1996) report the CUE of ten wheat cultivars to vary between 0.69 and 0.72 when measured at 23°C. Rescaling these values to measurements at 15°C using the data from Albrizio and Steduto (2003) leads to a range of 0.62 to 0.79.

Sink capacity traits. Shearman, Sylvester-Bradley et al. (2005) summarise ear and water soluble carbohydrate (WSC) dry weights at anthesis for eight wheat cultivars. From these values the fractional ear versus WSC investment pre-anthesis can be calculated to vary between 0.37 and 0.49. Keeping all other parameters at their default values s_1 can be calculated to vary between 357409 and 584695.

For 64 different wheat genotypes the number of grains per ear was found to vary between 32.5 and 55.2 (Clarke, Sylvester-Bradley et al. 2012). The same report showed that a 24% increase in ear dry matter weight at anthesis leads to a 9% increase in the number of grains per m^{-2}. Because the model assumed a constant shoot density this suggests a 9% increase in the number of grains per ear, *NG*. Given the assumption that the genetic variability in the number of grains per ear is represented by an upward or downward shift of the relationship between ear dry matter accumulation pre-anthesis and the number of grains per ear rather than a change in the shape of the relationship the maximum number of grains per ear, τ, can be calculated to vary between 57.37 and 97.44.

For two French wheat cultivars Bancal (unpublished data) recorded the increase in grain dry weights and WSC dry weights during the first 300 °C days after anthesis (roughly 3 weeks post-anthesis), which can be compared to the slow-fill period. From these values the fractional grain versus WSC investment post-anthesis can be calculated to vary between 0.50 and 0.59. Keeping all other parameters at their default values s_3 can be calculated to vary between 767462 and 1104396.

Shearman (2001) reports the potential grain weight of ten winter wheat cultivars to vary between 42.3 and 50.4 mg. Trujillo (PhD, unpublished) reports a similar range for 26 wheat cultivars of 39.5 to 56.2 mg in de-grained ears which is believed to be a good indicator for potential grain weight. The maximum grain DM content of the grain, V_{max}, is therefore assumed to vary between 0.040 and 0.056.

Stem storage capacity traits. For 64 different wheat genotypes the stem height at anthesis was found to vary between 0.64 and 1.10 m (Clarke, Sylvester-Bradley et al. 2012).

For 28 different wheat cultivars the stem diameter was found to vary between 3.24 and 4.12 mm (Berry, Sylvester-Bradley et al. 2007).

For ten spring wheat genotypes the fractional stem thickness was found to vary between 33 and 38% (Saint Pierre, Trethowan et al. 2010).

Shearman, Sylvester-Bradley et al. (2005) find that the stem WSC dry matter weights at anthesis plus 75 °C days for 8 wheat cultivars lie within the range of 244 to 391 g m^{-2}. The WSC dry matter weights per m^2 are given by the shoot density multiplied by the stem storage capacity. The stem storage capacity slope parameter, s_2, which is a measure for how efficiently a unit stem can be used for stem reserves storage can then be calculated to vary between 220341 and 353087.

Ehdaie, Alloush et al. (2006) found the stem specific weight (structural stem tissues and water soluble carbon) of nine spring wheat and two winter wheat cultivars to vary between 1.63 and 2.46 g m^{-1} stem. Given that roughly 66% of the total stem weight is made up of the structural tissues (Sylvester-Bradley 1998) this leads to a stem specific weight range of 1.08 to 1.62 g m^{-1} stem. Parameter *a* can then be calculated to vary between 257467 and 438069.

Traits associated to tissue weights. For low radiation levels as observed under field conditions Rawson, Gardner et al. (1987) found the specific leaf weight of two wheat cultivars to vary between 31.8 and 32.9 g m^{-2}. Shearman, Sylvester-Bradley et al. (2005) found the specific leaf weight of eight wheat cultivars to vary between 40.8 and 54.0. It is assumed that *c* represents a measure for the genetic variability in specific leaf weight, whereas *d* represents a measure of the effect of reduced overall assimilate availability due to, for example, shading on the specific leaf weight. From this *c* can be derived to vary between 26.5 and 48.7.

The cultivar mean total root mass at anthesis of six wheat cultivars was reported to vary between 661 and 842 kg ha^{-1} (Ford, Gregory et al. 2006), i.e. 0.11-0.15 g per shoot. For Mercia, the root length at anthesis was found to be 31 km m^{-2}, i.e. 51 m $shoot^{-1}$ whilst assuming a shoot density of 604 m^{-2} (HGCA 2008). The specific root weight was 0.0033 g m^{-1} (HGCA 2008), leading to a total root mass of 0.17 g per shoot. This is larger than that found for other cultivars, but the difference can be explained by the statement in the paper by Ford, Gregory et al. (2006) that the root biomass of modern varieties has declined from 1 t ha^{-1} to 0.75 t ha^{-1} (a 25% reduction) as shoot biomass has increased. The measurements in Ford, Gregory et al. (2006) represent relatively modern cultivars whereas Mercia is a historic cultivar. Assuming a direct relationship between root biomass and root length this explains the 13% larger root mass of Mercia. The root mass range was hence set to 0.11-0.17.

Literature cited

Albrizio, R. and P. Steduto (2003). "Photosynthesis, respiration and conservative carbon use efficiency of four field grown crops." Agricultural and Forest Meteorology **116**: 19-36.

Bancal, P. (2008). "Positive contribution of stem growth to grain number per spike in wheat." Field Crops Research **105**: 27-39.

Beed, F. D., N. D. Paveley and R. Sylvester-Bradley (2007). "Predictability of wheat growth and yield in light-limited conditions." Journal of Agricultural Science **145**: 63-79.
Berry, P. M., R. Sylvester-Bradley and S. Berry (2007). "Ideotype design for lodging-resistant wheat." Euphytica **154**: 165-179.
Bingham, I. J. and C. F. E. Topp (2009). "Potential contribution of selected canopy traits to the tolerance of foliar disease by spring barley." Plant Pathology **58**: 1010-1020.
Clarke, S., R. Sylvester-Bradley, J. Foulkes, D. Ginsburg, O. Gaju, P. J. Wemer, E. Flatman and L. Smith-Reeve (2012). Adapting wheat to global warming, HGCA**:** 131.
Driever, S. M., T. Lawson, P. J. Andralojc, C. A. Raines and M. A. J. Parry (2014). "Natural variation in photosynthetic capacity, groath, and yield in 64 field-grown wheat genotypes." Journal of Experimental Botany.
Ehdaie, B., G. A. Alloush, M. A. Madore and J. G. Waines (2006). "Genotypic variation for stem reserves and mobilization in wheat: I. Postanthesis changes in internode dry matter." Crop Science **46**: 735-746.
Eyal, Z. (1971). "Kinetics of pycnospore liberation in *Septoria tritici*." Can J Bot **49**: 1095-1099.
Ford, K. E., P. J. Gregory, M. J. Gooding and S. Pepler (2006). "Genotype and fungicide effects on late-season root growth of winter wheat." Plant and Soil **284**: 33-44.
Gent, M. P. N. (1994). "Photosynthate reserves during grain filling in winter wheat." Agronomy Journal **86**: 159-167.
Gifford, R. M. (1995). "Whole plant respiration and photosynthesis of wheat under increased CO_2 concentration and temperature: long-term vs. short-term distinctions for modelling." Global Change Biology **1**: 385-396.
HGCA (2008). The wheat growth guide.
Jamieson, P. D., M. A. Semenov, I. R. Brooking and G. S. Francis (1998). "*Sirius*: a mechanistic model of wheat response to environmental variation." European Journal of Agronomy **8**: 161-179.
Johnson, I. R. and J. H. M. Thornley (1984). "A model of instantaneous and daily canopy photosynthesis." Journal of Theoretical Biology **107**: 531–545.
Lawless, C., M. A. Semenov and P. D. Jamieson (2005). "A wheat canopy model linking leaf area and phenology." European Journal of Agronomy **22**: 19-32.
Lovell, D. J., T. Hunter, S. J. Powers, S. R. Parker and F. van den Bosch (2004). "Effect of temperature on latent period of septoria leaf blotch on winter wheat under outdoor conditions." Plant Pathol **53**: 170-181.
Milne, A., N. D. Paveley, E. Audsley and P. Livermore (2003). "A wheat canopy model for use in disease management decision support systems." Annals of Applied Biology **143**: 265-274.
Monje, O. and B. Bugbee (1998). "Adaptation to high CO_2 concentration in an optimal environment: radiation capture, canopy quantum yield and carbon use efficiency." Plant Cell and Environment **21**: 315-324.
Paveley, N., J. Blake, P. Gladders and V. Cockerell (2012). HGCA wheat disease management guide 2012. E. Boys**:** 1-32.
Paveley, N. D., D. Lockley, T. B. Vaughan, J. Thomas and K. Schmidt (2000). "Predicting effective fungicide doses through observation of leaf emergence." Plant Pathology **49**: 748-766.
Rawson, H. M., P. A. Gardner and M. J. Long (1987). "Sources of variation in specific leaf area in wheat grown at high temperature." Australian Journal of Plant Physiology **14**: 287-298.

Saint Pierre, C., R. Trethowan and M. Reynolds (2010). "Stem solidness and its relationship to water-soluble carbohydrates: association with wheat yield under water deficit." Functional Plant Biology **37**: 166-174.
Shearman, V. J. (2001). Changes in yield limiting processes associated with the genetic improvement of wheat PhD, University of Nottingham.
Shearman, V. J., R. Sylvester-Bradley, R. K. Scott and M. J. Foulkes (2005). "Physiological processes associated with wheat yield progress in the UK." Crop Science **45**: 175-185.
Singh, B. K. and C. F. Jenner (1984). "Factors controlling endosperm cell number and grain dry weight in wheat: effects of shading on intact plants and of variation in nutritional supply to detached, cultured ears." Australian Journal of Plant Physiology **11**: 151-163.
Spink, J., J. M. Foulkes, A. Gay, R. Bryson, P. Berry, R. Sylvester-Bradley, T. Semere, R. W. Clare, R. K. Scott, P. S. Kettlewell and G. Russell (2000). Reducing winter wheat production costs through crop intellegence information on variety and sowing date, rotational position, and canopy management in relation to drought and disease control. **HGCA Project Report 235:** 135.
Spink, J. H., P. Berry, C. Theobald, D. Sparkes, A. Wade and A. Roberts (2004). The effect of location and management on target drilling rate for winter wheat. **HGCA Project Report 361:** 154.
Spink, J. H., J. Whaley, T. Semere, A. Wade, D. Sparkes and J. Foulkes (2000). Prediction of optimum plant population in winter wheat. **HGCA Project Report No. 234:** 59.
Sylvester-Bradley, R. (1998). Assessments of wheat growth to support its production and improvement. **Volume I: The wheat growth digest; Methods for in-field crop assessment; Forecasting crop progress for wheat:** 128.
Sylvester-Bradley, R. (1998). Assessments of wheat growth to support its production and improvement. **Volume II: How to run a reference crop:** 78.
Sylvester-Bradley, R. (1998). Assessments of wheat growth to support its production and improvement. **Volume III: The dataset:** 50.
Sylvester-Bradley, R., P. M. Berry, J. Wiseman and B. Cottrill (2005). Yields of UK crops and livestock: physiological and technological constraints, and expectations of progress to 2050', DEFRA Project No IS0210**:** Final Report, 21 pp.
Tanaka, A. and M. Osaki (1983). "Growth and behavior of photosynthesized ^{14}C in various crops in relation to productivity." Soil Science and Plant Nutrition **29**: 147-158.
te Beest, D. E., M. W. Shaw, S. Pietravalle and F. van den Bosch (2009). "A predictive model for early-warning of Septoria leaf blotch on winter wheat." Eur J Plant Pathol **124**: 413-425.
Thorne, G. N., I. Pearman, W. Day and A. D. Todd (1988). "Estimation of radiation interception by winter wheat from measurements of leaf area." Journal of Agricultural Science **110**: 101-108.
Thornley, J. H. M. and I. R. Johnson (1990). Plant and crop modelling: a mathematical approach to plant and crop physiology. Oxford, Clarendon Press.
van den Boogaard, R., S. Goubitz, E. J. Veneklaas and H. Lambers (1996). "Carbon and nitrogen economy of four *Triticum aestivum* cultivars differing in relative growth rate and water use efficiency." Plant Cell and Environment **19**: 998-1004.
Vertregt, N. and F. W. T. Penning de Vries (1987). "A rapid method for determining the efficiency of biosynthesis of plant biomass." Journal of Theoretical Biology **128**: 109-119.

Phytopathology Supporting Information SI3

Article title: **Physiological and developmental traits determining yield tolerance of wheat to foliar diseases**
Authors: van den Berg, F., Paveley, N. D., Bingham, I. J. and van den Bosch, F.

Fig. SI3.1 Green area index for (**a**) individual leaf layers and (**b**) the total canopy. The observed data were derived from p.16 of the HGCA wheat growth guide (HGCA 2008) and include the GAI of the ear structures. The simulated green area indexes are based on the leaf lamina and sheaths only.

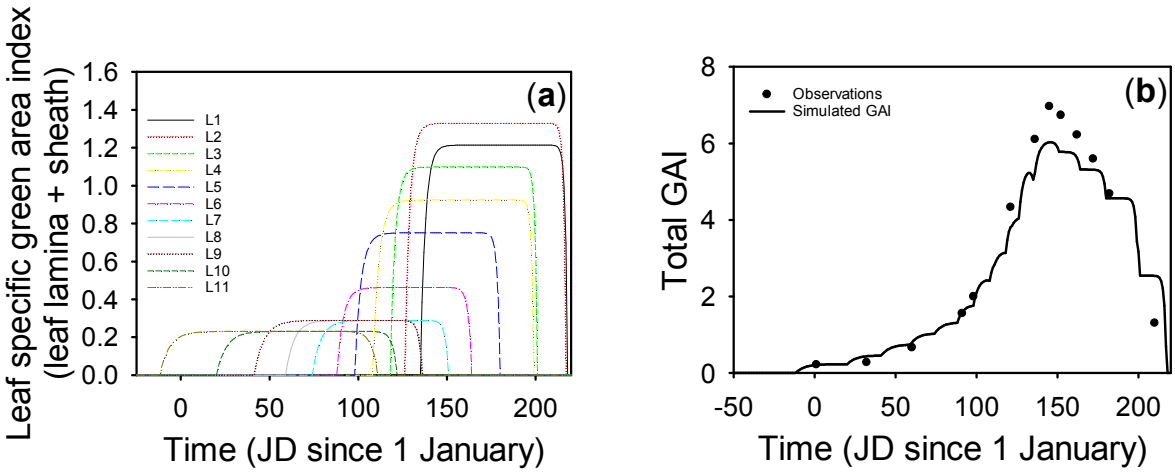

Figure SI3.1

HGCA (2008). The wheat growth guide.

Phytopathology Supporting Information SI3

Article title: **Physiological and developmental traits determining yield tolerance of wheat to foliar diseases**

Authors: van den Berg, F., Paveley, N. D., Bingham, I. J. and van den Bosch, F.

Additional model testing

The model's power to predict yield and yield components under different genotypic and environmental conditions was tested by comparing the model predictions with published data from five independent field experiments. For each data set both a qualitative and a quantitative comparison is made with the associated model outputs. In the model simulations the meteorological data such as incident radiation and temperature are kept at their default values, based on UK averages as explained in detail in Appendix SI1. It is also important to note that the experimental data are collected for a range of cultivars that may or may not include Mercia on which the default model parameters are based. This means that a direct quantitative comparison is not possible. However, a comparison of the percentage change in yield and yield components due to trait changes, can give further insights into the robustness of the model predictions. For the quantitative comparison the midpoint of the x-axis range across all yield components used in the published analysis was determined. For this midpoint value, its associated yield component value was estimated (extrapolation by a straight line took place where necessary). These values then represent the 100% reference point and subsequently all other data points were plotted as the percentage deviation from this reference point.

The main aim of the first experiment, referred to as the seed-rate experiment, was to study the relationship between seed rate (the number of viable seeds per hectare (ha)) and yield response; directly through yield and indirectly through separate yield components (Spink, JH *et al.*, 2000). The experiment considered up to 22 varieties over three years. The seed rates tested in this experiment were strongly correlated with the number of fertile ears per square meter. In the model the shoot density is assumed to represent main stems that all carry an individual fertile ear, and hence for comparison the shoot densities in the model are varied over the range of fertile ears per m^2 as found in the experiment, i.e. 300 – 700. The experiment results show that an increased number of ears per m^2 leads to an increased yield up to a clear optimum, a decreased number of grains per ear, a decrease in WSC storage per stem at GS65 and a roughly constant thousand grain weight (Fig. SI3.1). The model predicts that an increased shoot density leads to increased yields that seem to reach an optimum for higher densities, a decreased number of grains per ear, a decrease in WSC storage per stem at the end of the slow-fill period, with stem storage limitation for lower shoot densities and a roughly constant thousand grain weight (Fig. SI3.1; dash dotted line). Despite the model not explicitly including tillering, it still manages to reproduce the qualitative trends found within the experiments. A comparison of the percentage change in yield components due to changes in the number of ears per m^2 shows that the model predictions are also quite accurate from a quantitative point of view for the amount of WSC at

anthesis and thousand grain weight although the model seems to overestimate the yield increase for high shoot densities (Fig. SI3.1a).

In the second experiment the authors studied the effect of the presence of dwarfing genes on grain number and yield in wheat cultivars (Rebetzke *et al.*, 2011). Hereto the authors compared several near-isogenic and recombinant inbred lines that varied in plant height. They showed that reduced plant heights were associated with an increased grain yield, an increased number of grains per m^2 and an overall decrease in thousand grain weight although this effect was less clear (Fig. SI3.2). In the model the presence of the dwarfing gene is represented by a reduced stem height at anthesis. Furthermore, although dwarfing genes do not affect the stem diameter (Calderini *et al.*, 1996; Chen *et al.*, 2013), there is evidence that dwarfing genes might affect the stem wall thickness, whereby a 36% reduction in stem height leads to a 10% increase in wall thickness (Chen *et al.*, 2013). In the model this effect is represented by the following relationship

$$T_{stem} = 0.447 - 0.152 h_{stem}(t_{GS61}).$$

The qualitative effects of a reduced stem height as predicted by the model closely resemble the experimental data, whereby reduced stem heights at anthesis lead to increased yields and a higher number of grains per m^2. As in the experiments the effect on thousand grain weight is less clear whereby reduced stem heights seem to initially lead to an increase in thousand grain weight, whereas a further decrease in stem height leads to a decrease in thousand grain weight (Fig. SI3.2). However, there is quite a large quantitative difference between the effects of stem height on disease free yield and grains per square meter predicted by the model and those found in the experiment (Fig SI3.2). We do not consider this departure to be a result of poor model calibration as numerous combinations of parameter values were tested, without an improvement in fit. Instead, we believe that part of the problem lies in the nature of the dwarfing allele effects. If the assimilate supply is not increased in direct proportion to the reduction in stem height, for example because of pleiotropic reductions in leaf area and light interception, then increases in grain numbers observed experimentally will be smaller than those predicted by the model. The same outcome will occur if dwarfing alleles have negative pleiotropic effects on grain number formation in ways that offset or supress the impact of an increase in assimilate supply to the ear as these are not accounted for in the model.

The third experiment was designed to assess the influence of fungicides on the green leaf area decline of wheat flag leaves and its consequences for grain yield and mean grain weight (Gooding *et al.*, 2000). Hereto, the authors recorded the grain yield and mean grain weight as well as the area under the curve describing the percentage green leaf area of the flag leaf from first emergence to harvest. The paper used four data sources: three from published experiments conducted during the 1980s (Davies *et al.*, 1984; Gooding, 1988; Lawson, 1989) and one concerning two unpublished experiments conducted in the late 1990s. All experiments were conducted in the UK and although a total of ten winter wheat cultivars were covered by the experiments, once the data had been restricted to those in which *S. tritici* was the main pathogen

to be controlled this left us with a total of six different cultivars. Note that the fungicide regimes differed between the different experiments. Figure SI3.3 compares the experimental data from Gooding *et al.* (2000) with the model predictions and shows that the model can quite accurately predict the qualitative trends observed in the data. From a quantitative point of view the model predictions quite closely match the data for cultivar Consort but less well for the others. The data for cultivar Hereward seem to fit least well. Both cultivars Avalon and Mercia (cultivar representing the model prediction) are classed as historical cultivars, whereas Consort and Hereward are classed as modern cultivars. According to Clarke *et al.* (2012) the model predictions should therefore most closely match the effects found for Avalon, but the effects predicted by the model do in fact most closely match those found for the modern cultivar Consort (Fig. SI3.3).

The fourth experiment was designed to assess losses to yield components in four spring wheat cultivars as a result of infection by a range of *S. tritici* isolates (Ziv & Eyal, 1978). Hereto, the authors recorded the DM yield per head, the thousand grain weight and the number of grains per head as well as the percentage green leaf area of the top three leaves affected with *S. tritici* pycnidia at growth stage 10.5.4 (i.e. the onset of the rapid fill period). In the model the above described disease severity measure can be represented by

$$\left(1-\frac{\sum_{i=1}^{3} GA_i(t_{rapid-fill})[1-S_i(t_{rapid-fill})]}{\sum_{i=1}^{3} GA_i(t_{rapid-fill})}\right)*100\%.$$

Figure SI3.4 compares the experimental data from Ziv and Eyal (1978) with the model predictions and shows that they compare well in both a qualitative and a quantitative nature, whereby increased *S. tritici* severities lead to a reduction in grain DM per shoot, thousand grain weight and number of grains per ear. However, there seems to be a large quantitative departure between model prediction and experimental results for the relationship between green area loss and the change in the number of grains per ear (Fig SI3.4b). The relationship between % green area loss measured at the start of the rapid grain fill period and reduction in the number of grains per m^2 will depend on the rate and timing of disease epidemic development. As grain numbers are determined before anthesis, any reduction caused by disease must occur pre-anthesis. Losses in green leaf area after anthesis will not reduce grain numbers. Thus, differences between model predictions and experimental results in the relationship shown in SI3.4b could arise through differences in the rate of epidemic development and the relative proportions of pre- versus post-anthesis leaf area loss. A later onset but more rapid development of the epidemics in the model compared with experimental plants could account for the departure observed. This can unfortunately not be verified since the experimental study does not provide epidemic timing data.The fifth experiment was designed to assess how *S. tritici* affects yield and yield components under different nitrogen supplies and for 6 different cultivars (Simon *et al.*, 2002). Hereto, the authors recorded the yield, number of grains per ear and thousand grain weight in both the presence and absence of *S. tritici* inoculation, i.e. for each year, cultivar and nitrogen level combination there are only two measurements. The disease severity is measured as the area under the disease progress curve (AUDPC) of the top two canopy leaves accumulated over the duration of the leaf's life-span. Figure SI3.5 compares the experimental data (in the presence of fertilisation) with the model predictions and shows that the

model quite accurately predicts both the qualitative and quantitative trends, whereby infection by *S. tritici* results in a reduction in yield and both other yield components measured.

Although the data for these models are derived under quite contrasting conditions the effect that infection by *S. tritici* has on yield and yield components seem comparable. This can partially be explained by the following. Let's take a closer look at the comparison between the data from Ziv and Eyal (1978) and the model predictions. Spring wheat starts growing earlier than winter wheat and will mature quicker and might therefore have a different ability to collect assimilates leading to a higher or lower yield, number of grains and grain weight than winter wheat. This leads to a different interception point of the y-axis for spring wheat and winter wheat cultivars, although the variability between winter spring cultivars is much greater than that between some of the spring wheat cultivars and the winter wheat cultivar. This suggests that the cultivar effect is much higher than the sowing date effect. Furthermore, to enable comparison between the model and the data, disease severities in the model are chosen such that they match the disease pressures experienced in the data at specific plant growth stages. This means that although the exact epidemic progress curve might differ between the spring wheat and the winter wheat cultivars the overall disease pressures at the time of interest is the same. We therefore pose that although it might be hard to defend a direct quantitative comparison between these datasets and the model due to the very contrasting cultivar types and environmental conditions, a qualitative and indirect quantitative comparison of the trends as described here seems justified.

Fig. SI3.1 Effects of 'environmental' changes, represented through changes in seed rate, on yield and yield components. The experimental data are from Spink, JH *et al.* (2000); data from Table 2 are represented by the dash-dotted line and data from Table 1.6 and experimental years 96/97 and 97/98 are represented by the dotted and dashed line, respectively. The model predictions are represented by the solid red line. See main text for a detailed explanation of the x-axis.

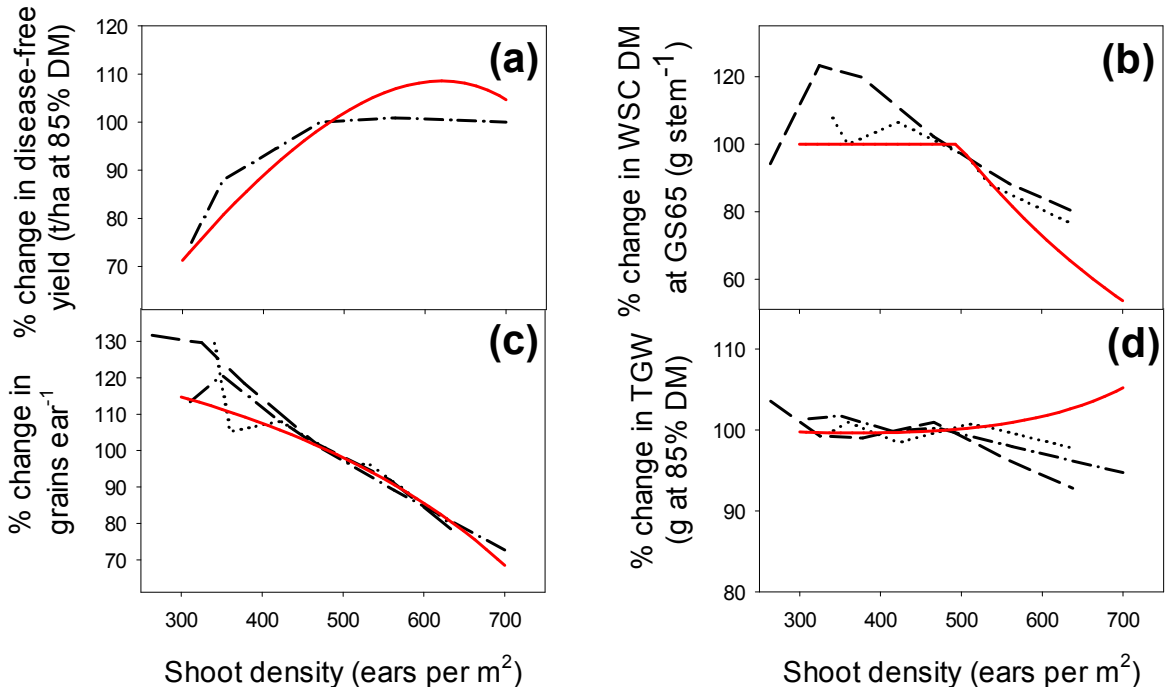

Figure SI3.1

Fig. SI3.2 Effects of the presence of a dwarfing allele, represented by a reduced stem height at anthesis, on yield and yield components according to data presented in Table 1 of Rebetzke *et al.* (2011). The dotted line represents the CM-18/Magnif M1 genotypes; the dashed line represents the Cranbrook/Haldberg genotypes and the red solid line represents the model predictions.

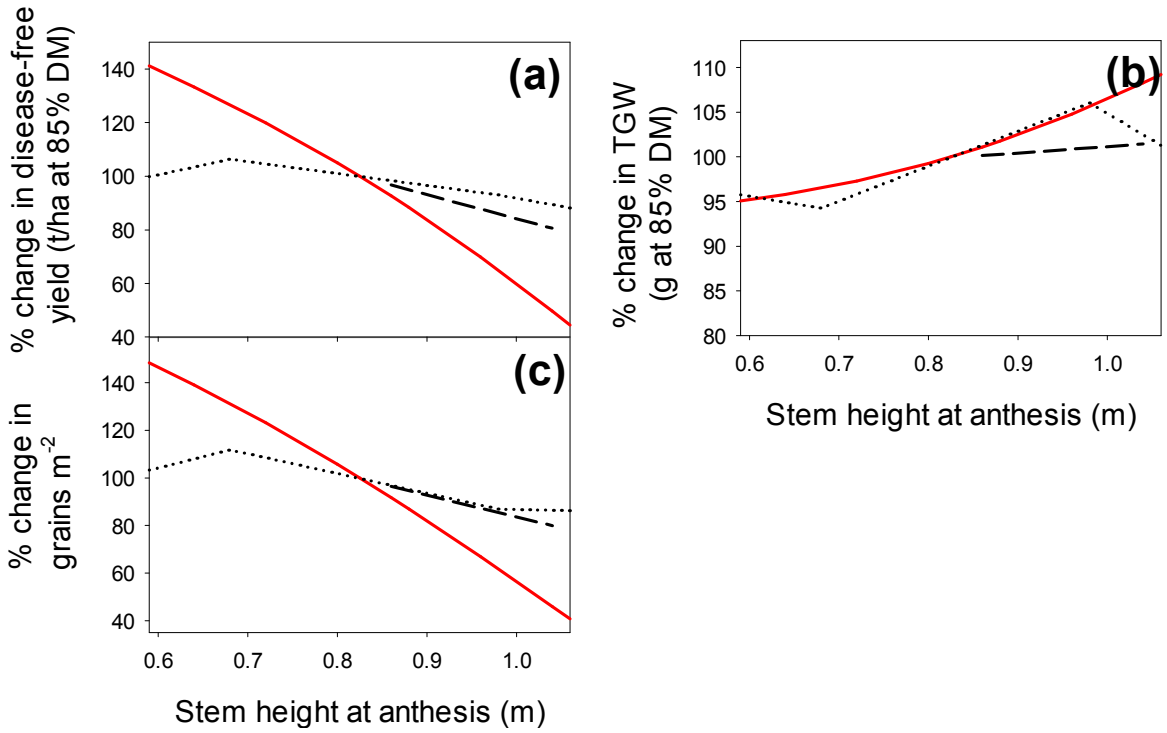

Figure SI3.2

Fig. SI3.3 Effects of *Septoria tritici* severity on yield and yield components according to data presented in Gooding *et al.* (2000). Disease severity is defined as the accumulated reduction in healthy area duration (HAD) of the flag leaf. The red solid line represents the model predictions. The other lines represent differences in cultivar (Avalon (A); Longbow (L); Mission (M); Brimstone (B); Hereward (H) and Consort (C)), fungicides applied (propiconazole (pr); flusilazole (fl); azoxystrobin (az); tridemorph (tr) with in brackets the dose in g ha^{-1}) and experimental year.

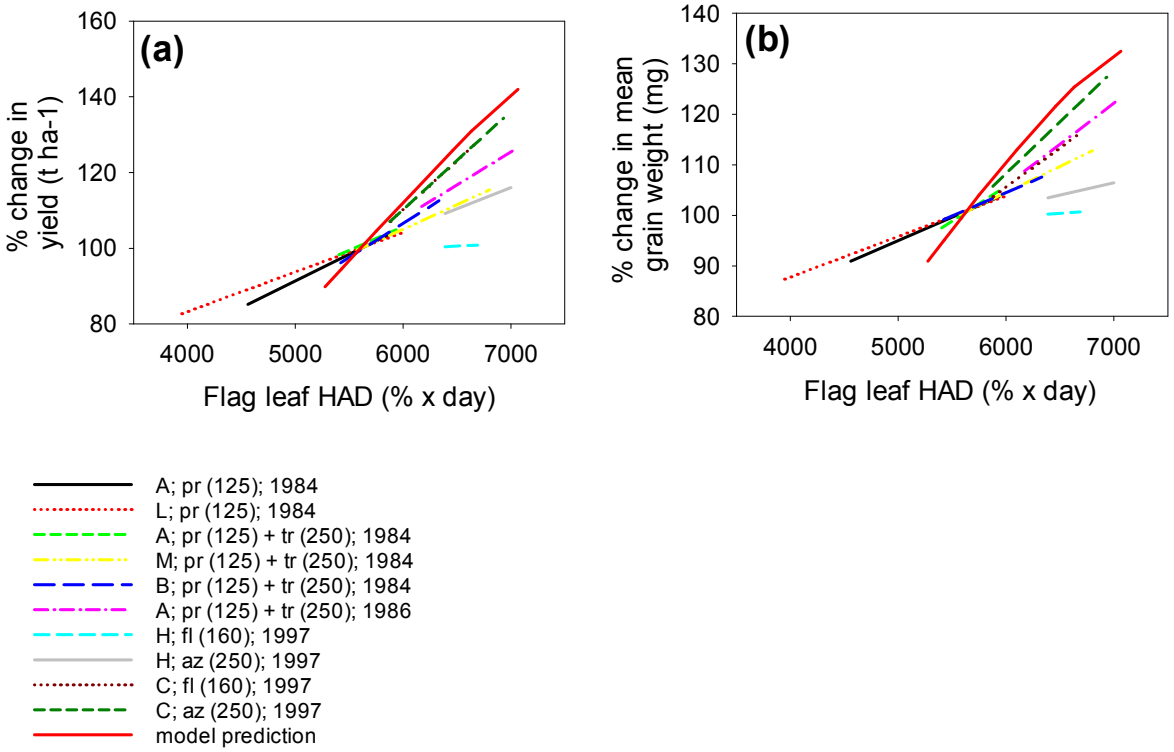

Figure SI3.3

Fig. SI3.4 Effects of *Septoria tritici* severity on yield and yield components according to data presented in Ziv and Eyal (1978). The solid red line represents the model predictions; the other lines represent different cultivars (Bet Dagan 131 (Be); Miriam (M); Yafit (Y); Barkai (Ba)) and experimental years; with GA, the green leaf area.

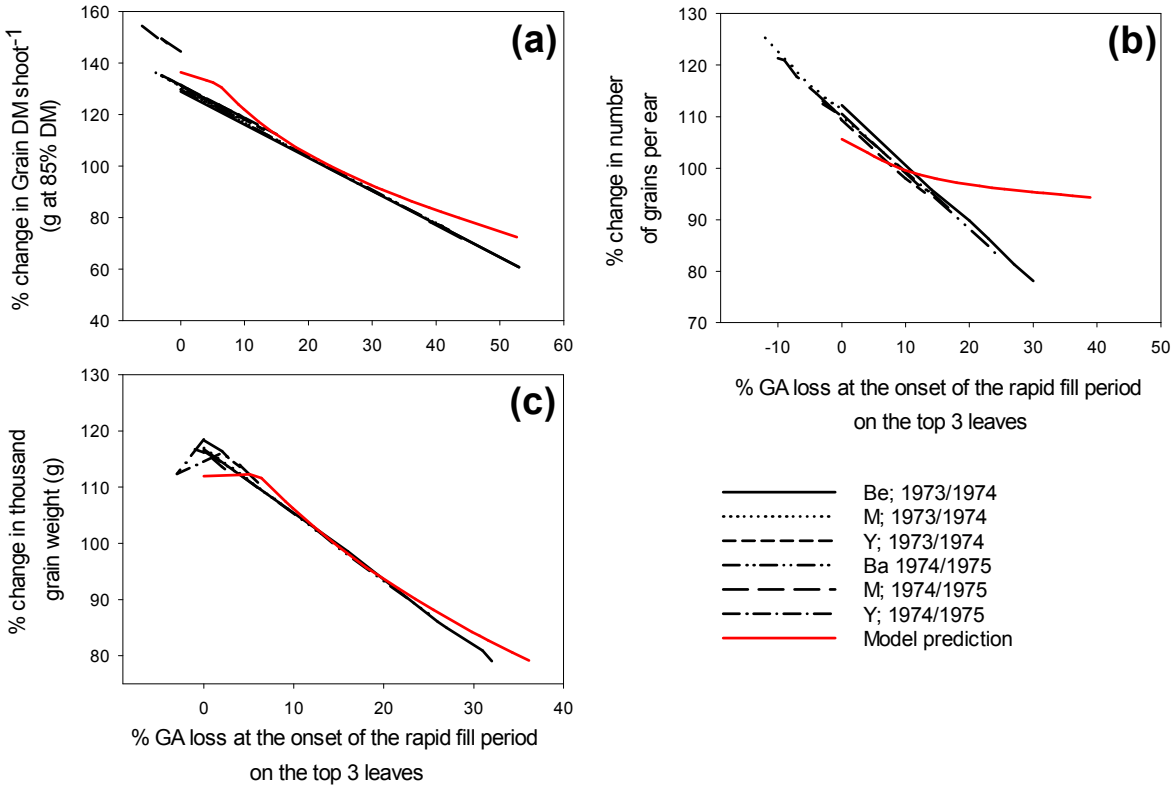

Figure SI3.4

Fig. SI3.5 Effects of *Septoria tritici* severity on yield and yield components according to data presented in Simon *et al.* (2002). The solid red line represents the model predictions; the other lines represent different cultivars (Buck Ombu (BO); Don Ernesto (DE); Klein Centauro (KC); Klein Dragon (KD); PROINTA Federal (PF) and PROINTA Isla Verde (PIV)) and experimental years in the presence of a nitrogen treatment.

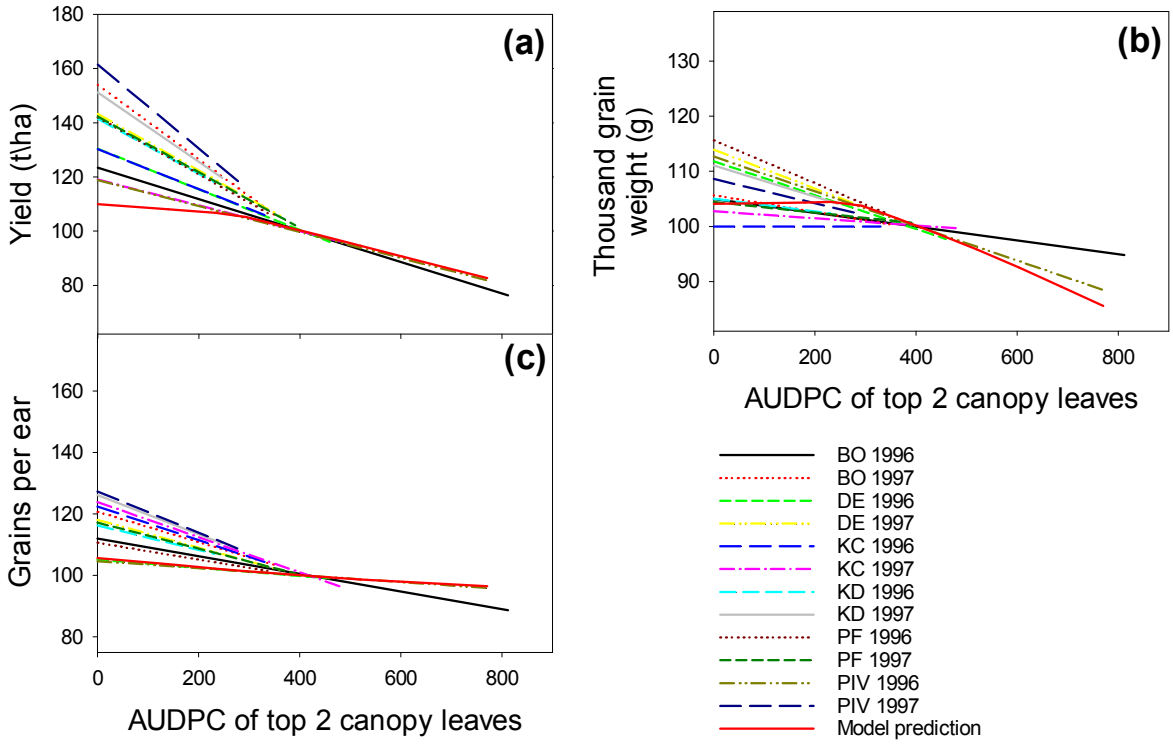

Figure SI3.5

Phytopathology Supporting Information SI4

Article title: **Physiological and developmental traits determining yield tolerance of wheat to foliar diseases**

Authors: van den Berg, F., Paveley, N. D., Bingham, I. J. and van den Bosch, F.

The effect of individual trait changes on tolerance trends

This appendix shows how tolerance is affected by changes in individual plant traits (squares in panels (**a**)). At the same time the graphs show how different components that might have a direct effect of tolerance are affected by the same trait change in both the absence of disease and the presence of a severe epidemic. The components considered are: (**a**) yield; (**b**) total realised sink size; (**c**) percentage of total sink filled at the end of the rapid-fill period; (**d**) HAD (green tissue area per unit ground area integrated over time); (**e**) number of grains per ear; (**f**) amount of water soluble carbon (WSC) per stem at the end of the slow-fill period (**g**) percentage of stem storage capacity used at the end of the slow-fill period and (**h**) HAD per grain. Squares represent tolerance, triangles represent disease-free/fully treated plants, whereas circles represent plants affected by a severe epidemic. Blank areas in the plot represent traits that lead to unviable plants, i.e. the assimilates collected pre-anthesis are not sufficient to cover the demand of the leaves, roots and stem structural tissues. To aid interpretation in all figures the intolerance axis has been reversed. Although the data points still represent intolerance, upward trends now represent a decreased intolerance (*sensu* increased tolerance). The x-axis is representative of the current genotypic variability for the trait in question as identified during a literature search.

The figures are grouped according to five different categories of traits, i.e. traits that are associated with: 1) Sink capacity; 2) carbon fixation ability; 3) Stem storage capacity and stem reserves remobilisation ability; 4) growth periods and 5) structural biomass. Some traits are associated with multiple categories, but are only shown in the first category of interest.

Sink capacity

Fig. SI4.1 Effect of changes in the fraction of ear versus stem reserves investment on disease tolerance.

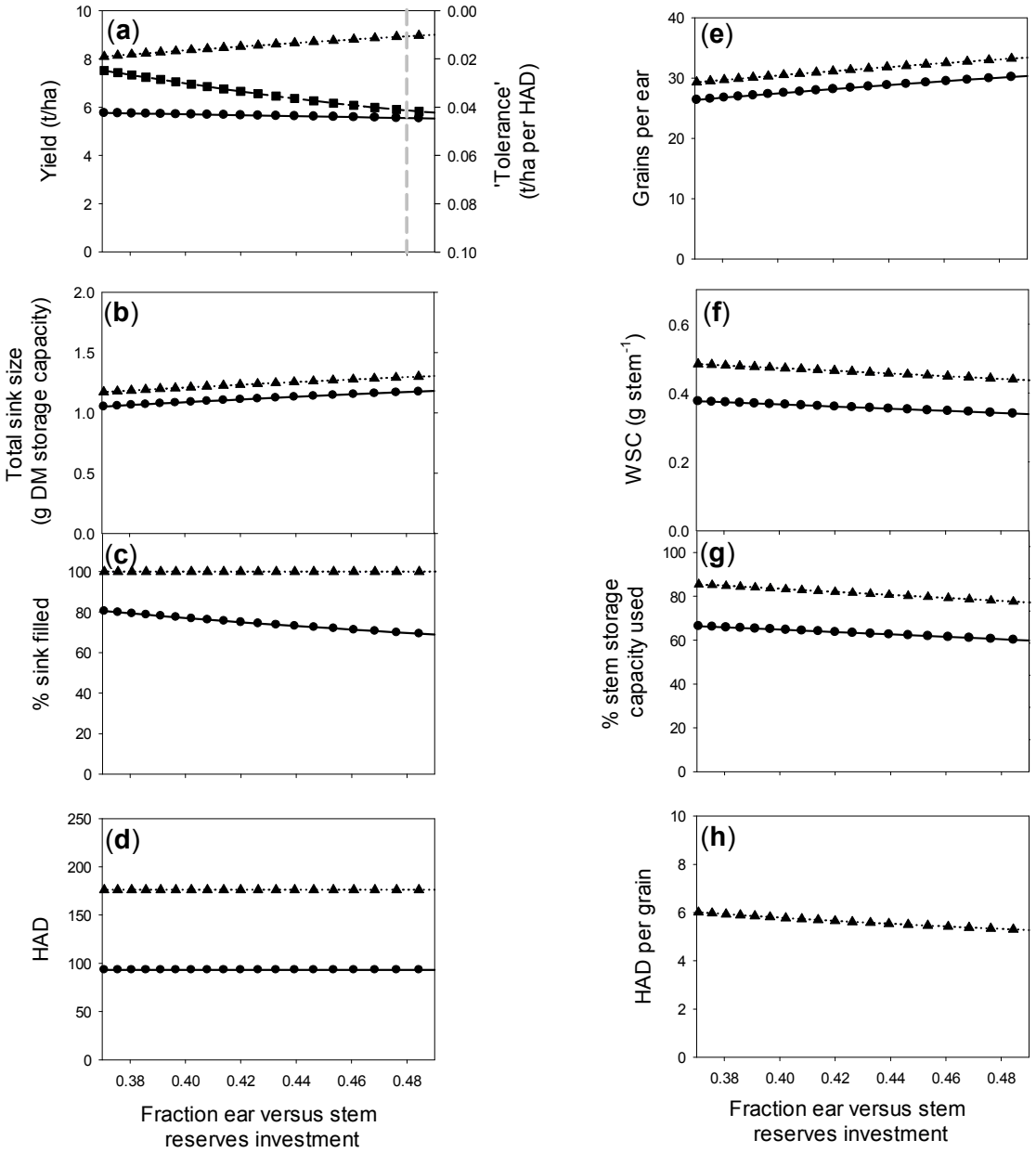

Figure SI5.1

Fig. SI5.2 Effect of changes in the maximum number of grains per ear on disease tolerance.

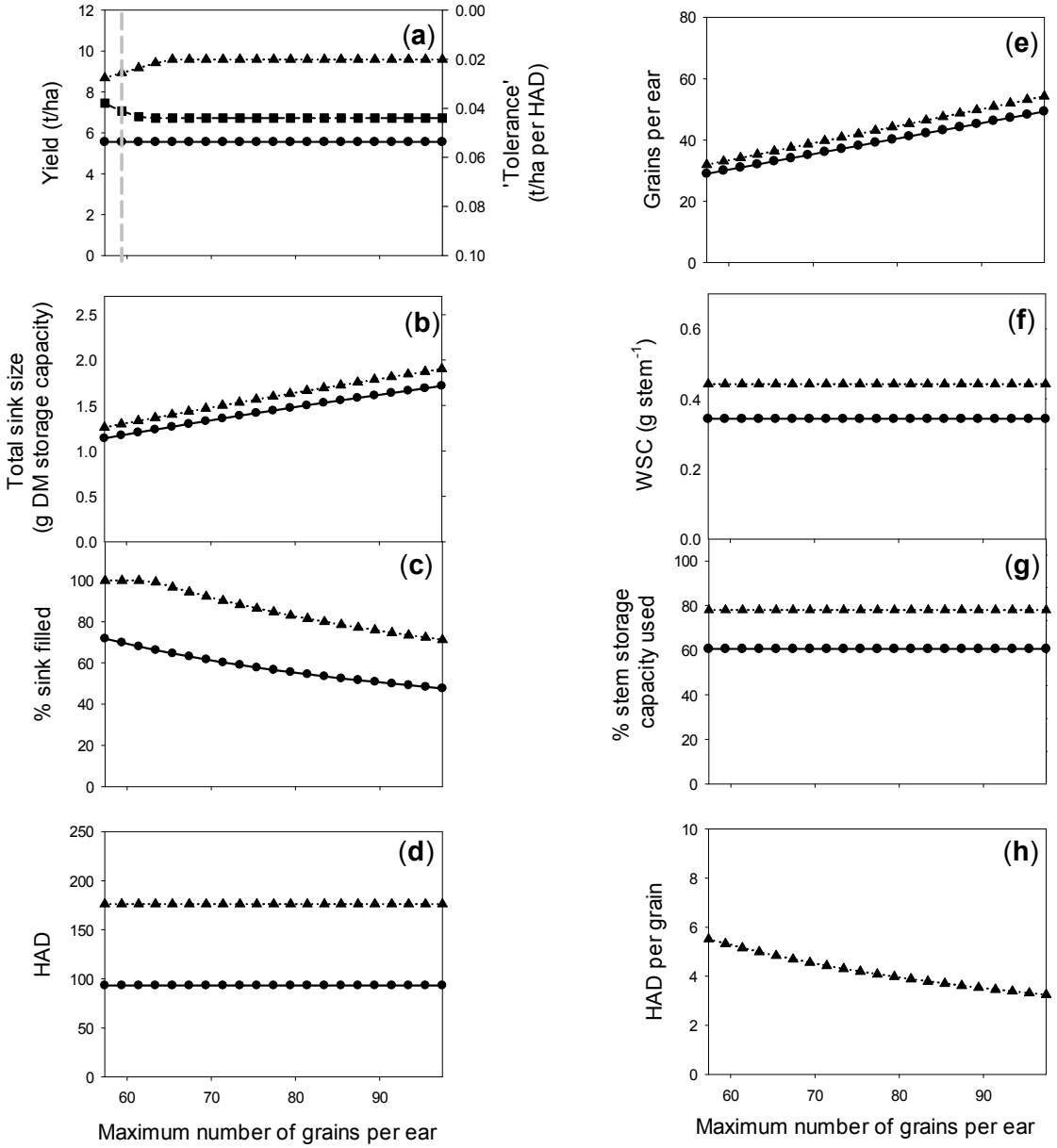

Figure SI4.2

Fig. SI4.3 Effect of changes in the fraction of grain versus stem reserves investment on disease tolerance.

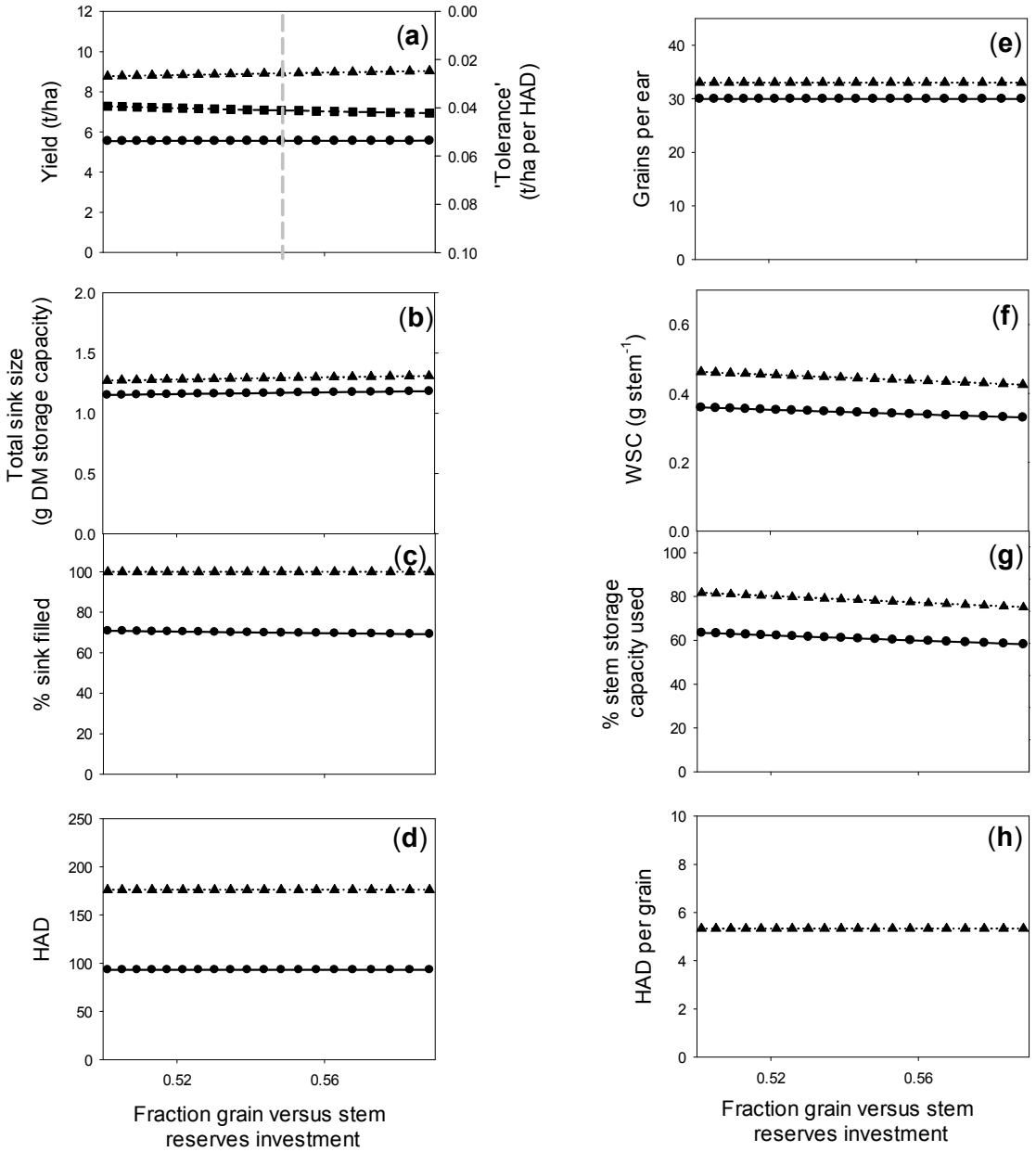

Figure SI4.3

Fig. SI4.4 Effect of changes in maximum potential grain volume on disease tolerance.

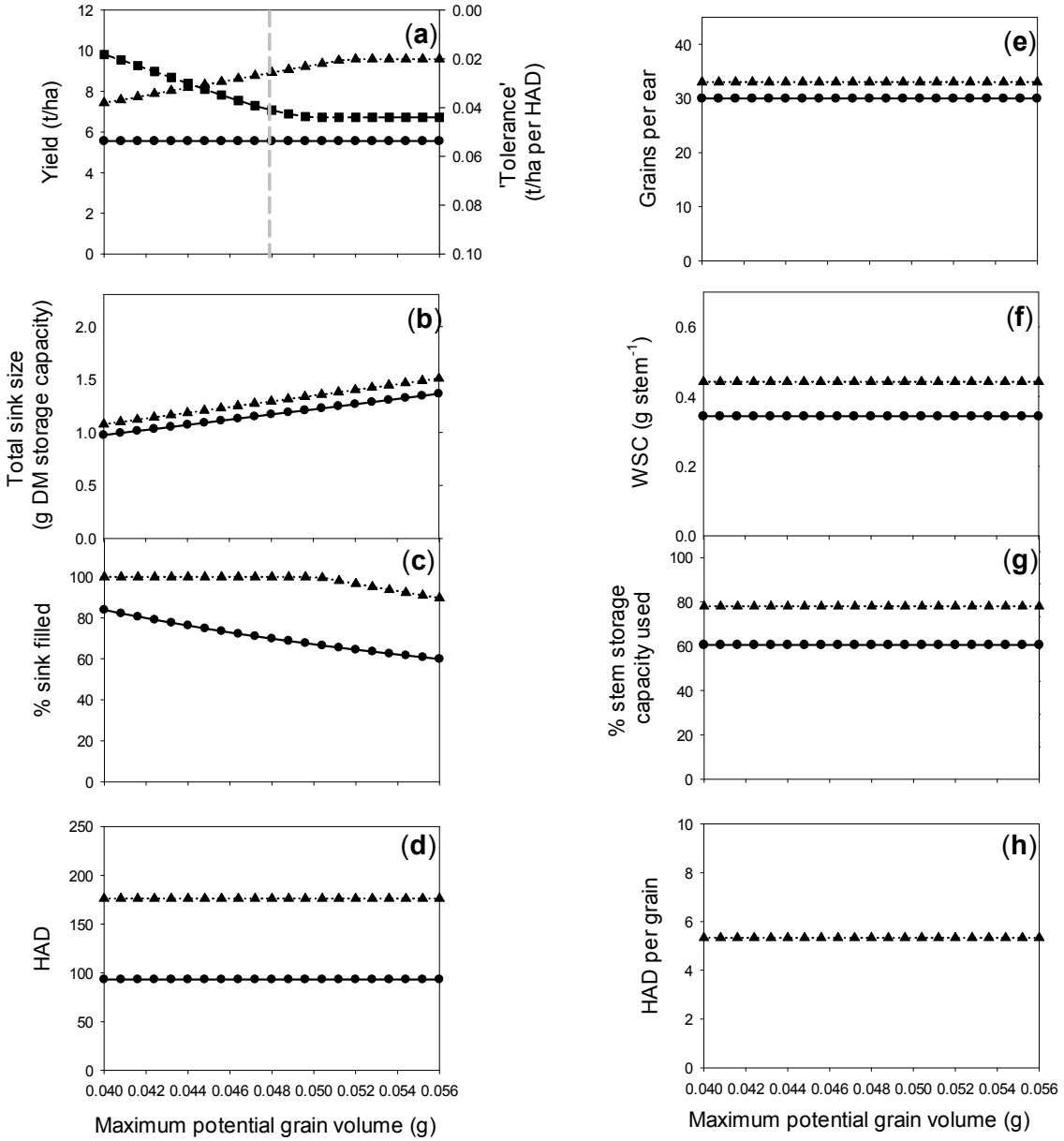

Figure SI4.4

Carbon fixation ability

Fig. SI4.5 Effect of changes in leaf distribution on disease tolerance.

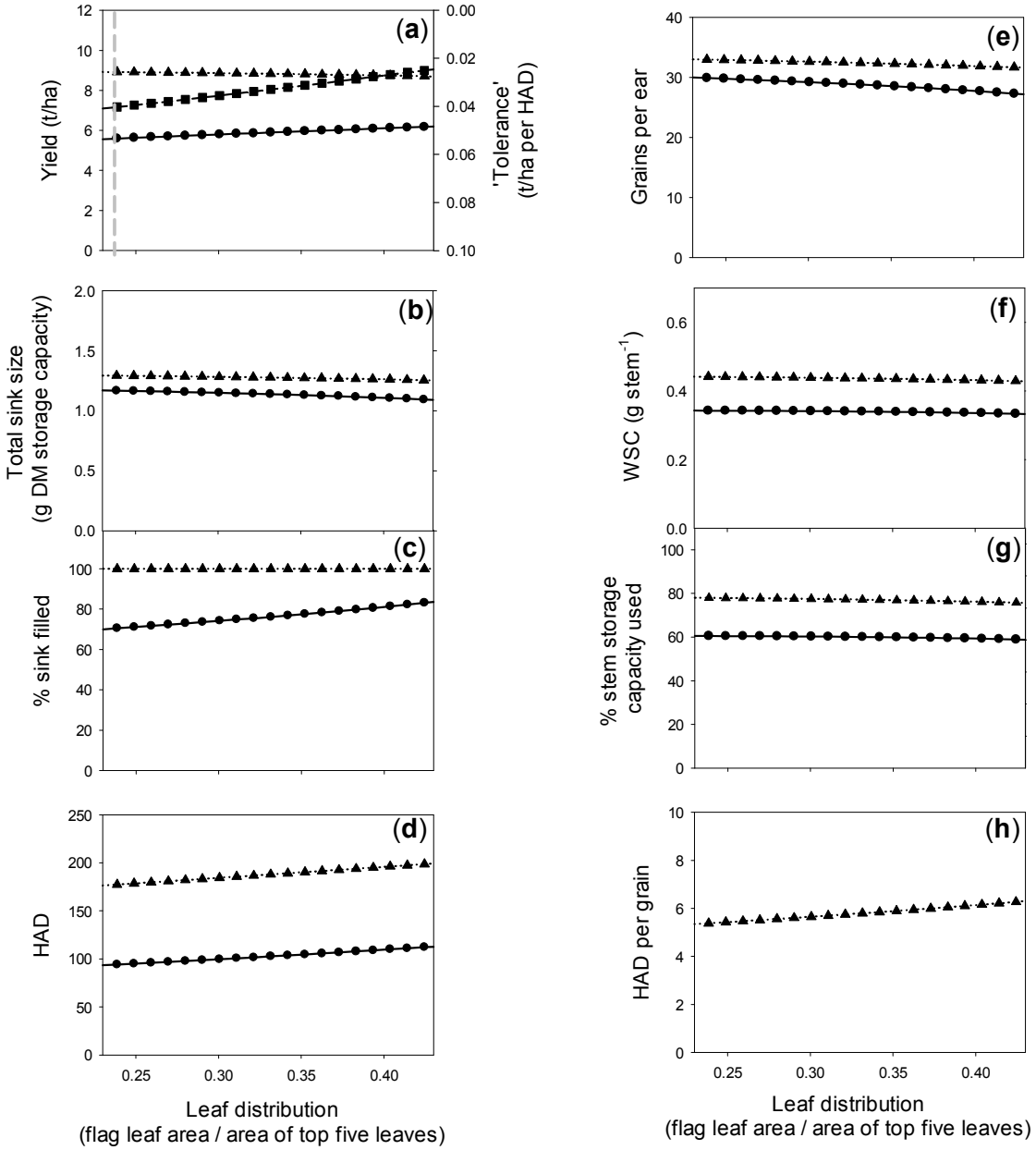

Figure SI4.5

Fig. SI4.6 Effect of changes in shoot density on disease tolerance.

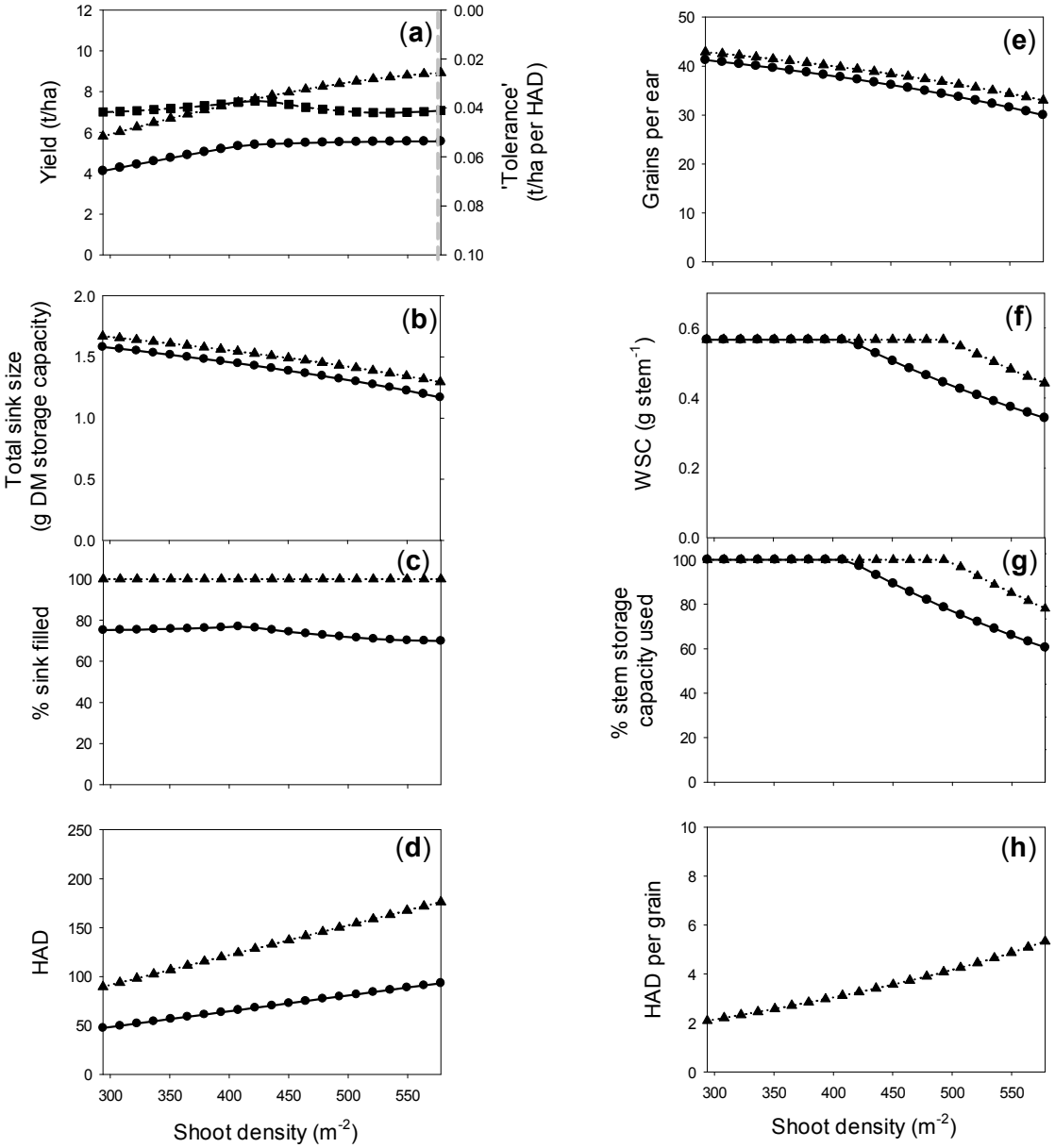

Figure SI4.6

Fig. SI4.7 Effect of changes in light extinction coefficient on disease tolerance.

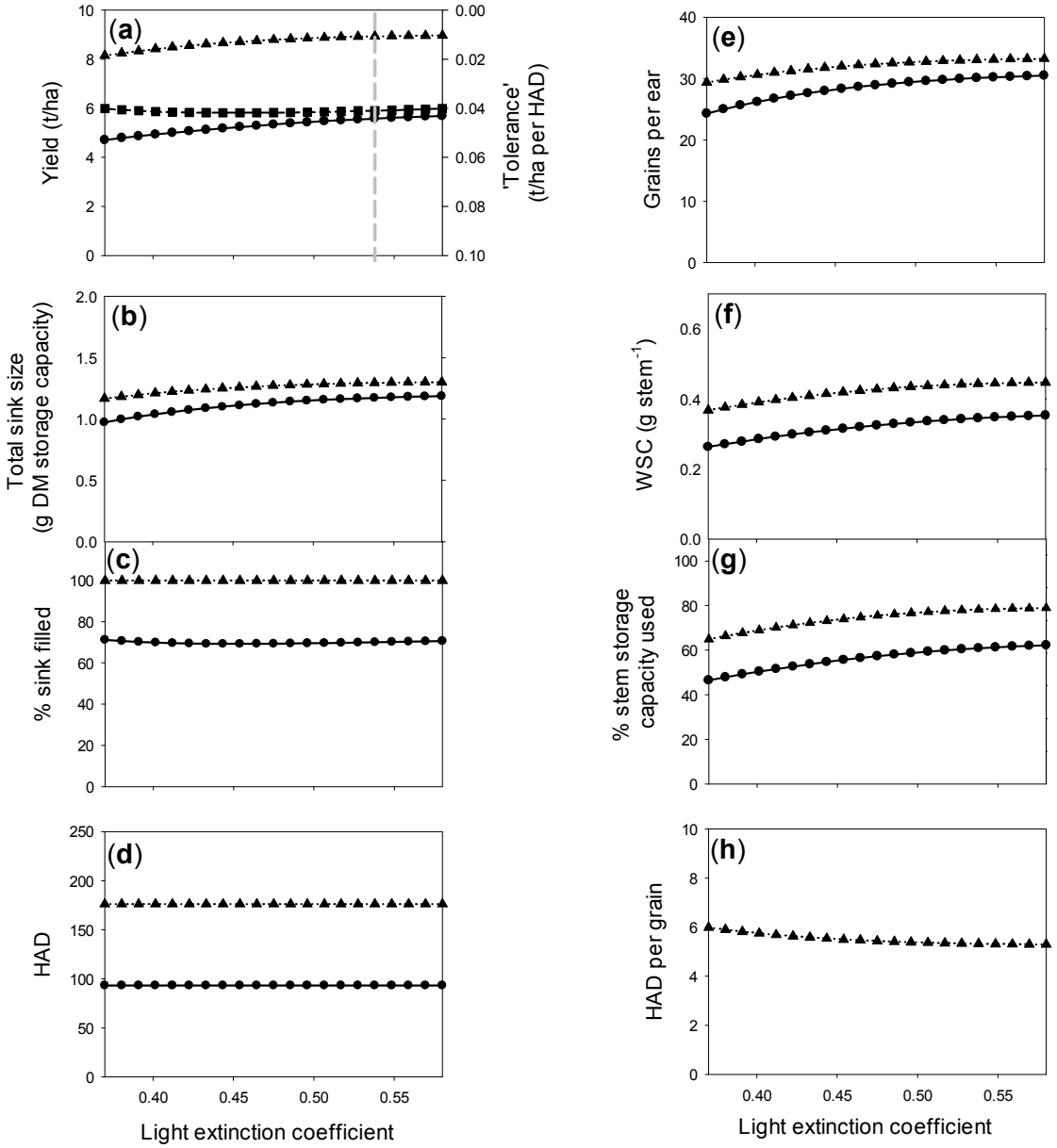

Figure SI4.7

Fig. SI4.8 Effect of changes in maximum photosynthetic capacity on disease tolerance.

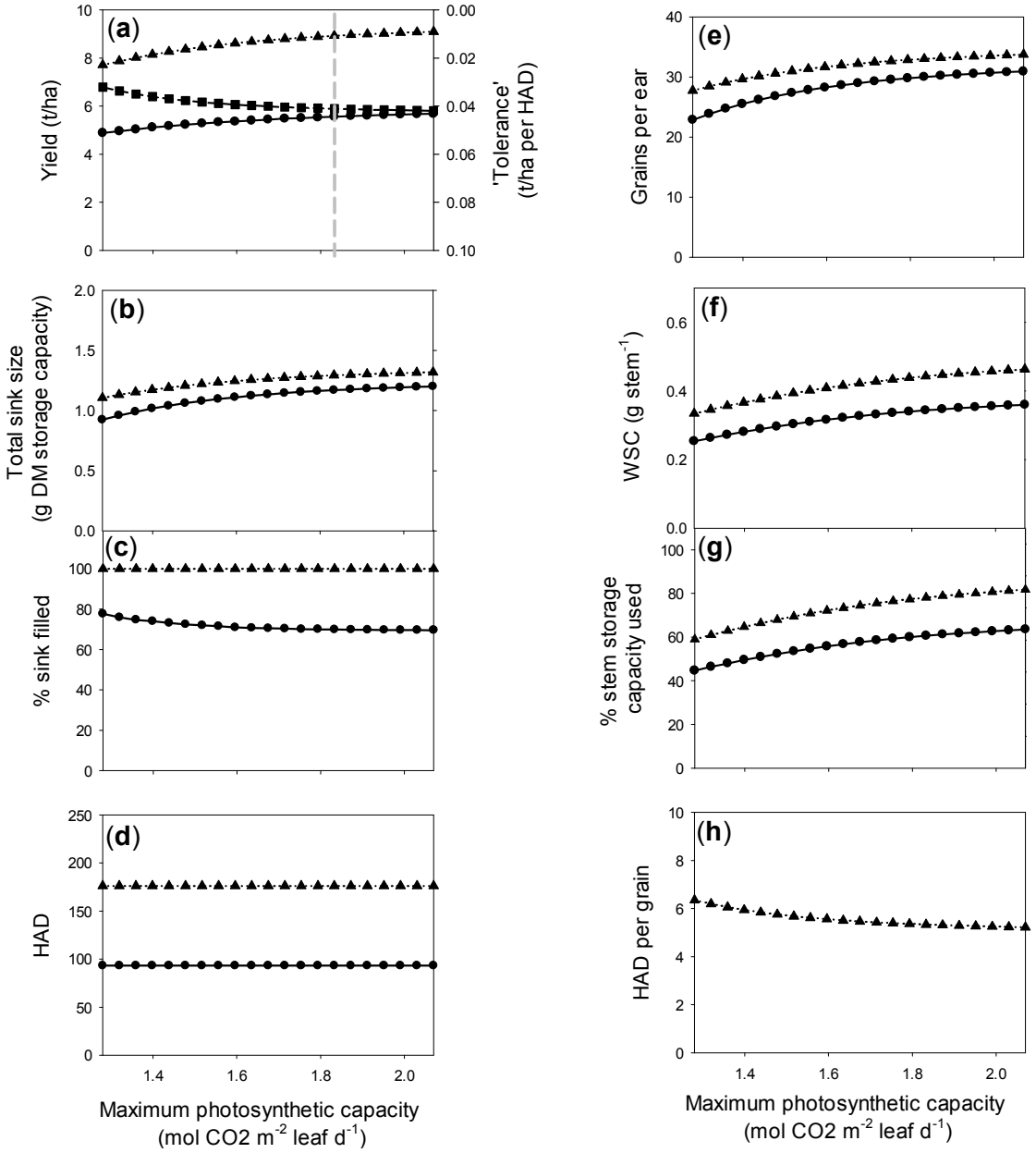

Figure SI4.8

Stem storage capacity and stem reserves remobilisation ability

Fig. SI4.9 Effect of changes in stem height at anthesis on disease tolerance.

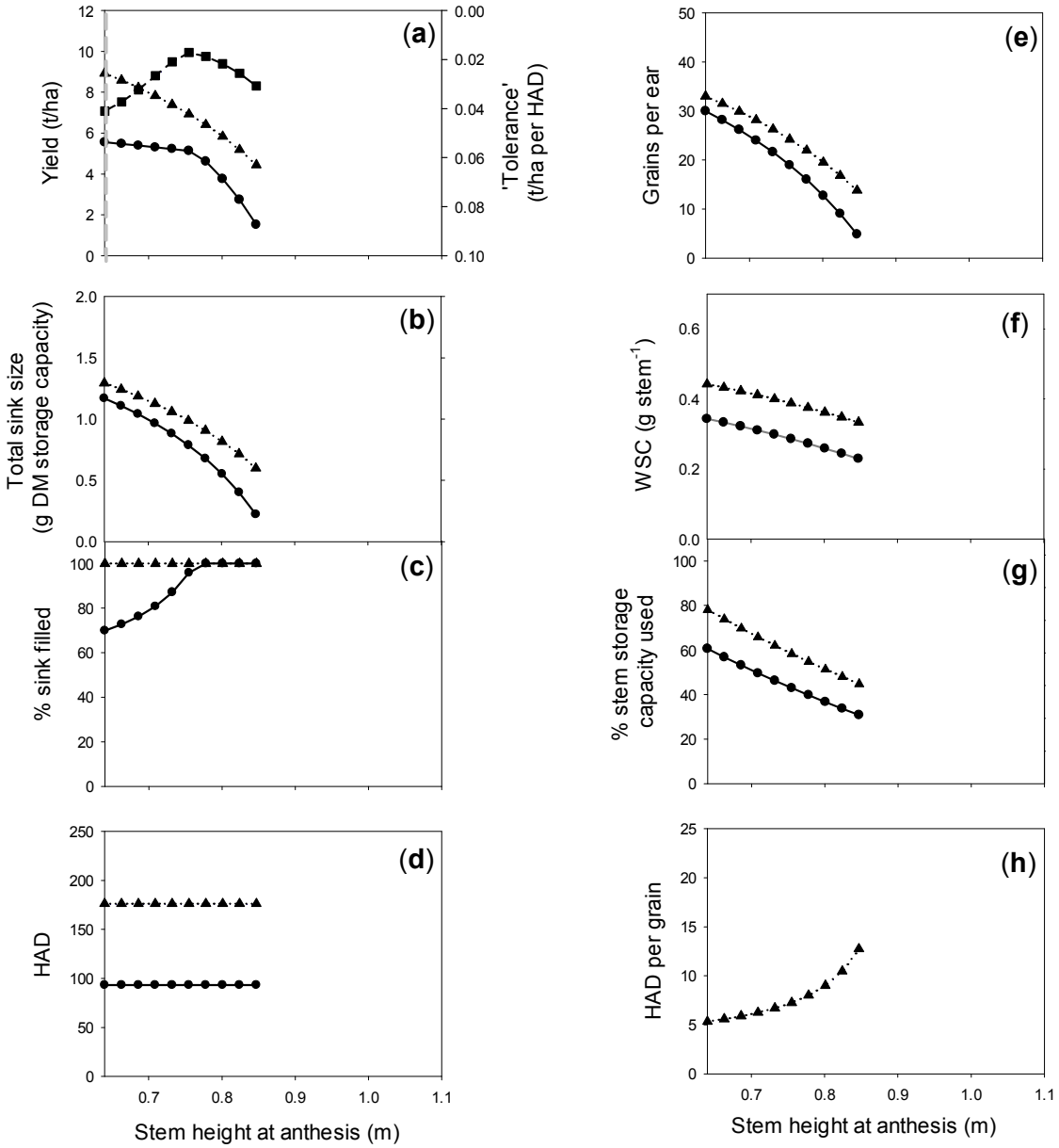

Figure SI4.9

Fig. SI4.10 Effect of changes in stem diameter on disease tolerance.

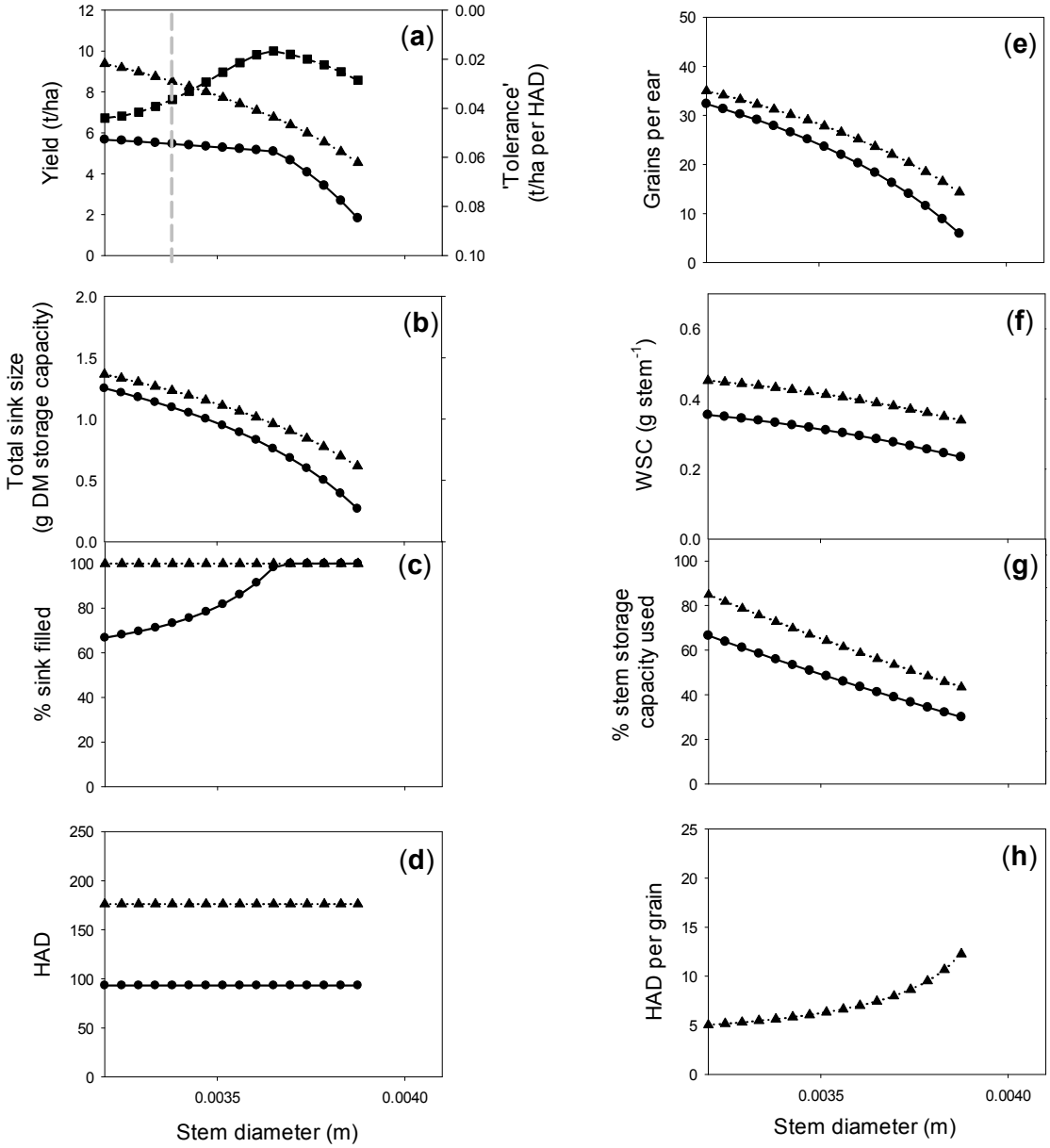

Figure SI4.10

Fig. SI4.11 Effect of changes in fractional stem thickness on disease tolerance.

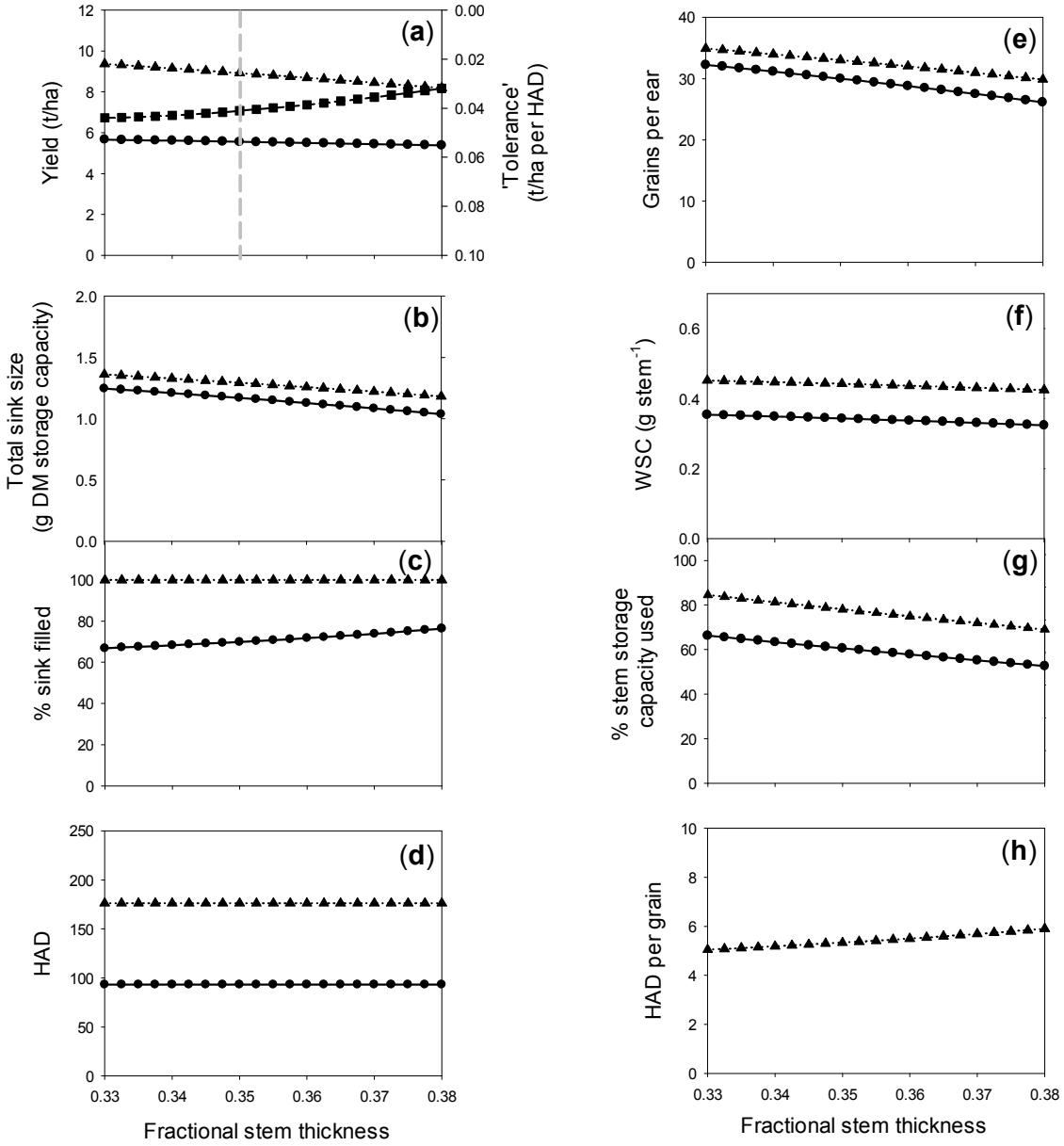

Figure SI4.11

Fig. SI4.12 Effect of changes in stem storage efficiency on disease tolerance.

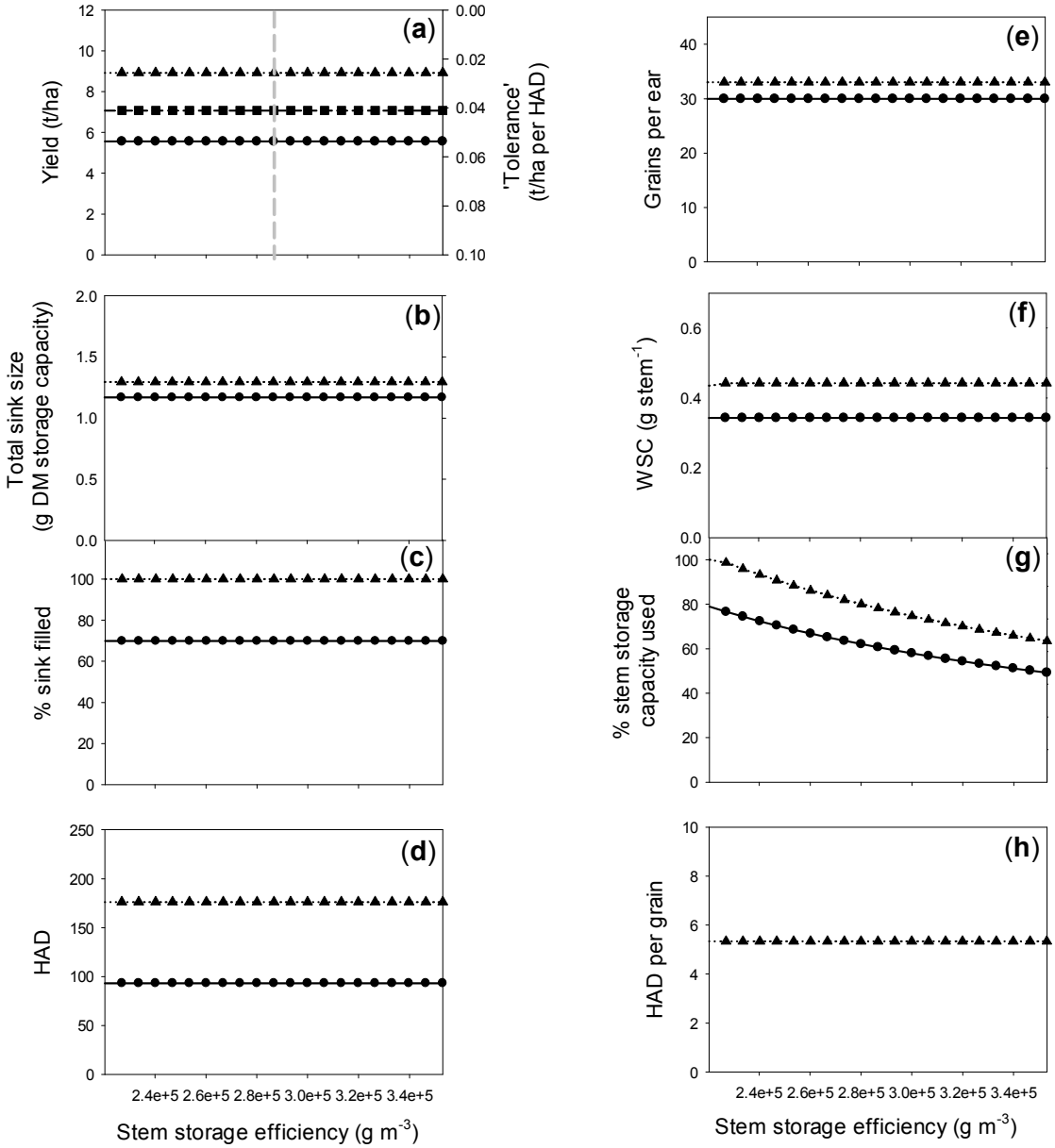

Figure SI4.12

Fig. SI4.13 Effect of changes in stem reserves remobilisation rate on disease tolerance.

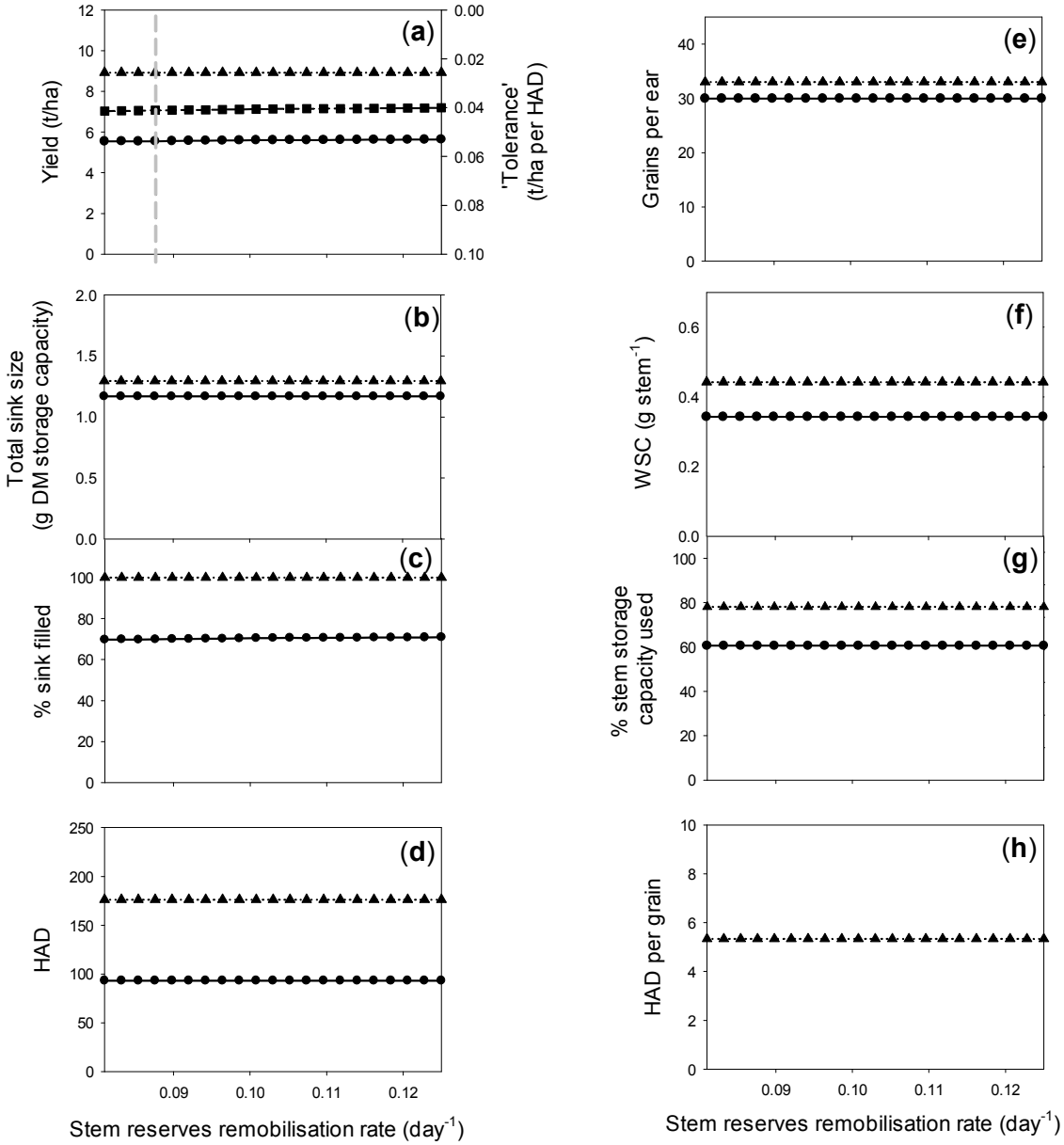

Figure SI4.13

Growth periods

Fig. SI4.14 Effect of changes in pre-anthesis period on disease tolerance.

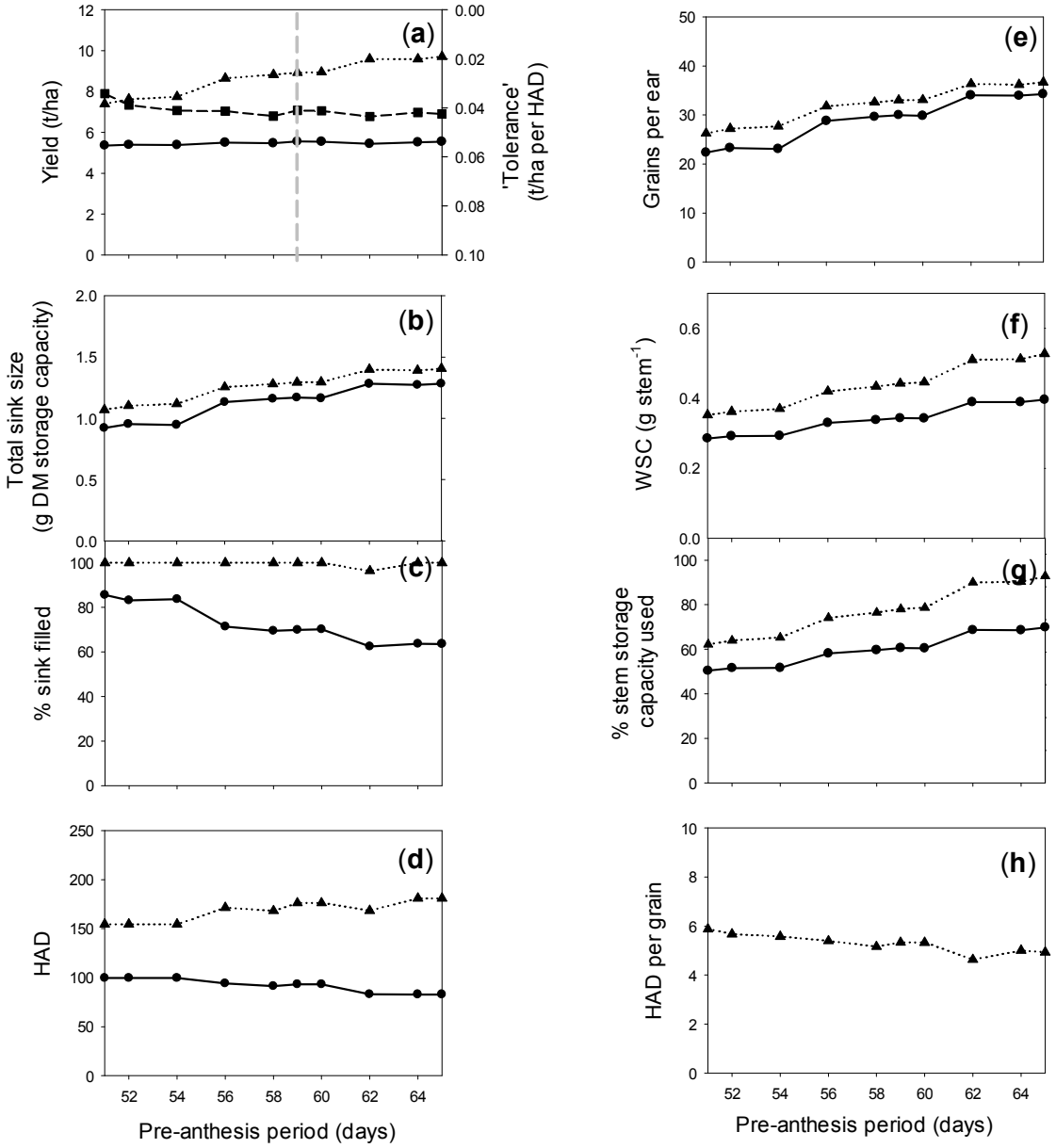

Figure SI4.14

Fig. SI4.15 Effect of changes in slow-fill period on disease tolerance.

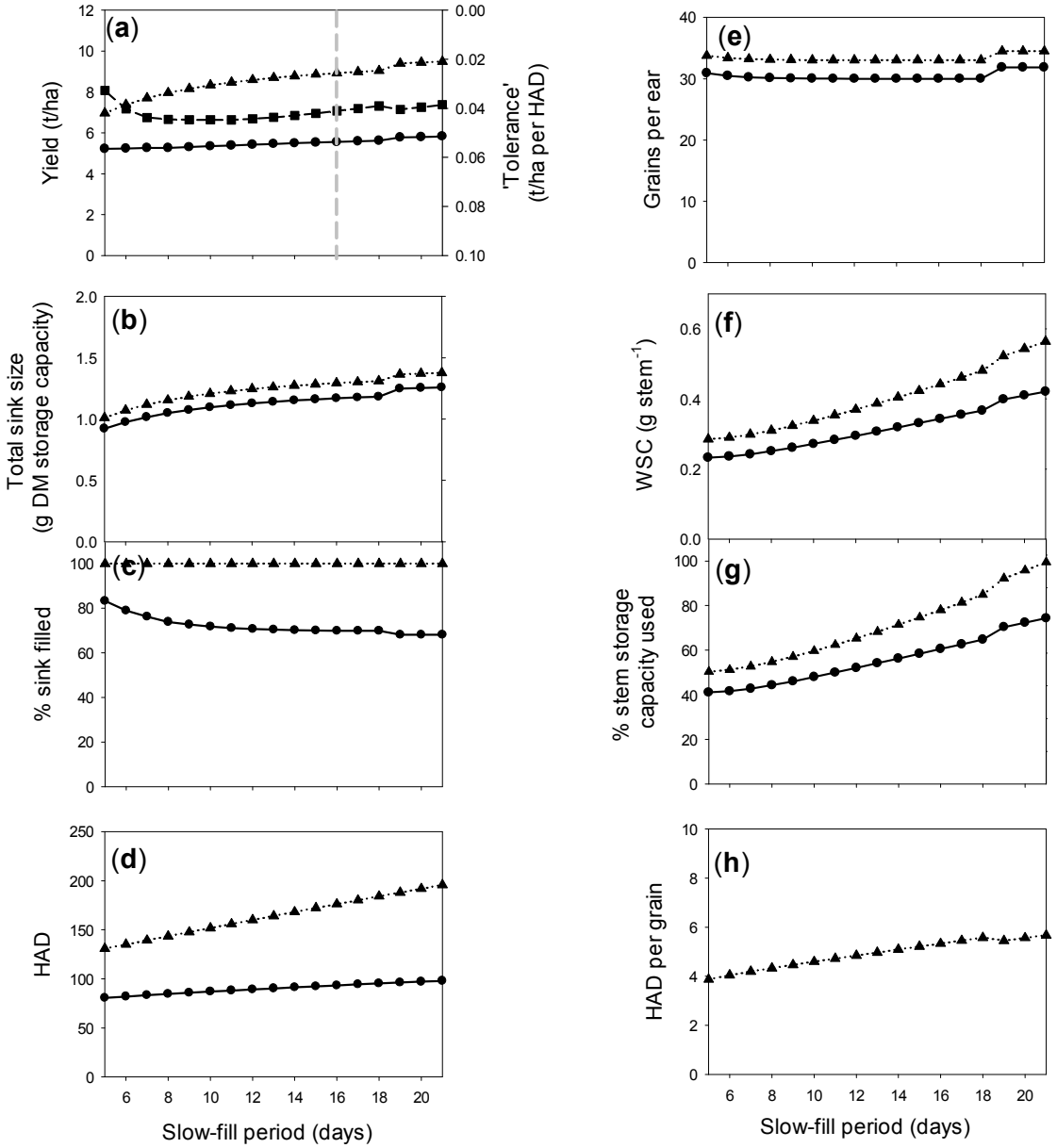

Figure SI4.15

Fig. SI4.16 Effect of changes in rapid-fill period on disease tolerance.

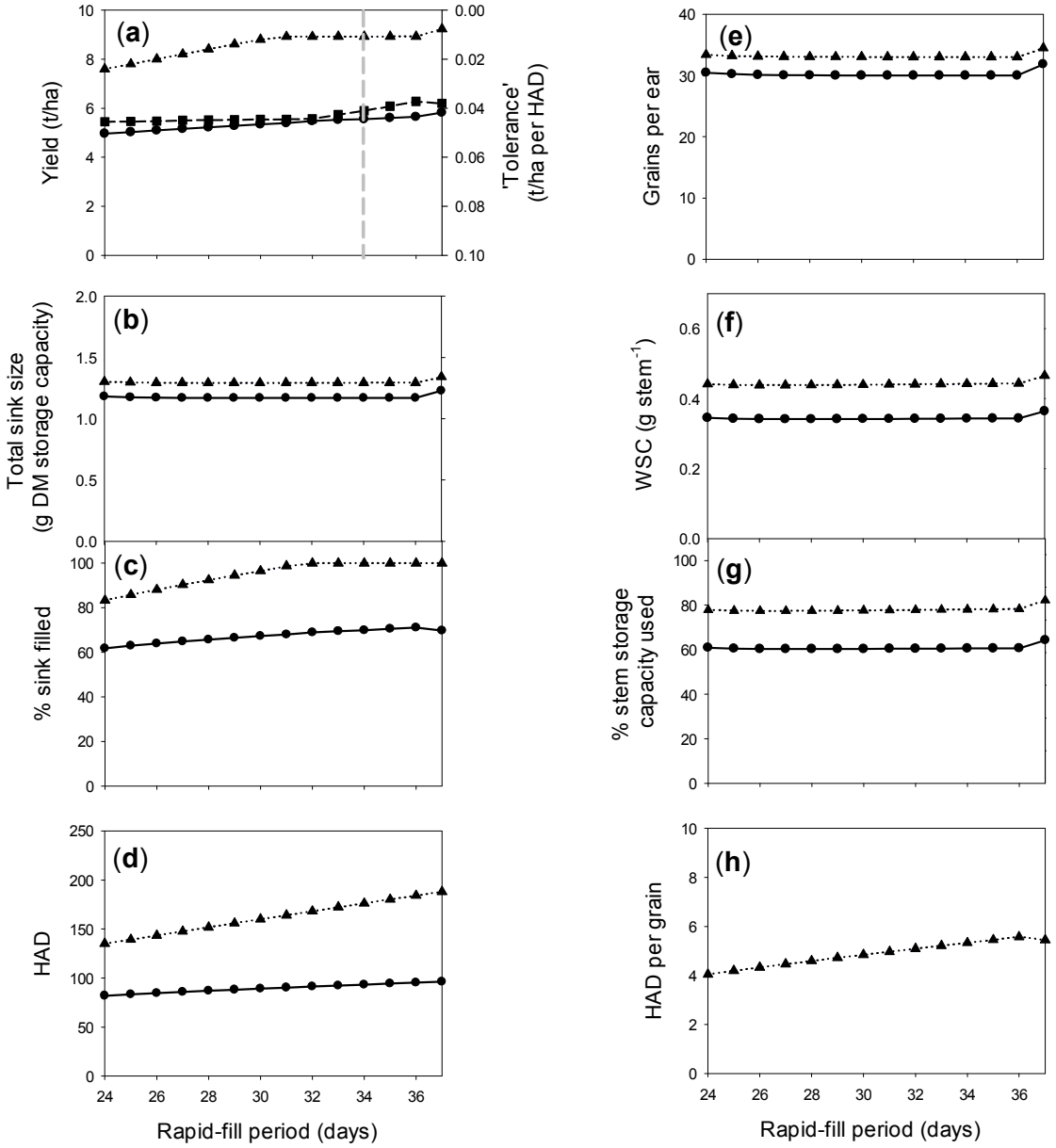

Figure SI4.16

Structural biomass

Fig. SI4.17 Effect of changes in leaf specific weight on disease tolerance.

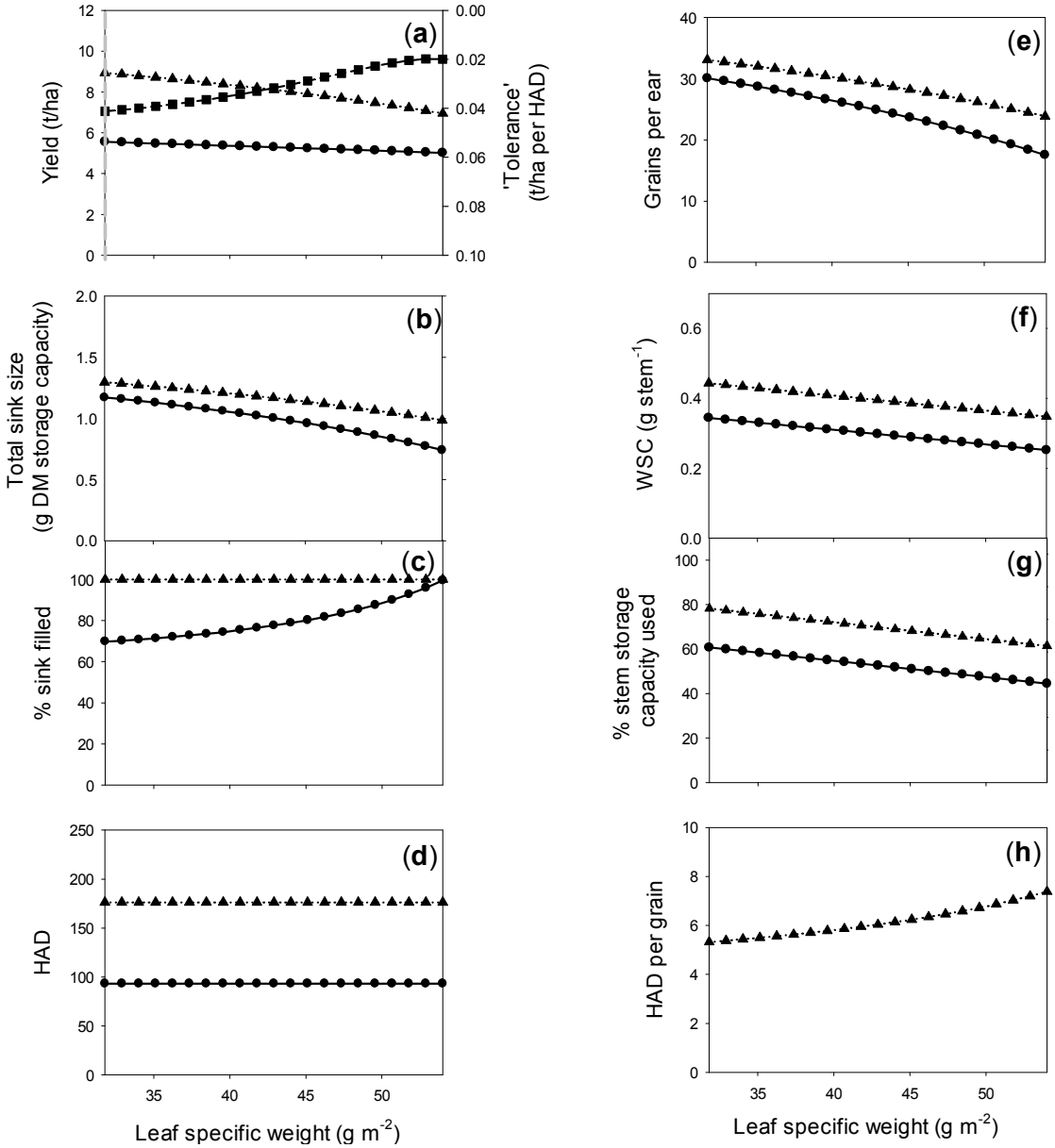

Figure SI4.17

Fig. SI4.18 Effect of changes in stem specific weight on disease tolerance.

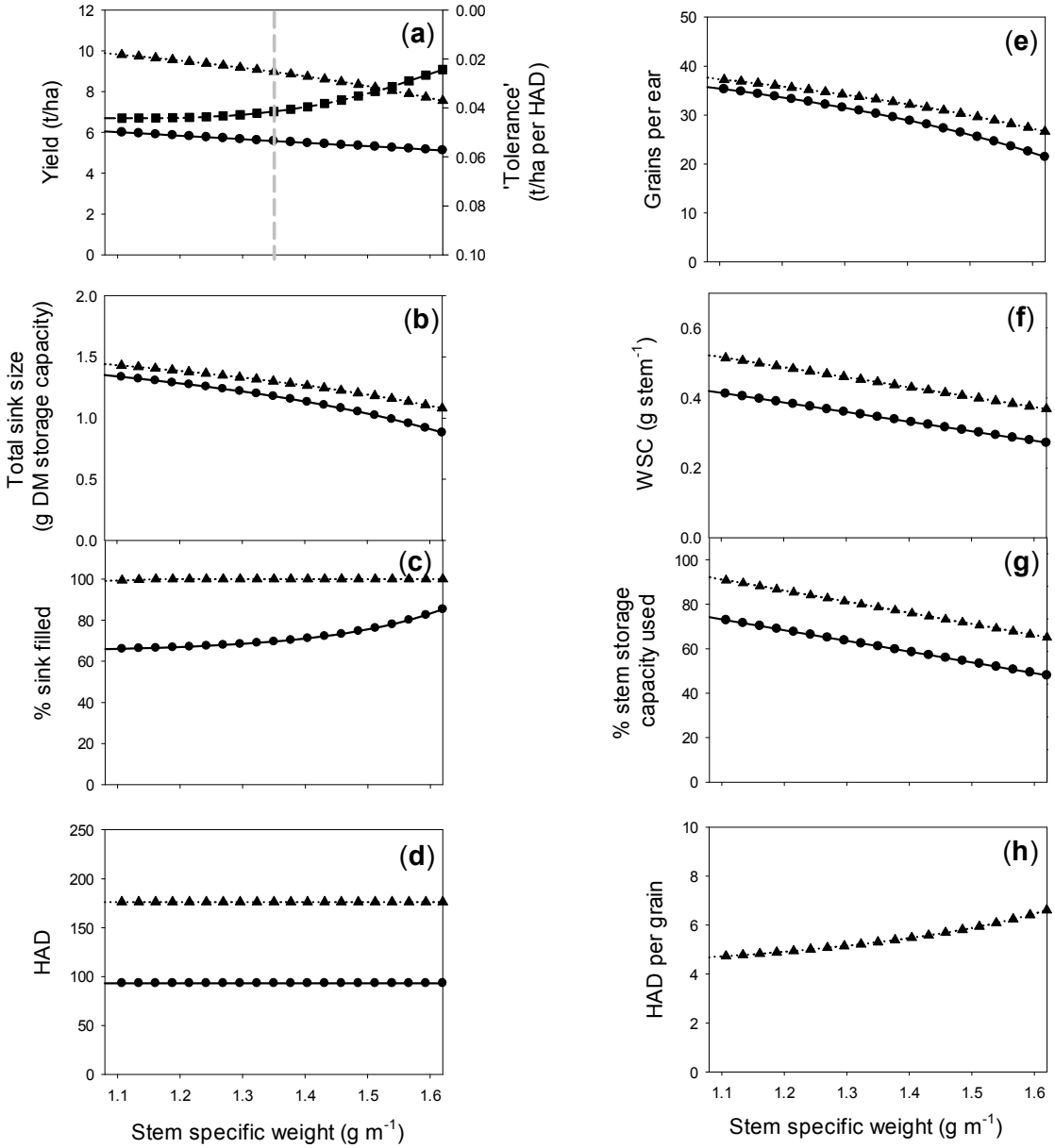

Figure SI4.18

Fig. SI4.19 Effect of changes in root mass on disease tolerance

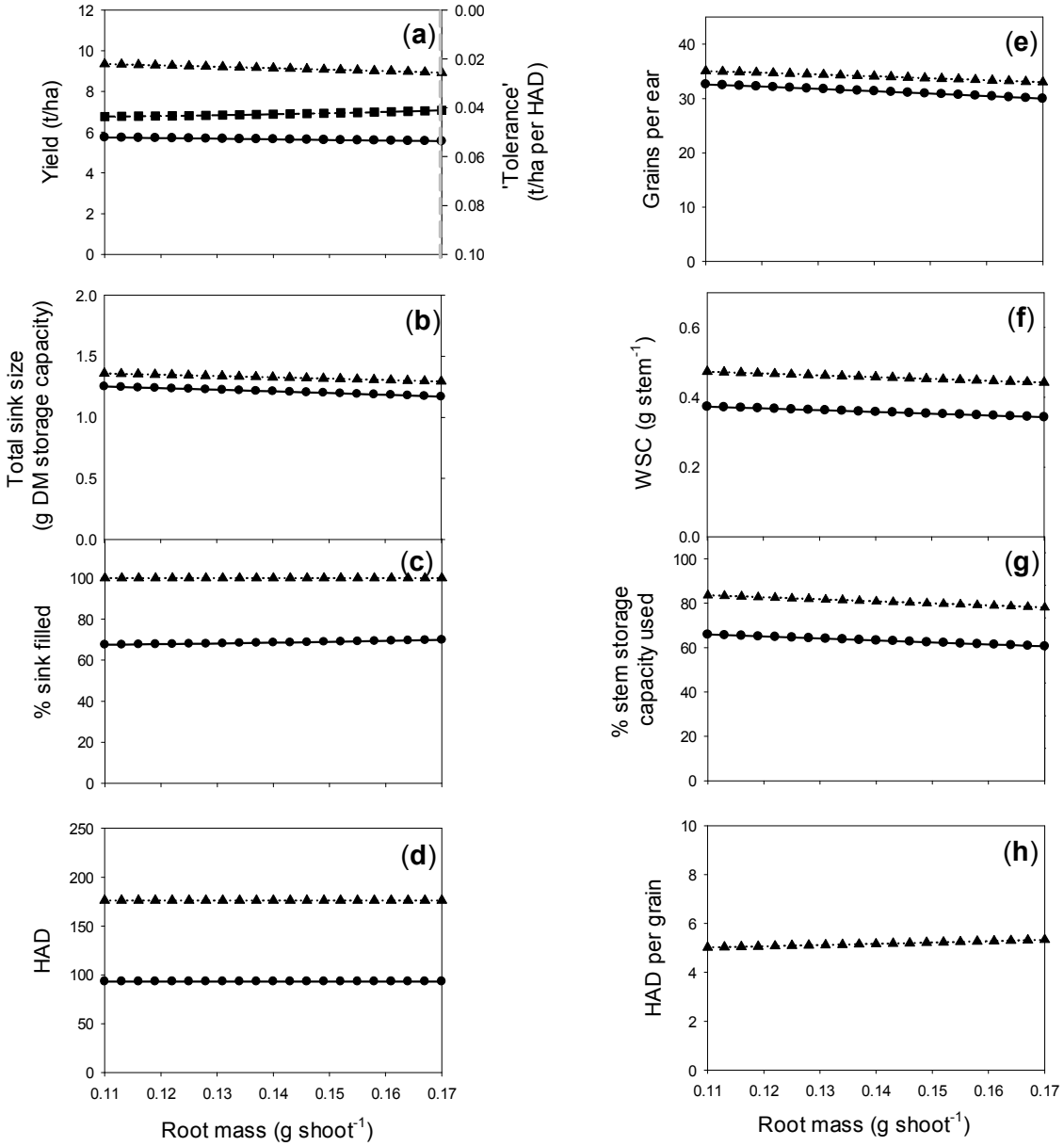

Figure SI4.19